THE INFLUENCE OF IRRADIANCE AND GENOTYPE ON THE CHANGE IN CARBON ALLOCATION BY FOUR SPECIES OF MICROALGAE UNDER INCREASING NUTRIENT STRESS

by

David S. Bowen

Submitted in partial fulfilment of the requirements
for the degree of Master of Science

at

Dalhousie University
Halifax, Nova Scotia
November 2012

DALHOUSIE UNIVERSITY

DEPARTMENT OF OCEANOGRAPHY

The undersigned hereby certify that they have read and recommend to the Faculty of Graduate Studies for acceptance a thesis entitled "THE INFLUENCE OF IRRADIANCE AND GENOTYPE ON THE CHANGE IN CARBON ALLOCATION BY FOUR SPECIES OF MICROALGAE UNDER INCREASING NUTRIENT STRESS" by David S. Bowen in partial fulfilment of the requirements for the degree of Master of Science.

Dated: November 27, 2012

Co-Supervisor: _____

Co-Supervisor: _____

Readers: _____

_____

_____

DALHOUSIE UNIVERSITY

DATE: November 27, 2012

AUTHOR: David S. Bowen

TITLE: THE INFLUENCE OF IRRADIANCE AND GENOTYPE ON THE CHANGE IN CARBON ALLOCATION BY FOUR SPECIES OF MICROALGAE UNDER INCREASING NUTRIENT STRESS

DEPARTMENT OR SCHOOL: Department of Oceanography

DEGREE: MSc CONVOCATION: May YEAR: 2013

_____

Signature of Author

To the future of green energy

Table of Contents

List of Tables

List of Figures

Abstract

During nutrient-replete growth of microalgae, new photosynthate is allocated toward three different biochemical pools: light harvesting compounds, the biosynthetic apparatus and energy storage. The mechanisms governing allocation of photosynthate between the energy storage compounds carbohydrate and lipid are not well understood. For biofuel production, it is desirable to identify conditions and algal strains that allocate maximum amounts of photosynthate to lipid. This thesis assessed the allocation of photosynthate toward the energy storage pool, and to lipid vs. carbohydrate, at two light levels and during ongoing nitrogen-starvation, for two diatoms and two chlorophytes. Nitrogen-starvation resulted in an increase in the photosynthate allocated toward energy storage, however the magnitude of change was determined by a combination of species and light level. Of the four species studied, the diatom *Chaetoceros muelleri*, grown in high light, accumulated lipid during N-starvation at a relatively high rate, making it a good candidate for biofuel production.

List of Abbreviations and Symbols Used

Symbol	Definition	Units
α	Initial slope of the P-I curve	g C · [g chl *a*]$^{-1}$ · [h]$^{-1}$ · (µmol quanta m^{-2} s^{-1})$^{-1}$
B	Biosynthetic apparatus	N/A
β	Photoinhibition factor	g C · [g chl *a*]$^{-1}$ · [h]$^{-1}$· (µmol quanta m^{-2} s^{-1})$^{-1}$
C_i	Carbon content for compound *i*	µmol C L^{-1}
Carb	Carbohydrate	g L^{-1} or mol L^{-1}
CCMP	Center for Culture of Marine Phytoplankton (now NCMA)	N/A
chl *a*	Chlorophyll *a*	g m^{-3}
CV	Coefficient of variation	N/A
D	Dilution ratio	Dimensionless
DW	Dry weight	g L^{-1}
E	Energy stores	N/A
ECS	Elemental combustion system	N/A
F_0'	Minimum fluorescence. Prime indicates cultures were not dark adapted	RFU
F_t'	Fluorescence at time *t*. Prime indicates cultures were not dark adapted	RFU
F_m'	Maximum fluorescence. Prime indicates cultures were not dark adapted	RFU

Symbol	Definition	Units
F_v'	Variable fluorescence. $F_v' = F_m' - F_0'$. Prime indicates cultures were not dark adapted	RFU
F_v'/F_m'	Quantum yield of photosystem II. Determined without dark adaptation	Dimensionless
Γ_i	Slope of a linear curve fit between an individual compound (*i*) and particulate organic carbon during N-starvation	mol C_i · [mol C]$^{-1}$
$\hat{\Gamma}_{TLG}$	Calculated carbon allocated toward lipid during N-starvation	mol C_{TLG} · [mol C]$^{-1}$
HPLC	High Performance Liquid Chromatography	N/A
HL	High light	N/A
I	Irradiance	µmol quanta m^{-2} s^{-1}
LL	Low light	N/A
L	Light harvesting compounds	N/A
$\mu_{F'}$	Growth rate determined from *in vivo* fluorescence	d^{-1}
NCMA	National Center for Marine Algae and Microbiota (formerly CCMP)	N/A
NO_3^-	Nitrate	µmol L^{-1}
P^B	Photosynthetic rate, normalized to chl *a*	g C · [g chl *a*]$^{-1}$ · [h]$^{-1}$

Symbol	Definition	Units
P_S^B	Maximum photosynthetic rate without photoinhibition	g C · [g chl *a*]$^{-1}$ · [h]$^{-1}$
PAR	Photosynthetically available radiation	μmol quanta m^{-2} s^{-1}
POC	Particulate organic carbon	μmol L^{-1}
PON	Particulate organic nitrogen	μmol L^{-1}
ψ_i	Carbon normalized to particulate organic nitrogen, for compound *i*	mol C$_i$ · [mol N]$^{-1}$
$\Delta\psi_i$	Relative change in the carbon:nitrogen ratio between nutrient replete and starved conditions, for compound *i*	mol C$_i$ · [mol N]$^{-1}$
$\Delta\widehat{\psi}_{POC}$	Calculated change in total carbon, normalized to particulate organic nitrogen. $\Delta\widehat{\psi}_{POC} = \Delta\psi_{Carb} + \Delta\psi_{TLG}$.	mol C · [mol N]$^{-1}$
R	Nutrient replete	N/A
RFU	Relative fluorescence units	N/A
S	Nutrient starved	N/A
t	Time	Defined in text
TLG	Total lipid as determined via gravimetric means	g L^{-1} or mol C L^{-1}
TLI	Total lipid as determined via inferred means	mol C L^{-1}
ζ_{POC}	Rate of carbon allocation toward energy storage compounds	mol C · [mol N]$^{-1}$ · d^{-1}

Acknowledgements

The work presented here is only a portion of what was achieved with the team of people I had the fortune of working with. First, to my supervisor John Cullen, thank you for all of the advice and patience you have provided throughout this thesis. Hugh MacIntyre, your move to Dalhousie came at a time that greatly benefited my project. Thank you for your insight on the depths of algal physiology. Markus Kienast, your reassurance and direction throughout have been greatly appreciated, thank you. Marlon Lewis, thank you for the assistance and providing me with the opportunity to ponder the unexpected impacts of bacteria. Patrick McGinn, thank you for your insightful comments on a short time scale.

Audrey Barnett, thank you for your tireless patience teaching me the finer points of Matlab®. Cathy Ryan your continued assistance and witty commentary on sampling early in the morning was greatly welcomed. Flavienne Bruyant, thank you for the crash course in the mass culturing of microalgae and the chance to pursue unexpected opportunities. Without the laboratory assistance of Yinglin Zou, Matthew Beck, Cheryl Rafuse, Joe Cullen, Trina Whitsitt, Robert Lennox and Katie Kowarski this project would not have been possible. Thank you. Thanks to Jonathan Pye and Richard Davis for technical assistance. Chris Jones, thank you for all of the statistical analysis advice. The Plankton Lab, both past and present, for their continued guidance throughout this thesis. Thanks to Steve McKenna and Ron Melanson for providing access to seawater from the National Research Center – Institute of Marine Bioscience Research Facility. Finally, to my family and friends, your support throughout has been unmatched. Thank you.

Financial support was provided by Dalhousie University and Cellana.

Chapter 1: Introduction

Global energy demands have increased concurrent with rising concentrations of atmospheric greenhouse gases, promoting the search for alternative energy sources with low carbon emissions (Huntley & Redalje, 2007, Saxena *et al.*, 2009). The burning of fossil fuels releases gases such as carbon dioxide (CO_2), sulfur dioxide (SO_2), and nitrogen oxides (NO_x) into the atmosphere that contribute to climate change (Forster *et al.*, 2007), ocean acidification (Doney *et al.*, 2009) and acid rain (Galloway & Likens, 1981). The increasing use of alternative biological sources for fuel helps to mitigate the emission of greenhouse gases (Huntley & Redalje, 2007, Sims *et al.*, 2010). Current biological sources utilized include photosynthetic organisms and organic components of municipal waste. The focus here will be placed on photosynthetically produced biofuels, such as the production of the energy stores carbohydrate and lipid, by plants and microbes.

1.1 First- and Next-Generations of Biofuels: The Case for Algae

First-generation biofuels consist of food crops, such as corn, soybean and sugarcane, that can also be used as a source of biofuel. Some problems that arise from using these sources include reducing resource availability, direct competition with food production and uncertain energy returns (Schenk *et al.*, 2008, Naik *et al.*, 2010). Resources include potable water, which has become increasingly important as access becomes restricted in developing countries (Schenk *et al.*, 2008) and high quality agricultural lands, which could be used indirectly for livestock production (Nigam & Singh, 2011). The direct competition for food production is worrisome, as it is believed

that the increase of cereal crops being used for biofuel production has increased global food prices (Naik *et al.*, 2010, Sims *et al.*, 2010). Additionally, cereal crops have been shown to have an uncertain net energy balance (NEB); defined as the energy returned for the energy required to produce the biofuel source (Hill *et al.*, 2006). For example, corn has been shown to have an NEB between 0.71, a net loss, (Pimentel & Patzek, 2005) to 1.25, a net gain (Hill *et al.*, 2006).

Next-generation biofuels focus on ligno-cellulosic feedstocks (Scott *et al.*, 2010). These feedstocks range from those that can be cultured on poor agricultural lands, for example Jatropha and switchgrass (Nigam & Singh, 2011) to processing byproducts, such as cereal straw and sugar cane bagasse, to wastes such as organic components of municipal solid wastes (Sims *et al.*, 2010). Unlike first-generation biofuels, next-generation biofuels do not directly compete for resource availability, or divert crops that could otherwise be used for food. Another advantage of next generation biofuels is the potential for a carbon neutral impact on CO_2 concentrations (Naik *et al.*, 2010).

Another next-generation biofuel feedstock source is microalgae. These microbes have a physiological versatility that allows them to alter the allocation of photosynthate, in response to environment (Laws & Bannister, 1980, Shifrin & Chisholm, 1980, Thomas *et al.*, 1984a, Renaud *et al.*, 2002) or between species (Wilhelm *et al.*, 2006, Maberly *et al.*, 2010, Hockin *et al.*, 2012). An option that would help resolve the land usage issue would be mass cultures of microalgae on non-arable land, as long as there is access to an appropriate water source. For freshwater facilities, this could be near a wastewater outflow (Oswald & Golueke, 1960) while marine facilities would either be near a saltwater aquifer or seawater (Ferrell & Sarisky-Reed, 2010).

1.2 Historical Overview

Microalgae were first proposed to be mass cultured for production of foodstuff in the 1950's (Burlew, 1953), then for wastewater treatment in the 1960's (Oswald & Golueke, 1960, Ferrell & Sarisky-Reed, 2010), in addition to being considered as a source of oxygen and protein for space travel (Powell *et al.*, 1961). Shortly after this, the oil shortage of the early and mid 1970s spurred western countries to investigate alternative energy sources, such as aquatic microbes and terrestrial plants (Canakci & VanGerpen, 2001, Chisti, 2007, Ferrell & Sarisky-Reed, 2010). While the mass culture of microalgae for production of energy became a prevalent research topic in the 1970's, it is important to note that the idea that microalgae could be used as an energy source originated in the mid 1950's. During this time, Meier (1955) and Oswald and Golueke (1960) proposed that microalgal carbohydrate could be anaerobically digested to produce methane gas.

Between 1978 and 1996, the United States Department of Energy oversaw the Aquatic Species Program (ASP), "a relatively small research effort intended to look at the use of aquatic plants as a source of energy" (Sheehan *et al.*, 1998). Initially ASP focused its research on hydrogen production by algae, but in the early 1980s this switched to finding sources of biodiesel (Sheehan *et al.*, 1998). In 1996, funding to ASP was discontinued for multiple reasons, one of which was that it was not financially feasible given the existing technology. At the time, the price of oil was roughly $20 per barrel (http://www.ioga.com/Special/crudeoil_Hist.htm).

Building on ASP, and research that has been carried out since, the United States Department of Energy's Biomass Program was funded in 2009 to "invest in the research,

development, and deployment of commercial algal biofuel processes" (Ferrell & Sarisky-Reed, 2010). The resurgence of interest in microalgae as a source for biofuel feedstock was partially due to the increase in fuel price, desire to reduce reliance on foreign fuel sources, and to create economic opportunities (Ferrell & Sarisky-Reed, 2010).

Additionally, in 2009, Sustainable Energy Ireland released a report on the potential of using microalgae as source of biofuel (Bruxton *et al.*, 2009). While identifying the global interest in using microalgae for biofuel, Sustainable Energy Ireland acknowledged that the climate in Ireland would limit the microalgae's potential. However, given the higher photosynthetic efficiency of microalgae vs. terrestrial plants, and "significant lipid content" relative to other biofuel sources, interest remains high (Bruxton *et al.*, 2009).

While different programs have pursued mass scale microalgae biofuel production, one of the key obstacles to commercialization is the maximization of yields to make production economical (Hu *et al.*, 2008).

1.3 Example of Current Mass Microalgal Culturing Success

The physiological versatility of phytoplankton has made these photosynthetic microbes ideal candidates for the mass production of various biochemical compounds, which can have industrial uses. For example, the microalga *Haematococcus pluvialis* has successfully been mass cultured for the production of the "high value metabolite" astaxanthin (Olaizola, 2000). This pigment has various applications, two of which are as a food colouring agent in aquaculture and as an antioxidant in nutraceuticals (Lorenz & Cysewski, 2000, Olaizola, 2000, Guerin *et al.*, 2003). The commercial production of astaxanthin, in microalgae, is mostly limited to *Haematococcus* sp. as this species has

been shown to accumulate large amounts under nutrient stress. Similarly, other biochemical compounds, such as lipid, are produced by all microalgae; however, the cellular concentration, and composition, differs between species and with culture conditions.

1.4 Fundamental Issues

While research supports the use of microalgae for a biofuel feedstock source, the application on a mass scale encounters fundamental issues that still need to be overcome. These issues include determining efficient ways to culture (Huntley & Redalje, 2007), harvest and process the algae (Burlew, 1953, Scott *et al.*, 2010), as well as preventing biological contamination (Gummert *et al.*, 1953). However, maximizing the yield of lipid is the main challenge that must be addressed in order to commercially generate photosynthetically produced biofuels (Huntley & Redalje, 2007).

Two different culturing regimes have been implemented for the mass culturing of microalgae: continuous reactor and a two-stage regime. In a continuous reactor, algae are maintained in balanced growth with cultures being semi-continuously harvested throughout the culture's duration (Goldman, 1979, Rodolfi *et al.*, 2009). A two-stage regime combines the continuous reactor, i.e. photobioreactor, which maintains nutrient-replete cultures with a second stage that takes place in either the same photobioreactor or open ponds. During this second stage, cultures would become nutrient-starved prior to harvest (Huntley & Redalje, 2007).

In terms of maximizing lipid content, the strain of microalgae that was harvested from a continuous reactor would have to have a high lipid fraction while growing under nutrient-replete conditions, or perhaps chronic nutrient stress. However, it has been

previously shown that high lipid content and rapid growth tend to be mutually exclusive, in that slow-growing algae typically having a higher lipid fraction than those that are fast growing (Griffiths & Harrison, 2009, Rodolfi *et al.*, 2009). For example, Shifrin and Chisholm (1980) reported that of 7 strains of microalgae grown under N-replete conditions, the largest lipid fraction (> 40%) was observed in *Monallantus salina,* a green alga that grew at a rate of 1.4 divisions d^{-1}, approximately half that of the next-slowest growing alga.

The advantage of a two-stage regime is that cultures that have a relatively low lipid fraction, yet high growth rate, under N-replete conditions are not necessarily excluded. Instead the focus is placed on the lipid fraction that is accumulated in response to nutrient starvation (Huntley & Redalje, 2007). In this case, a successful algal candidate would be able to produce photosynthetic biomass efficiently while mass cultured, and photosynthesize primarily lipid in response to nutrient starvation.

1.5 Algal Physiology and Lipid Production

Photoautotrophic microalgae utilize light energy to photosynthesize organic compounds, thus allowing for cellular growth and division. Photons are captured by pigments associated with photosystem II and photosystem I and their energy used to drive hydrolysis and electron transport, ultimately producing adenosine triphosphate (ATP) and nicotinamide adenine dinucleotide phosphate (NADPH), during the light reactions (Falkowski & Raven, 2007). These compounds then provide energy and reductant for the Calvin – Benson – Bassham (CBB) cycle (dark reactions) (Falkowski & Raven, 2007). The products of the CBB cycle are referred to here as photosynthate.

Microalgal physiology has a plasticity that allows the allocation of photosynthate between biochemical pools to be variable. During nutrient-replete conditions, allocation can be influenced by factors such as light level (Renaud *et al.*, 1991, Sukenik & Wahnon, 1991, Terry *et al.*, 1983, Brown *et al.*, 1993) and temperature (Utting, 1985, Thompson *et al.*, 1992, Renaud *et al.*, 2002). The responses to environmental stimuli differ between species (Parsons *et al.*, 1961, Moal *et al.*, 1987, Renaud *et al.*, 2002). Renaud *et al.* (1999) reported on the chemical composition of 18 different species of marine microalgae under constant nutrient-replete conditions. There were interspecific differences in the allocation of photosynthate between carbohydrate, lipid, and protein, as a percent of dry weight. For example, the diatom *Chaetoceros* sp. allocated 6.2% of dry weight (DW) toward carbohydrate, 17.0% DW toward lipid, 36.7% DW toward protein, and 21.2% DW was ash. The remaining 18.9% DW was not accounted for. By comparison, *Isochrysis* sp. allocated 15.5% DW toward carbohydrate, 23.4% DW toward lipid, 29.5% DW toward protein, and 13.2% DW was ash. The remaining 18.4% DW was unaccounted for. Observing all species, a general trend was apparent. Under constant nutrient-replete conditions, photosynthate was allocated primarily toward protein, lipid then carbohydrate. Similar to the patterns reported in Renaud *et al.* (1999), Parsons *et al.* (1961) found that the majority of photosynthate was allocated toward protein under nutrient-replete conditions. However, unlike the pattern found by Renaud *et al.* (1999), more photosynthate was allocated toward carbohydrate than lipid.

In general, increases in light level result in an increase in allocation of photosynthate toward energy storage compounds (carbohydrates and lipids), with a corresponding decrease in the allocation toward proteins (Renaud *et al.*, 1991, Thompson

et al., 1993) and light harvesting compounds. An increase in light absorption beyond that which can be utilized efficiently cues the down-regulation of light-harvesting pigments, and a corresponding up-regulation in photosynthate allocated toward the energy storage compounds (Geider *et al.*, 1996). This shift influences cellular lipid composition, as energy storage lipids are non-polar whereas structural lipids are polar (Williams & Laurens, 2010).

The effect of temperature on photosynthate allocation toward lipid is difficult to generalize (Shifrin & Chisholm, 1980, Hu *et al.*, 2008). For example, Thompson *et al.* (1992) reported the cellular lipid quota (pg $cell^{-1}$) for eight species of marine microalgae: three showed an increase in the allocation of photosynthate to lipid in response to increasing temperature (e.g. *Chaetoceros calcitrans*), whereas five showed a decrease (e.g. *C. gracialis*). While the allocation of photosynthate to lipid in response to varying temperature is difficult to generalize, it is thought that the influence of temperature on fatty acid composition can be generalized: lower temperatures correspond to greater number of unsaturated fatty acids whereas higher temperatures correspond to a greater concentration of saturated fatty acids (Hu *et al.*, 2008).

The depletion of ambient nitrogen elicits the strongest changes in photosynthate allocation between biochemical pools. Nitrogenous compounds, such as proteins, can no longer be accumulated so any new photosynthate is allocated toward non-nitrogenous compounds, such as carbohydrate and/or lipid (Shifrin & Chisholm, 1981, Richardson & Cullen, 1995, Larson & Rees, 1996). As with changes in light level, the depletion of nitrogen results in changes in lipid composition. Non-polar lipids, i.e. energy storage

lipids, are primarily synthesized under nitrogen-starved conditions, whereas polar, i.e. structural lipids, are not (Singh & Kumar, 1992, Yu *et al.*, 2009).

Research has shown that there is a difference between species in the allocation of photosynthate between lipid vs. carbohydrate during N-starvation (Thomas *et al.*, 1984a, b, c, Chu *et al.*, 1996). In some cases, species primarily accumulate lipid during N-starvation, e.g. *Monollantus salina* (Shifrin & Chisholm, 1981, Thomas *et al.*, 1984c), whereas others accumulate carbohydrate, e.g. *Dunaliella primolecta* (Thomas *et al.*, 1984b). The accumulation of total energy storage compounds during N-starvation also varies between species. Presuming that increases in the C:N ratio during N-starvation indicate increases in total energy stores, it has been observed that responses vary between species (Larson & Rees, 1996, Utting, 1985).

Figure 1.1, from Geider *et al.* (1996), shows the generalized allocation of photosynthate between the three biochemical pools light harvesting complex (L), biosynthetic apparatus (B), and energy storage (E), as influenced by irradiance, under nutrient replete balanced growth. A decrease in light levels results in greater amounts of carbon being allocated toward the light-harvesting complex, thereby maximizing the capture of photons. At high irradiance, the allocation of carbon toward light-harvesting complexes is down-regulated, while the allocation of carbon toward energy stores is up-regulated (Geider *et al.*, 1996).

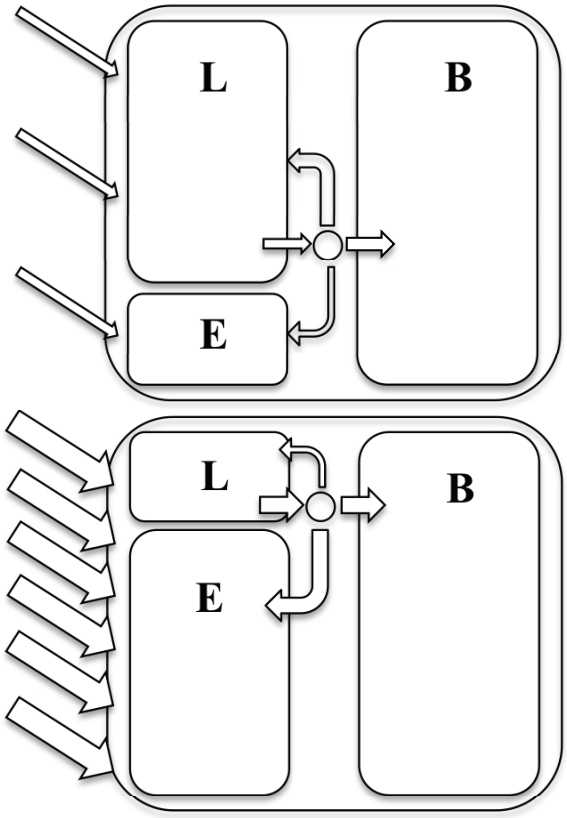

Figure 1.1. Regulation of photosynthate allocation, to three different biochemical pools, in response to growth irradiance, under balanced growth. (Upper) In low light, photosynthate is primarily allocated toward the light harvesting complex (L) and biosynthetic apparatus (B), with the least amount going toward energy reserves (E). (Lower) In high light, more photosynthate goes to E than L. Redrawn Geider *et al*. (1996) with symbols altered for consistency with this thesis.

The opposite occurs under nutrient (e.g. NO_3^-) stress: when NO_3^- is readily available, the carbon allocated toward the light harvesting complexes and the biosynthetic apparatus is up-regulated while carbon going to energy stores is down-regulated. The effects of restricted availability of NO_3^- are in some ways similar to those of high light: an excess of photosynthesis, in relation to nitrogen assimilation, results in up-regulation of carbon allocated to energy stores whereas carbon allocated to light-harvesting complexes and the biosynthetic apparatus is by necessity down-regulated (Geider *et al.*, 1998). When ambient NO_3^- is depleted, the synthesis of light-harvesting complexes and the biosynthetic apparatus is slowed or halted and carbon is allocated toward energy stores.

1.6 Optimizing Lipid Production in the Mass Culture of Microalgae: Goal and Objectives

This research is focused on finding a microalgal strain that produces large quantities of lipid under nutrient starvation, and defining optimum conditions for this production. The key question was: what influences do genotype (i.e. species) and light level have on the accumulation of lipid by microalgae during nutrient starvation? To answer this question, experiments were conducted on four species of microalgae, each grown at two light levels during nutrient replete conditions and subsequent N-starvation. We developed metrics of lipid accumulation during these experiments and analyzed results to identify the best performance and to provide a tool for screening other species of microalgae.

Chapter 2: Materials and Methods

2.1 Phytoplankton Culturing

The diatoms *Chaetoceros muelleri* var. *subsaplsum* Lemmermann (CCMP 1316) and *Thalassiosira pseudonana* (Hustedt) Hasle et Heimdal (CCMP 1335) were obtained from the National Center for Marine Algae and Microbiota (NCMA) and the chlorophytes *Dunaliella salina* and *Tetraselmis* sp., both isolated in Hawaii, were obtained from the University of Hawaii.

Cultures were grown in medium which consisted of natural seawater enriched with modified f/2 nutrients and vitamins (Guillard & Ryther, 1962, Guillard, 1975). Seawater was obtained from Ketch Harbour, NS, Canada, 3 months prior to the start of experiments. Medium was 0.2 μm sterile filtered, using a Whatman PolyCap 75AS Filter Capsule, prior to the addition of culture. To ensure that nitrogen was the only nutrient to become depleted during experiments, nitrate concentrations were reduced to 100 μM from f/2 levels (880 μM) and the cultures were enriched with 200 mg Na_2CO_3 L^{-1} and f/20 trace metal solution (adequate to support growth in cultures with only 100 μM nitrate, J. Cullen and colleagues, unpublished). Cultures were grown in an environmental incubator (MLR-531H, Sanyo, San Diego, CA, USA), equipped with cool-white fluorescent lamps (FL40SS W/37, Mitsubishi/Osram) using neutral density filters and white diffusion filters attached to the inside of the chamber windows to adjust and equalize irradiance within the chamber. Cultures were acclimated to either low light (LL), 175 μmol quanta m^{-2} s^{-1}, or high light (HL), 600 μmol quanta m^{-2} s^{-1} photosynthetically available radiation (PAR) on a 12h:12h light:dark cycle at 30ºC under nitrogen replete (N-replete) conditions. Positions within the incubator were determined prior to

experiments such that irradiance was similar between culture vessels. During experiments, PAR was measured, in each position, using an US-SQLS light sensor (Walz, Effeltrich, Germany), to ensure irradiance had not changed. Based on the position being measured and the culture vessel to be used, the US-SQLS/L sensor was placed in either a tube or flask, with the sensor submerged in NanoPure™ water.

At each light level, non-axenic algal stock cultures of 40 mL volume were maintained for a minimum of 8 generations in 25 mm x 115 mm Pyrex tubes (Fisher Scientific) loosely fitted with polypropylene caps (Nalgene, VWR) to be used as an inoculum source for acclimated (N-replete, R) and perturbation (N-starved, S) experimental cultures. These N-replete and N-starved experimental cultures of 600 mL volume were maintained in loosely capped 650 mL polystyrene flasks (Cellstar, VWR). To obtain the necessary volume required for sampling, a "ramp-up" process was implemented where culture from tubes were diluted with new media, applying the same dilution ratio used on all tubes, until the desired volume was obtained. Three flasks of experimental culture were maintained for each sampling period to accommodate total volume and replication requirements for all measurements. Sampling took place over six non-consecutive days (see details below); the first three were used to assess cultures for the N-replete regime while the latter three were for the N-starvation regime, when changes in chemical composition and physiological status in response to ongoing nutrient stress were assessed (Figure 2.1).

2.2 Growth Measurements

Growth rates of the cultures were monitored following the semi-continuous culture methodology of Brand *et al*. (1981) that allowed for the rapid determination of

acclimated growth rates in multiple cultures of phytoplankton. The principle is that when phytoplankton are acclimated, any measure of phytoplankton biomass increases at a constant rate. Consequently, the Brand *et al.* (1981) methodology relies on measurements of *in vivo* fluorescence, even though fluorescence cannot generally be assumed to be an accurate measure of biomass (Cullen, 1982). Cultures were not dark adapted prior to fluorescence measurements. Instead, prior to measurement, cultures were placed into a light box that had an irradiance matching the culture's growth chamber. *In vivo* fluorescence (F', RFU) was read on both tubes and flasks daily, at algal mid-day, on a Turner Designs 10-AU fluorometer equipped with a fluorescence chamber that allowed the capped tube to be placed directly in fluorometer. All tubes were gently inverted three times before being measured to ensure homogeneity of the culture. In order to measure fluorescence on flask cultures, flasks were gently inverted three times prior to sub-samples being aseptically transferred to a sterile capped tube, which was then measured. The subsample was transferred back to its parent flask aseptically, post-measurements.

Growth rate ($\mu_{F'}$, d^{-1}), nominally over the prior 24 h, was calculated over a discrete period of time (Δt, d):

$$\mu_t = \frac{1}{\Delta t} \cdot \ln\left(\frac{F_t'(1-D)}{F_{t-1}'} \right) \tag{2.1}$$

using *in vivo* fluorescence values, during illumination, from the day prior (F_{t-1}', RFU) and time of sampling (F_t', RFU) corrected for dilution ($D = (mL\ new\ vol.)/(mL\ total\ vol.)$).

Immediately afterwards, the quantum yield of photosystem II (PS II), F_v'/F_m' (dimensionless) (Genty *et al.*, 1989), with no dark acclimation, was measured using a Fluorescence Induction and Relaxation (FIRe) fluorometer (Satlantic, Halifax, N.S.):

$$\frac{F_v'}{F_m'} = \frac{F_m' - F_0'}{F_m'} \tag{2.2}$$

where the maximum (F_m', RFU) and minimum (F_0', RFU) fluorescence values were used to determine F_v'/F_m' (dimensionless), to be used in this case as an indicator of nutrient stress. Tubes were placed in a custom-built black cuvette holder that was connected to the FIRe using a fiber optic probe, with the connection being made 4 cm above the bottom of the tube (i.e. approximately in the middle of the sample). The fiber optic probe was split so it both delivers the excitation beam from the light source and returns the fluorescence signal to the detector. Parameters were derived using single turnover induction data from the FIRe, fit to the relationship of Kolber *et al.* (1998).

The daily dilution ratio for the next day was based on the growth rate over the preceding 24 h, ($\mu_{F'}$, d^{-1}), calculated through re-arrangement of equation. 2.1, so the estimated biomass would remain constant. Cultures were diluted daily, under aseptic conditions, at the end of photoperiod during N-replete growth. After 8 generations under constant conditions, algal cultures were considered acclimated, and used to inoculate flasks for measurements of cellular characteristics under either N-replete or N-starved conditions. As with tubes, the N-replete flasks were diluted at the end of photoperiod the day prior to measurements. The N-starvation regime was initiated by dilutions being stopped 48 h prior to the first measurement, with the expectation being that N-starvation would occur within the 24 h prior to measurements being made. Subsequent measurements took place on the following days (Figure 2.1). Due to the sampling protocol, there were multiple days of semi-continuous dilutions without sampling between samplings for the N-replete (R1 – R3) and N-starvation (S1 – S3) regimes (Figure 2.1). To ensure that neither these non-sampling days nor the change in volume

and culture vessel disrupted balanced growth, dilution-corrected *in vivo* fluorescence measurements were compared between tubes and flasks (Figure 2.2). Matching *in vivo* fluorescence values and trends established that neither had altered the culture's growth (Figure 2.2). As such, it was determined that the non-sampling days could be omitted for interpretation, and the reference point, S0, from which changes due to N-starvation were compared, could be established at R3.

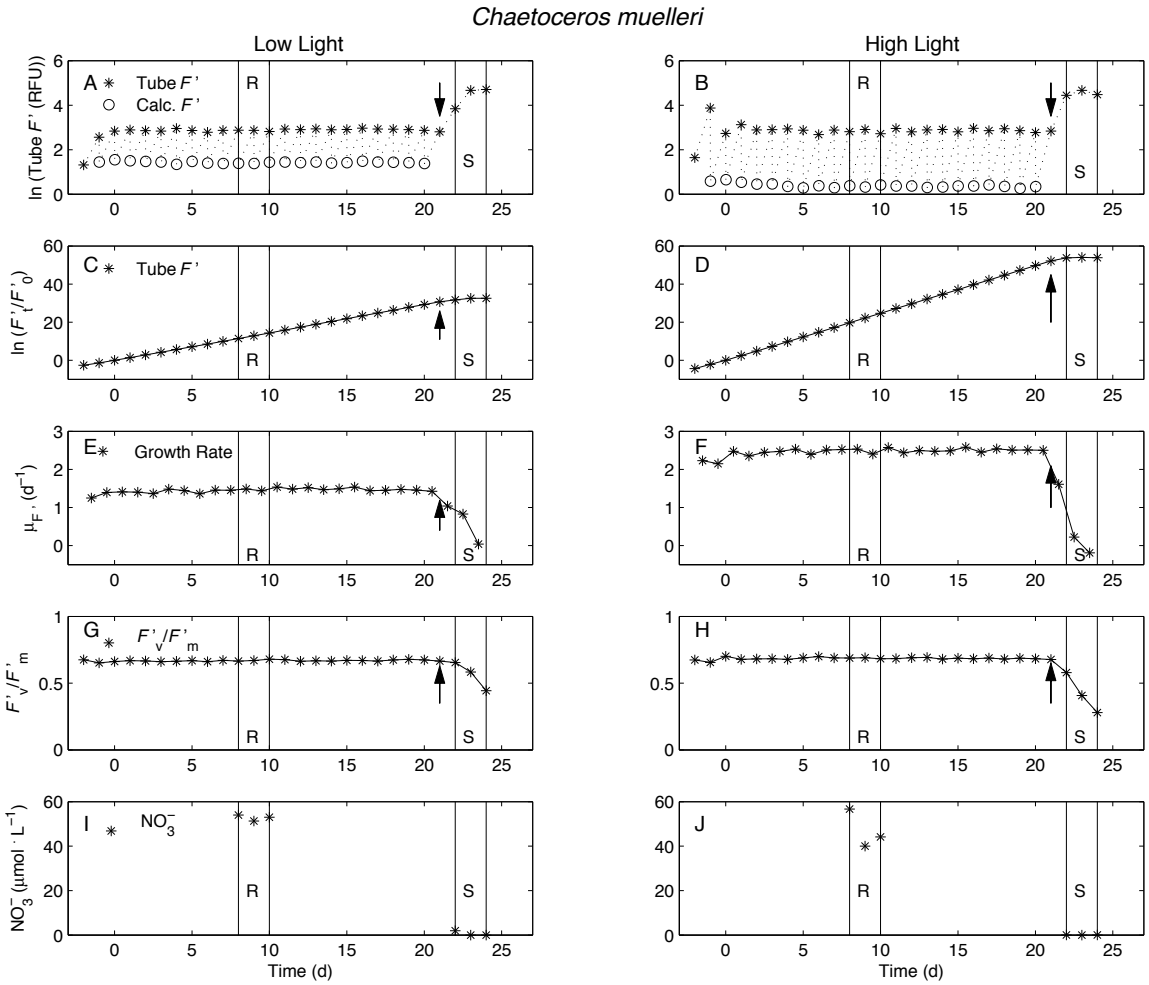

Figure 2.1. Measurements of chlorophyll fluorescence, calculated growth rates and available nitrogen for tube cultures of *Chaetoceros muelleri* grown under low and high light. Cultures were sampled during N-replete (assayed in time period R) and increasingly N-starved (S) conditions that developed after daily dilutions were stopped (arrow). (A, B) Measured *in vivo* fluorescence (log-transformed *F'* in RFU) is shown with stars. Open circles show the calculated value immediately after dilution. (C, D) The log-transform of fluorescence corrected for dilution (F_t'), normalized to its value on day 0 (F_0') shows steady nutrient-replete growth (Brand *et al.*, 1981) that stops after nitrate is depleted. (E, F) Growth rate, $\mu_{F'}$ (d^{-1}), is calculated from dilution-corrected fluorescence (Equation 1.1). (G, H) The quantum yield of Photosystem II activity, F_v'/F_m' (dimensionless), which is used as an indicator of nutrient stress. (I, J) Nitrate concentration (μmol L^{-1}) measured during the R and S assay periods.

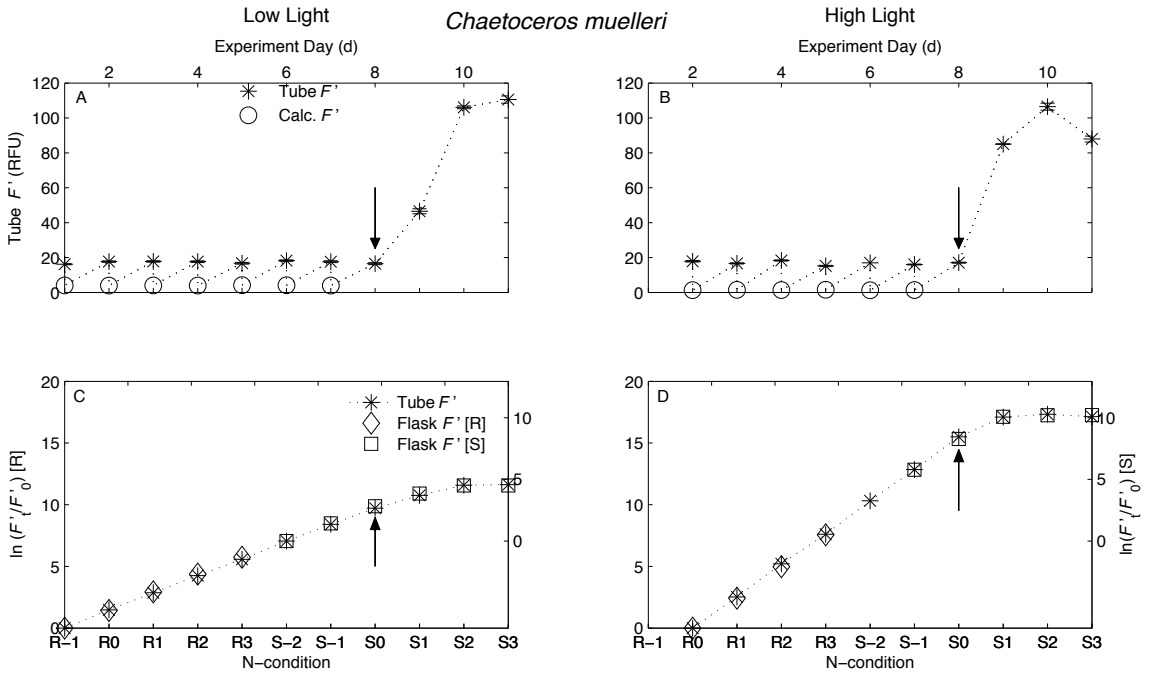

Figure 2.2. Fluorescence measurements made on tube and flask cultures leading up to, and during, the replete and progressively N-starved growth regimes. (A, B) Measurements (*) and calculated values (o) of *in vivo* fluorescence (F' , RFU) made on cultures of *Chaetoceros muelleri* acclimated to low light (left panes) and high light (right panes) and grown in tubes. Calculated values are for the tubes following daily dilution. (C, D) Log-transformed fluorescence values, corrected for dilution (F_t'/F_0' , dimensionless), made on tubes (*), N-replete flasks (◊) and N-starved flasks (□). Flasks were inoculated from tubes and grown in parallel to assess N-replete growth and N-starvation. Arrow indicates the cessation of nutrient resupply by dilution and the onset of nitrogen-starvation. Dilution-corrected fluorescence plots show the matching fluorescence values and trends that existed for tubes and corresponding flasks that existed prior to and during the N-replete and N-starved regimes. Differences between these independent measurements are too small to be detected in these plots.

2.3 Sample processing

2.3.1 Nutrients

Nutrient concentration in the medium (μmol L^{-1}) was determined on duplicate 7 mL samples of 0.7 μm culture filtrate (25 mm GF/F Whatman). Culture filtrate was frozen at -20ºC until analyzed for nitrate, silicate and phosphate, following the method outlined in Tréguer and Lecorre (1975), using an AutoAnalyzer (Bran + Lubbe, Montreal, PQ, Canada).

2.3.2 Chlorophyll a

Triplicate 0.1 mL samples of culture were injected directly into 6 mL of cold 100% methanol (ACS reagent grade) and extracted for a minimum of 24 h at -20ºC, prior to fluorometric analysis (Welschmeyer, 1994) using a 10-005R Turner Designs fluorometer (Turner Designs, San Diego, CA, USA) calibrated with a solution of pure chlorophyll *a* (Sigma-Aldrich) dissolved in 100% methanol.

2.3.3 Particulate Organic Carbon and Particulate Organic Nitrogen

The particulate organic carbon (POC) and particulate organic nitrogen (PON) concentration (mol C L^{-1}, mol N L^{-1}) of the culture were measured in tandem. Triplicate 10 mL samples of culture were gently filtered onto 21 mm glass fiber filters (Grade 691, VWR; 1.5 μm pore size), which had been pre-combusted for 6 h at 450ºC. The same volume of sterile medium was filtered for blanks, and treated identically to the culture samples. Filtration towers were rinsed with 0.22 μm filtered seawater (FSW) immediately afterwards to ensure that residual cells and detrital matter had been rinsed from the towers onto the filter. Nitrate levels of the FSW were unknown, however as water was collected after the spring bloom it was presumed that nitrate levels were minimal. Filters

were placed on pieces of pre-combusted aluminium foil, dried for 12 h at 60ºC, folded inside the aluminium foil and stored in a Petri dish within a vacuum-sealed desiccator until analysis. Samples were analyzed using an elemental combustion system (ECS, Costech, Valencia, CA, USA), following the manufacturers recommended protocol, with acetanilide as a standard.

2.3.4 Intracellular Carbohydrate

Triplicate samples of 5 – 10 mL were filtered under gentle vacuum (10 mmHg) onto 21 mm filters (Grade 691, VWR; 1.5 µm pore size) that had been pre-combusted for 6 h at 450ºC. The blanks consisted of the same volume of sterile-filtered medium, and were treated identically to the culture samples. Filters were placed on pieces of pre-combusted aluminium foil, placed in a Petri dish and frozen at -80ºC until analysis. Samples were analyzed as described below following the phenol/sulfuric acid method outlined in Dubois *et al*. (1956), as modified by Sun *et al*. (1984), using laminarin as a standard. However, units expressed here will be g carbohydrate (*Carb*), or mol C_{Carb}, for clarity. No significant difference was found between D-glucose and Laminarin when used with the phenol-sulfuric acid method (data not shown), unlike with other standards (Mecozzi, 2005).

Filters were brought to room temperature and placed into 13 mm x 100 mm borosilicate glass tubes (VWR) to which 400 µL NanoPure water was added, while other tubes contained a dilution series of Laminarin standard (400 µL total) for the standard curve. Standard curves were prepared on each day of analysis. 500 µL of 5% (w/v) phenol was added to all tubes, which were vortex-mixed for 5 – 10 s, followed by the rapid addition of 2 mL of ACS reagent grade 95% sulfuric acid and vortex-mixed again

for 5 – 10 s. Capped tubes were immediately placed into a 95°C water bath for 30 min, vortexed for 5 – 10 s and placed back into the water bath for another 30 min. The reaction mixture was then poured into micro-centrifuge tubes and centrifuged at 3341 g for 10 min. Supernatant was decanted into disposable ultra-microcuvettes (15 mm window, BrandTech, Fisher) and optical density (dimensionless) between 460 – 510 nm read on a dual-beam spectrophotometer (Cary 4000, Varian, Agilent, Mississauga, ON), using NanoPure™ in the reference cuvette. Concentration was calculated from optical density at the wavelength of maximum absorption between 480 – 490 nm, using the Laminarin dilution series for the standard curve.

2.3.5 Gravimetric Lipids

Total lipid includes structural (polar) lipids and neutral lipids that serve for energy storage (Williams & Laurens, 2010). The total lipid concentration of a culture was determined using gravimetric measurements in which single, 450 mL, samples of culture were filtered onto 47 mm glass fiber filters (Grade 691, VWR; 1.5 μm pore size) that had been pre-combusted for 6 h at 450ºC. Triplicate 350 mL FSW blanks were processed concurrently during each sampling day. Due to FSW volume concerns, a smaller volume was used to filter for blanks than the volume of culture filtered for samples. All filters were rinsed with three 30 mL aliquots of 0.5 M ammonium formate, 90 mL total, each rinse being allowed to soak the filter for 30 s. Ammonium formate was used to remove soluble salts that could have interfered with analysis if left on the filter (Conover, 1966). As an additional diagnostic, triplicate unused pre-combusted filters were analyzed for each day's sampling. Filters were placed on pre-combusted pieces of aluminum foil, folded and frozen at -80ºC until analysis. Lipid extraction was based on the method

established by Bligh and Dyer (1959). Briefly, samples were freeze-dried for 24 h at -40ºC, and the lipid fraction extracted on an ASE 350 solvent extraction system (Dionex, Sunnyvale, CA, USA), using a solution of HPLC grade chloroform and HPLC grade methanol (1:1.85 v/v). The extracted samples were contained in pre-weighed glass vials, and evaporated to dryness for approximately 2h (Genevac EZ-2 Plus Personal Evaporator, Gardiner, NY, USA). The gravimetric lipid concentration (mg L^{-1}) was determined by re-weighing (Sartorius SemiMicro Balance ME235P-SD, 1.0 µg precision, Sartorius, Bohemia, NY, USA) the vials post-evaporation and subtracting the tared weight of the vial from its post-evaporation weight. Sample and FSW blank weights were corrected for diagnostic error by subtracting the averaged values of diagnostic blanks (n = 3). Subsequently, a final lipid weight was determined by subtracting the averaged diagnostic blank corrected FSW blank weight (n=3) from the diagnostic blank corrected sample weight. The method depends on accurate weighing and minimal contamination as the tare weight of the vials averaged about 25 g and lipid weights were often well under 5 mg.

2.3.6 Nile Red Lipids

A secondary, qualitative, method was used to estimate total lipid concentration. Culture samples were stained with the fluorochrome Nile Red (Sigma-Aldrich) following methodology outlined in Elsey *et al.* (2007) and Chen *et al.* (2009). Single 2 mL aliquots of culture were taken from individual flasks and placed into internally threaded cryovials (2.0 mL, Fisher). Corresponding blanks for each treatment were prepared by combining 2 mL of culture from each of the three flasks for each treatment and gently filtering through a 25 mm Whatmann GF/F filter (0.7 µm pore size) in a syringe mount. 2 mL of this filtrate was placed in a cryovial for analysis. A secondary blank was prepared by

pipetting 2 mL of sterile medium into a cryovial. The culture filtrate blank was used to account for any fluorescence that may have been a result of the Nile Red fluorochrome bonding to excreted organic matter. The sterile medium blank accounted for any fluorescence that occurred if the fluorochrome bound to medium components.

Triplicate 300 µL sub-samples of unstained culture from each cryovial were pipetted into the wells of a 96-well plate, and 1 µL acetone was added to each. Then, 3 µL of Nile Red (Sigma-Aldrich) solution (1:1 w/v, diluted in HPLC grade acetone) was added to each cryovial and vortex-mixed for 5 s. Triplicate 300 µL sub-samples of stained culture were pipetted onto the plate and fluorescence (RFU) was read using a Synergy 4 (BioTek, Winooski, VT, USA) plate reader, following Chen *et al*. (2009). The peak value and value taken 30 min. after the start of the assay were used in the data analysis.

As part of an exploratory study, the concentrated lipid emulsion Chemically Defined Lipid Concentrate (CDLC, Invitrogen, Burlington, ON, Canada) was tested as a standard. However, the method was found to be unsuitable for quantitative analysis in our study because under the same conditions and CDLC concentrations, replicable dilution series could not be obtained under the same operational conditions and CDLC concentrations. Instead, following each run, the lipid fluorescence values were normalized to the fluorescence signal of a standard plate supplied by BioTek. The normalized lipid fluorescence values were then used as a qualitative indicator of lipid concentration, used in the evaluation of apparent outliers in gravimetric lipid measurements.

2.3.7 Photosynthetic Rate via Photosynthesis vs. Irradiance Curves

Photosynthetic production of particulate and dissolved organic carbon was measured as a function of irradiance in parallel studies and results were used here to estimate the possible production of extracellular polysaccharides unaccounted for in this thesis. Photosynthesis as a function of irradiance was measured following the method of Lewis and Smith (1983) as outlined in Richardson *et al*. (1996) and fit to the equation described by Platt *et al.* (1980):

$$P^B = P_s^B \left(1 - e^{-\alpha I / P_s^B}\right)\left(e^{\left(-\beta I / P_s^B\right)}\right) \tag{2.3}$$

where P^B is the photosynthetic rate, normalized to chlorophyll (g C · [g Chl *a*]$^{-1}$ · [h]$^{-1}$), P_s^B is the maximum photosynthetic rate in the absence of photoinhibition (g C · [g Chl *a*]$^{-1}$ · [h]$^{-1}$), I is the irradiance (µmol quanta m^{-2} s^{-1}), α is the initial slope of the *P-I* curve (g C · [g Chl *a*]$^{-1}$ · [h]$^{-1}$ (µmol quanta m^{-2} s^{-1})$^{-1}$) and β is the parameter describing the reduction in the photosynthetic rate at high irradiance (g C · [g Chl *a*]$^{-1}$ · [h]$^{-1}$ · [µmol quanta m^{-2} s^{-1}]$^{-1}$).

2.3.8 Extracellular Polysaccharide

Attempts to directly measure the production of extracellular polysaccharides were made during these experiments. Triplicate 50 mL samples of culture filtrate (25 mm Whatman GF/F) were frozen at -20ºC until analyzed using the phenol/sulfuric acid method (Dubois *et al.*, 1956), as modified by Sun *et al.* (1984), with further modifications made to reagent volumes that would allow for filtrate to be analyzed, instead of particulate matter. Results were inconsistent, possibly due to ionic interference with the chemical reaction (Panagiotopoulos & Sempere, 2005). Development of a new method was beyond the scope of this thesis.

2.4 Equations

Because this thesis is focused on the allocation of carbon between carbohydrate and total lipid, conversion factors from Geider and La Roche (2002) were applied to account for the carbon content of each compound. All chemical compounds, measured and calculated, were normalized to particulate organic nitrogen, to account for differences in biomass between the treatments and to focus on changes in energy storage compounds during N-starvation.

2.4.1 Carbon Content of Carbohydrate and Lipid

Particulate organic carbon in phytoplankton (g L^{-1}) was partitioned into the contributions from lipid (C_{lipid}), based on total gravimetric lipid (TLG, g L^{-1}), and carbohydrate (C_{carb}) using conversions (g C · [g DW]$^{-1}$) from Geider and LaRoche (2002): $C_{lipid} = TLG \cdot 0.76$ g C · [g DW_{lipid}]$^{-1}$; $C_{carb} = Carb \cdot 0.40$ g C · [g DW_{carb}]$^{-1}$.

2.4.2 Particulate Organic Nitrogen Normalization

The carbon concentration of carbohydrate (mol C_{Carb} · L^{-1}) and gravimetric total lipid (mol C_{TLG} · L^{-1}), were normalized to the corresponding PON (mol N L^{-1}), to remove biases similar to those described above:

$$\psi_i = \frac{mol\ C_i\ L^{-1}}{mol\ N\ L^{-1}} \tag{2.4}$$

where the PON-normalized carbon concentration (ψ_i, mol C_i · [mol N]$^{-1}$) is calculated from the carbon (mol C_i L^{-1}), of the individual compounds (i), and PON (mol N L^{-1}) concentrations.

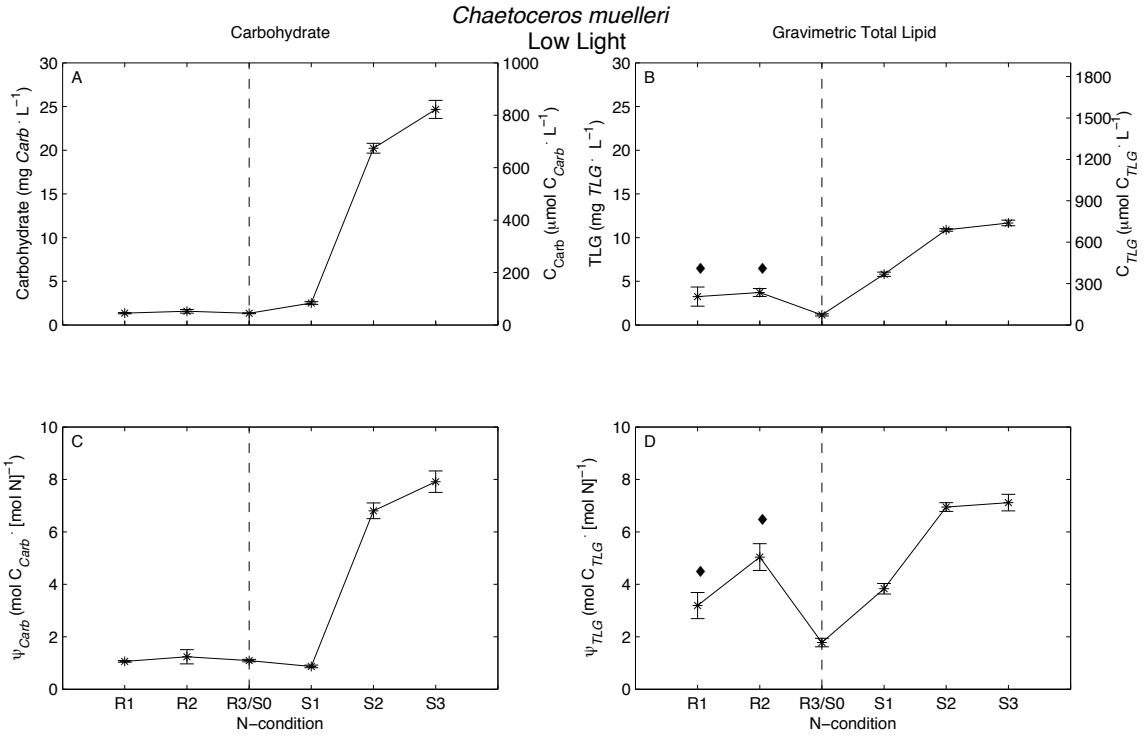

Figure 2.3. Measurements of carbohydrate (left panes) and gravimetric total lipid (right panes) during N-replete (R1 – R3) and N-starved (S0 – S3) regimes for the diatom *Chaetoceros muelleri* low light treatment. (A, B) Carbohydrate and gravimetric total lipid (left axes) were used to calculate the carbon content of carbohydrate and gravimetric total lipid (right axes) using conversion factors from Geider and LaRoche (2002), as explained in Section 2.4.1. (C, D) Carbon content for both chemical compounds were then normalized to the corresponding particulate organic nitrogen concentration, as explained in Section 2.4.2. Error bars indicate standard error of triplicate measurements, except where they indicate the range of duplicates (♦, n = 2). Dashed line represents the final N-replete data point, after which NO_3^- is depleted (< 10 µmol NO_3^- L^{-1}) and further measurements are made under N-starved conditions.

Chapter 3: Results

3.1 General Trends in Chemical Composition and Physiological Status

The change in carbon allocation toward non-nitrogenous compounds associated with energy storage, i.e. carbohydrate and total lipid, in response to a nitrogen-starvation regime was examined using microalgal cultures. To establish appropriate baselines from which changes in physiological status and chemical composition could be determined, four microalgal species, *Chaetoceros muelleri, Dunaliella salina, Thalassiosira pseudonana* and *Tetraselmis* sp., were acclimated to both low light (LL) and high light (HL), under nutrient-replete conditions. For each of these eight treatments, measurements of chemical composition and physiological status were taken during growth in N-replete and N-starvation regimes.

All treatments showed similar changes during the transition from N-replete growth to N-starvation; however the magnitude and timing of the responses varied between species and treatments. Results from one treatment (LL, *Chaetoceros muelleri*) are presented here to illustrate a typical result and to reveal analytical errors that arose during the study. A comparison of the eight treatments follows, utilizing some metrics that are described in this section.

Nutrient-replete growth – Daily dilutions of the treatments were designed to ensure balanced growth, during which all biomass measures would increase at the same rate, and physiological status measurements would be constant, day-to-day (Brand *et al.*, 1981, MacIntyre & Cullen, 2005). During the N-replete regime (R1 – R3, Figure 3.1) expectations for balanced, N-replete growth were mostly fulfilled. Growth rate, calculated from *in vivo* fluorescence, was steady (CV = 0.02, n = 9) throughout the N-

replete regime (Figure 3.1 A). F_v'/F_m' (dimensionless), a measure of physiological status, was high and also nearly constant (CV = 0.02, n = 9) throughout the N-replete regime, consistent with results for N-replete cultures in balanced growth (Eppley & Renger, 1974) (Figure 3.1 B). Measurements of available NO_3^- confirmed that NO_3^- was not depleted during the N-replete regime (Figure 3.1 C). Combined with the corresponding measurements of PON (Figure 3.1 D), the initial 100 μmol N L^{-1} in the growth medium was accounted for (Dortch *et al.*, 1984), as expected. However, mass balance was not observed in all cultures (see Appendix A.5). The imbalance was most obvious with cultures that stuck to the vessels walls, e.g. *Tetraselmis* sp.. The POC:PON ratio (ψ_{POC}, mol C · [mol N]$^{-1}$, Figure 3.1 E) of the algae was steady and close to the Redfield Ratio of 6.625 mol C · [mol N]$^{-1}$ (Redfield, 1958). The chl *a*:PON ratio (g chl *a* · [mol N]$^{-1}$, Figure 3.1 F) and the ratio of carbohydrate C to PON (ψ_{Carb}, mol C_{Carb} · [mol N]$^{-1}$, Figure 3.1 G) were likewise nearly constant, consistent with balanced growth.

Gravimetric measurements of total lipid were an exception. The ratio of gravimetrically-determined total lipid carbon to PON (ψ_{TLG}, mol C_{TLG} · [mol N]$^{-1}$, Figure 3.1 H) varied 3-fold during the N-replete regime. This anomalous variation is best explained by significant analytical error in the gravimetric determination of total lipid due to the relatively low biomass concentrations and lipid content observed during N-replete growth in these experiments (see section 3.2.2).

The results from the LL treatment of *C. muelleri* indicate that the growth rate, physiological status and chemical composition of the microalga acclimated to N-replete conditions can be characterized by measurements made on R3, and that these measurements can be used as a baseline (S0, the start of the N-starvation regime) to

describe responses to N-starvation. Gravimetric measurements of total lipid concentration are an exception, and an alternate estimation of lipid accumulation in response to N-starvation must be utilized instead (see section 3.2.2).

Response to nitrogen starvation – During the N-starvation regime (S0 – S3, Figure 3.1), changes in chemical composition and physiological status were observed. These changes began with the depletion of NO_3^- with concurrent accumulation of PON (Figure 3.1 C, D), which increased more than two-fold from S0 to S1. During this time, chemical composition (Figure 3.1 E – H) and physiological status (Figure 3.1 B) changed little, as the stress of N-depletion was just beginning. Changes in carbon allocation became apparent on S2, the second day of the N-starvation regime, but the first with depleted NO_3^-. At this point ψ_{POC} increased (Figure 3.1 E) as carbon was allocated toward non-nitrogenous compounds (Figure 3.1 G, H). There were minimal changes in chl *a*:PON during the experiment (Figure 3.1 F), indicating that there was neither net synthesis nor preferential degradation of chlorophyll when the cells entered N-starvation (Morris, 1981, Richardson & Cullen, 1995).

The largest increases for ψ_{POC}, ψ_{Carb} and ψ_{TLG} were noted on S2, followed by a relatively small increase on S3. Relative to the S0 baseline (ψ_{POC} = 6.57 ± 0.13, mean±SE, mol C · [mol N]$^{-1}$), the overall increase in ψ_{POC} was 11.38 ± 0.68 (mean±SE) mol C · [mol N]$^{-1}$ (Figure 3.1 E), ψ_{Carb} was 6.82 ± 0.41 (mean±SE) mol C_{Carb} · [mol N]$^{-1}$ (Figure 3.1 G) and ψ_{TLG} was 5.33 ± 0.35 (mean±SE) mol C_{TLG} · [mol N]$^{-1}$ (Figure 3.1 H). Parameterization for each compound in terms of mol C_i · [mol N]$^{-1}$, allows for direct comparison of carbon allocation during the N-starvation regime: if particulate carbon is assumed to be allocated only toward carbohydrate and total lipid during the N-starvation

regime, the relative change in ψ_{POC}, for any given day should be equivalent to the summation of change in ψ_{Carb} and ψ_{TLG} (see section 3.2.2). In this example, the change in ψ_{Carb} and ψ_{TLG} was 12.15 mol C · [mol N]$^{-1}$, corresponding to 107% of the change in ψ_{POC}, with 56% of that change attributed to carbohydrate and 44% to lipid.

Growth rates calculated from fluorescence ($\mu_{F'}$, d^{-1}) using the Brand *et al*. (1981) methodology are not accurate during nutrient-starvation because the underlying assumptions of constant chl *a* quotas and quantum yields of fluorescence do not hold. However the decline of $\mu_{F'}$ can be used qualitatively to show responses to N-depletion, here beginning on day S2 when nitrate was depleted (Figure 3.1 B). In addition to this, decreasing values of F_v'/F_m' (dimensionless) for cultures in unbalanced growth can be used as indicators of nutrient stress (Parkhill *et al.*, 2001, Suggett *et al.*, 2009, Hockin *et al.*, 2012), which was not evident for this treatment until the day following NO_3^- depletion (Figure 3.1 B). With ongoing N-starvation, observed trends of both $\mu_{F'}$ and F_v'/F_m' matched expectations for N-starvation (Berges & Falkowski, 1998, Parkhill *et al.*, 2001). On S3, fluorescence had stopped increasing, consistent with no more accumulation of biomass (Figure 3.1A), whereas F_v'/F_m' had not stopped decreasing as stressful conditions continued (Figure 3.1 B).

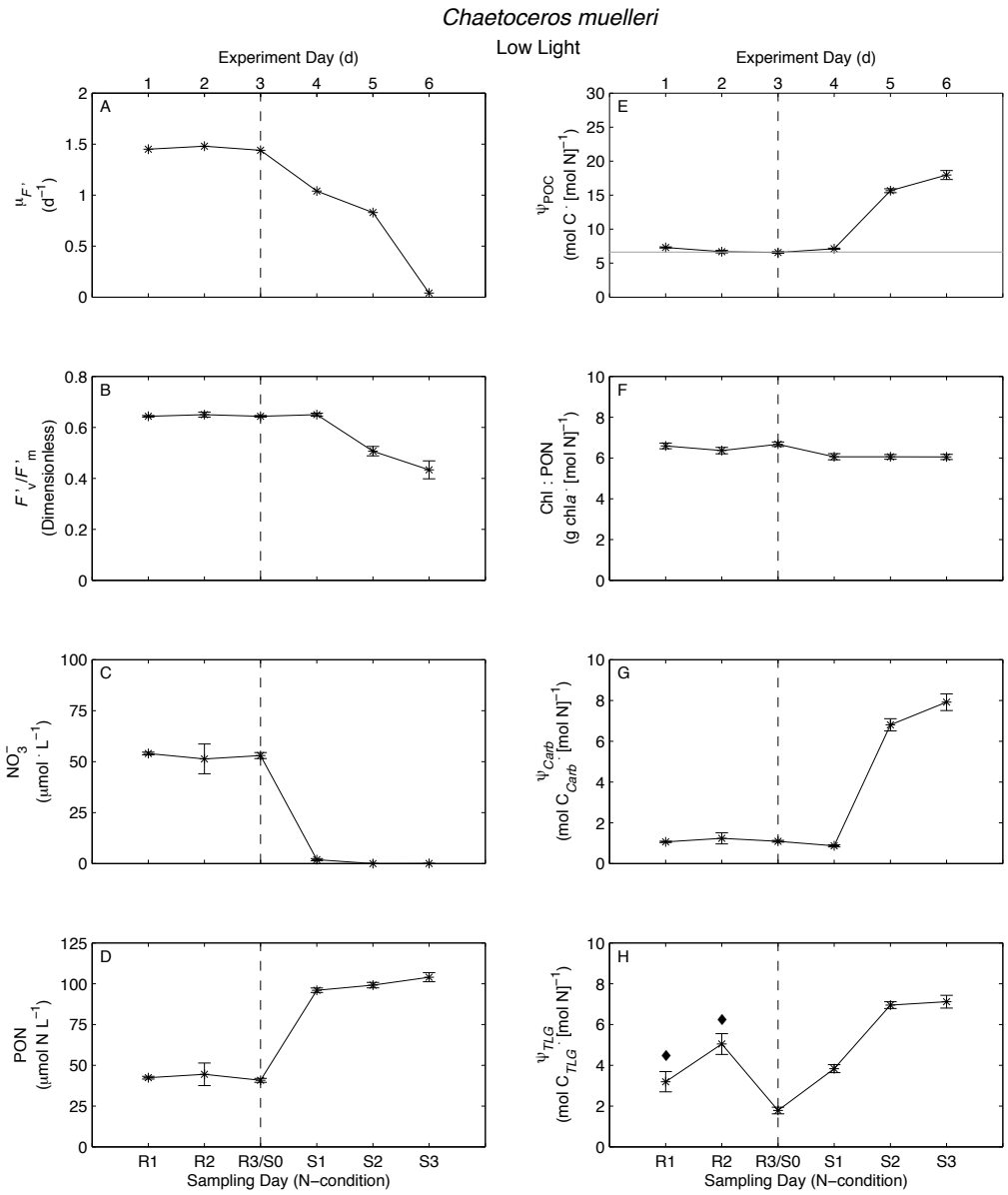

Figure 3.1. Changes in the chemical composition and physiological status of the diatom *Chaetoceros muelleri* acclimated to low light (175 µmol quanta m^{-2} s^{-1}), during periods of nutrient replete growth (R1 – R3) and a regime of nutrient starvation (S0 – S3). (A) Growth rate estimated from fluorescence ($\mu_{F'}$, d^{-1}), (B) Photochemical efficiency (F_v'/F_m' dimensionless), (C) Nitrate concentration (NO_3^-, µmol N L^{-1}), (D) Particulate N (PON, µmol N L^{-1}), (E) Particulate C, normalized to PON (ψ_{POC}, mol C · [mol N]$^{-1}$), (F) Chlorophyll *a,* normalized to PON (g chl *a* · [mol N]$^{-1}$), (G) Carbohydrate-carbon normalized to PON (ψ_{Carb}, mol C_{Carb} · [mol N]$^{-1}$) and (H) Carbon in gravimetrically determined lipid normalized to PON (ψ_{TLG}, mol C_{TLG} · [mol N]$^{-1}$). Error bars indicate standard error (n = 3) or range (♦,n = 2) for independent cultures. Vertical dashed lines represent the beginning of the N-starvation regime i.e., one day after the final dilution after which NO_3^- will begin to run out. Horizontal bar in E represents the Redfield Ratio of ψ_{POC} = 6.625 mol C · [mol N]$^{-1}$ (Redfield, 1958).

3.2 Metrics of Carbon Allocation

To determine how carbon allocation was related to species, irradiance and N-starvation, metrics were developed to describe these changes. The first metric describes the relative change in chemical composition with ongoing N-starvation; the second replaces gravimetric total lipid, allowing for a more accurate total lipid estimate; the third describes the proportional allocation of carbon between carbohydrate and total lipid; and the fourth shows the rate of carbon allocation towards non-nitrogenous compounds during N-starvation.

3.2.1 Relative Change in Carbon During N-starvation

During the N-starvation regime, the relative change in a compound's carbon content normalized to PON can be expressed as:

$$\Delta\psi_i St = \psi_i St - \psi_i S0 \tag{3.1}$$

where the change in carbon content normalized to PON (ψ_i, mol C_i · [mol N]$^{-1}$), for a given compound (i) on day St, during the N-starvation regime (t = 1, 2, or 3), is the difference between that day's concentration ($\psi_i St$, mol C_i · [mol N]$^{-1}$) and the N-replete baseline ($\psi_i R3/S0$, mol C_i · [mol N]$^{-1}$). For illustration, the increase of POC during the N-starvation regime in Figure 3.1 E is expressed as $\Delta\psi_{POC}$ in Figure 3.2 A. In some treatments, for example the low-light treatment of *Chaetoceros muelleri* (Figure 3.2 A), there was a delayed response in the carbon being allocated toward non-nitrogenous compounds. This resulted with $\Delta\psi_{POC}$ showing minimal increase in response to initial N-starvation regime, as carbon was still being allocated toward nitrogenous compounds as residual N was being taken up.

3.2.2 Inferred Total Lipid

N-replete measurements of ψ_{TLG} expressed a variability that was unexpected, because chemical composition, in addition to physiological status measurements, should have been consistent from day to day under balanced growth (Eppley & Renger, 1974, Brand *et al.*, 1981). Lipid content close to, or lower than, the limit of quantification (+10 SE of blanks, see Appendix A.4) was likely responsible for the significant variability observed for several of the N-replete cultures. Due to this uncertainty in the N-replete measurements, the N-starved measurements are questionable, particularly in reference to the R3/S0 value. Additionally, during the N-starvation regime, changes in *TLG* were inconsistent with those of POC and *Carb*, assuming that changes in ψ_{POC} were due to changes in ψ_{Carb} and ψ_{TLG}:

$$\Delta\widehat{\psi}_{POC} = \Delta\psi_{Carb} + \Delta\psi_{TLG} \tag{3.2}$$

where $\Delta\widehat{\psi}_{POC}$, mol C · [mol N]$^{-1}$, is the calculated change in POC:PON during N-starvation, assuming that it is attributed entirely to changes in measured *Carb* and *TLG*. In the data shown in Figure 3.2, the assumption behind equation 3.2 was violated as the calculated change in POC, $\Delta\widehat{\psi}_{POC}$, was higher on days S1 – S3 than the observed $\Delta\psi_{POC}$; for example, on S1 $\Delta\widehat{\psi}_{POC}$ was 300% greater than $\Delta\psi_{POC}$. When the calculated changes are compared to measurements, the extent that $\Delta\widehat{\psi}_{POC}$ deviated from $\Delta\psi_{POC}$ becomes apparent (Figure 3.3A). Considering only the change in carbohydrate-carbon ($\Delta\psi_{Carb}$, Figure 3.3 B) as it corresponds to $\Delta\psi_{POC}$, the majority of data were within realistic limits, i.e. less than $\Delta\psi_{POC}$. This further suggested that gravimetric total lipid measurements contained errors that could not be accounted for.

In an attempt to assess the relative allocation of carbon to lipid during N-starvation, the variable "inferred total lipid", $\Delta\psi_{TLI}$ (mol C_{TLI} · [mol N]$^{-1}$) was estimated as the difference between POC and carbohydrates (Figure 3.2 E):

$$\Delta\psi_{TLI}St = \Delta\psi_{POC}St - \Delta\psi_{Carb}St \tag{3.3}$$

where the change in inferred total lipid carbon ($\Delta\psi_{TLI}$) for a given N-starved day (St) was the difference between the increase in POC ($\Delta\psi_{POC}$) and increase in carbohydrate-carbon ($\Delta\psi_{Carb}$) for the same day. The estimate is based on the implicit assumption that changes in POC were due solely to increases in the net synthesis of energy stores, in this case carbohydrates and total lipids.

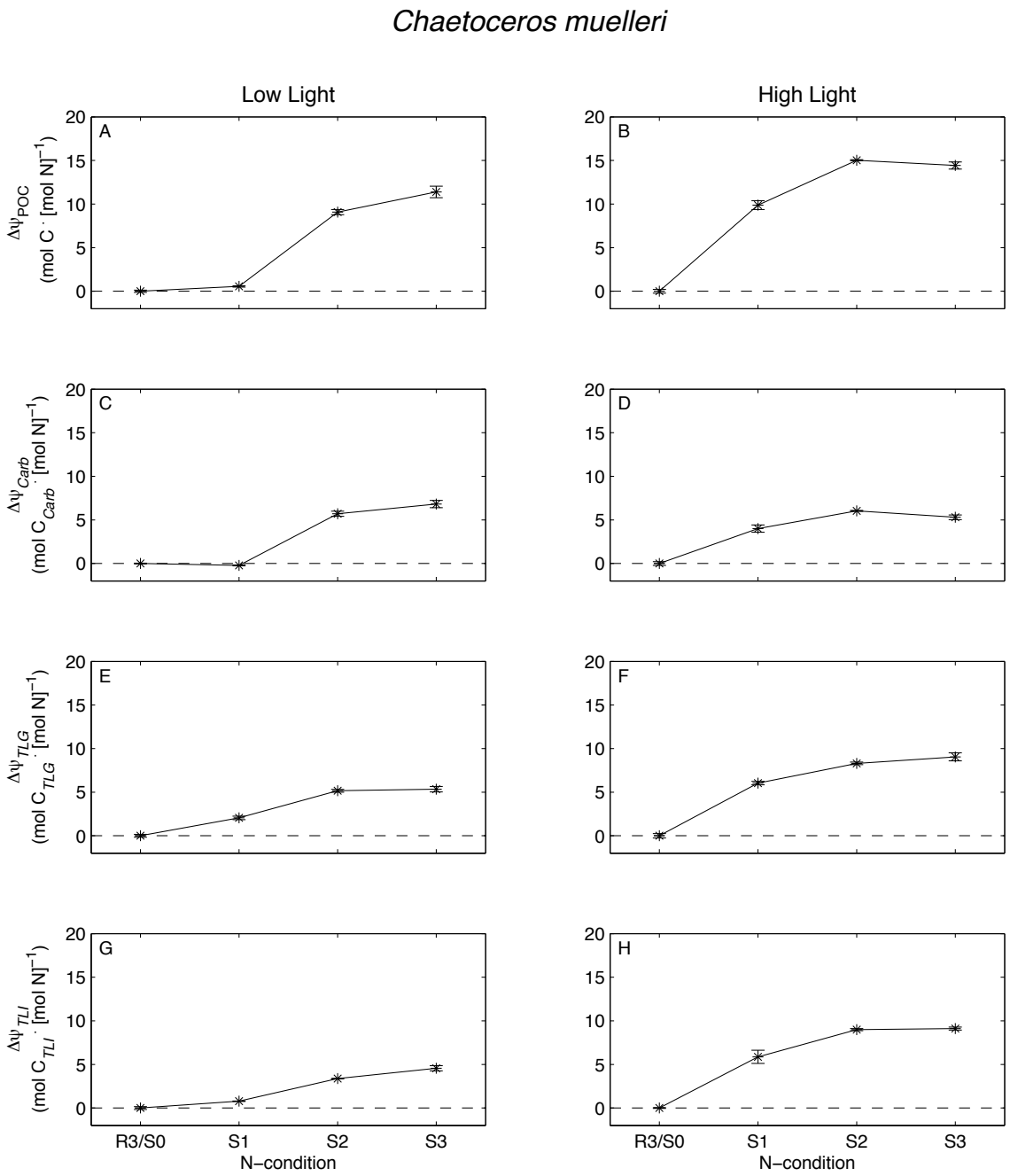

Figure 3.2. The relative change in PON-normalized carbon, during the N-starvation regime, $\Delta\psi_i$ (mol C_i · [mol N]$^{-1}$), for the compounds (*i*) of (A, B) particulate organic carbon, $\Delta\psi_{POC}$, (C, D), carbohydrate, $\Delta\psi_{Carb}$, (E, F), gravimetric total lipid, $\Delta\psi_{TLG}$ and (G, H) inferred total lipid, $\Delta\psi_{TLI}$, during the N-starvation regime, for the low light (175 µmol quanta m^{-2} s^{-1}, left panes) and high light (600 µmol quanta m^{-2} s^{-1}, right panes) treatments of the diatom *Chaetoceros muelleri*. The dashed horizontal line demarks R3/S0, the baseline against which $\Delta\psi_i$ is expressed. Error bars indicate the standard error (n = 3) of the measurement, for independent cultures. The LL cultures are the same as what was shown in Figure 3.1.

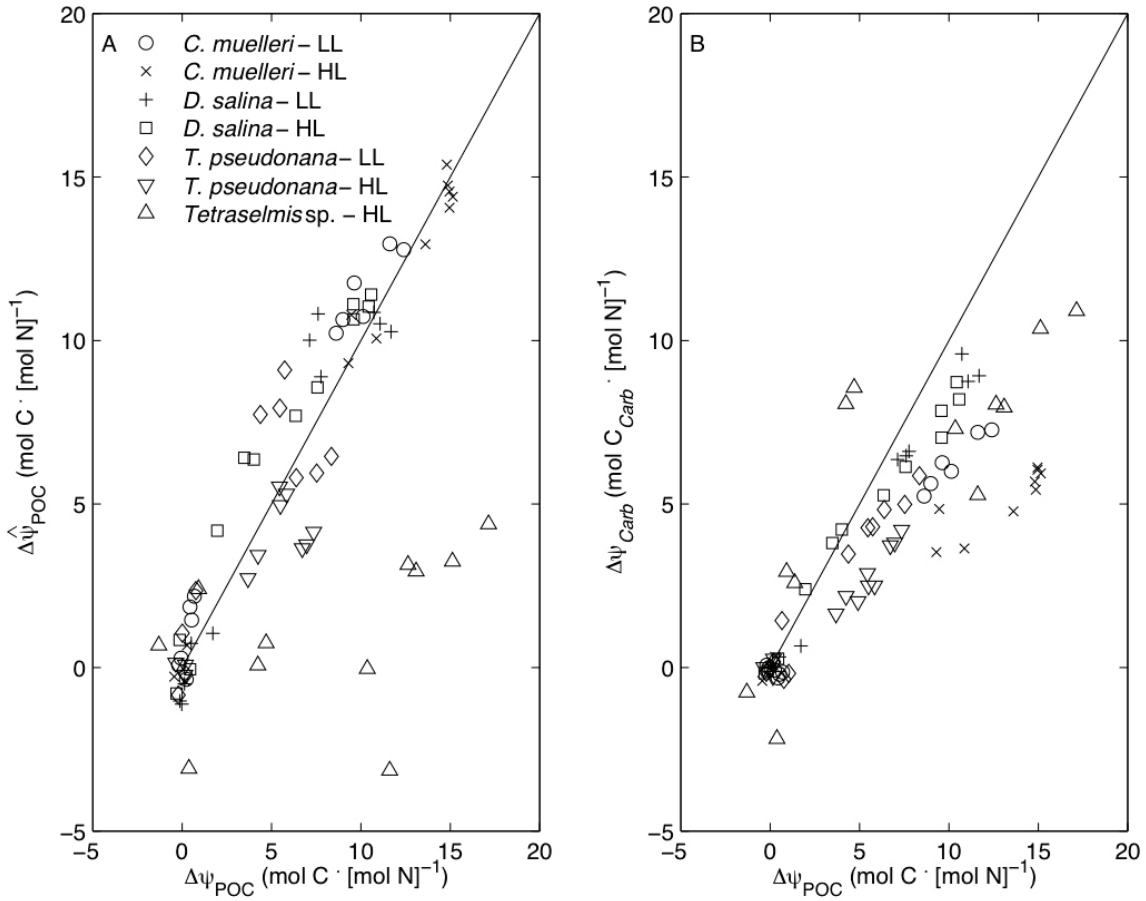

Figure 3.3. (A) The calculated change in total carbon during the N-starvation regime, assuming all C is accumulated as *Carb* + *TLG* ($\Delta\widehat{\psi}_{POC}$, mol C · [mol N]$^{-1}$) , and (B) change in carbohydrate-carbon during the N-starvation regime ($\Delta\psi_{Carb}$) as related to the measured change in POC ($\Delta\psi_{POC}$, mol C · [mol N]$^{-1}$), for 4 species of microalgae, 3 of which were grown under two light treatments, and 1 *Tetraselmis* sp. only grown at HL. The solid line indicates the theoretical maximum change if the measurement of $\Delta\psi_{POC}$ is accurate (see Section 3.2.2).

3.2.3 Proportion of Energy Storage Carbon Allocated Toward Lipid or Carbohydrate

The third metric describes the proportion of carbon allocated to each of the two non-nitrogenous compounds during the N-starvation regime. The linear slope (Γ_i, mol C_i · [mol C]$^{-1}$, *i* = *Carb* or *TLG*) was calculated in a regression of ψ_{Carb} and ψ_{TLG} against POC, ψ_{POC} for sampling days R3/S0 through S3. The slopes Γ_{Carb} (mol C_{Carb} · [mol C]$^{-1}$) and Γ_{TLG} (mol C_{TLG} · [mol C]$^{-1}$) represents the proportion of carbon being allocated toward each non-nitrogenous compound (Figure 3.4 A – D). Due to the issues associated with *TLG*, a slope for *TLI* was also calculated, simply as 1 - Γ_{Carb}, the difference between the accumulation of POC and *Carb.* Because they differ only in their intercepts, a linear regression performed on ψ_i vs. ψ_{POC} yields the same slopes as $\Delta\psi_i$ vs. $\Delta\psi_{POC}$. While the example provided in Figure 3.4 is described for ψ_i vs. ψ_{POC}, further results will be discussed as $\Delta\psi_i$ vs. $\Delta\psi_{POC}$. This will allow for $\Delta\psi_{TLI}$ to be shown.

3.3.4 Rate of Increase of Carbon During the Nitrogen Starvation Regime

The fourth metric represents the rate of carbon allocation towards non-nitrogenous compounds. The linear slope (ζ_{POC}, mol C · [mol N]$^{-1}$ · d^{-1}) was calculated for the increase ψ_{POC} (mol C · [mol N]$^{-1}$) for the duration of the N-starvation regime (*t*, d) (Figure 3.4 E – F).

As with Γ_i, ζ_{POC} results are the same whether ψ_{POC} or $\Delta\psi_{POC}$ values are regressed against time. Again, the example provided in Figure 3.4 is described for ψ_{POC}, with further results being described as $\Delta\psi_{POC}$.

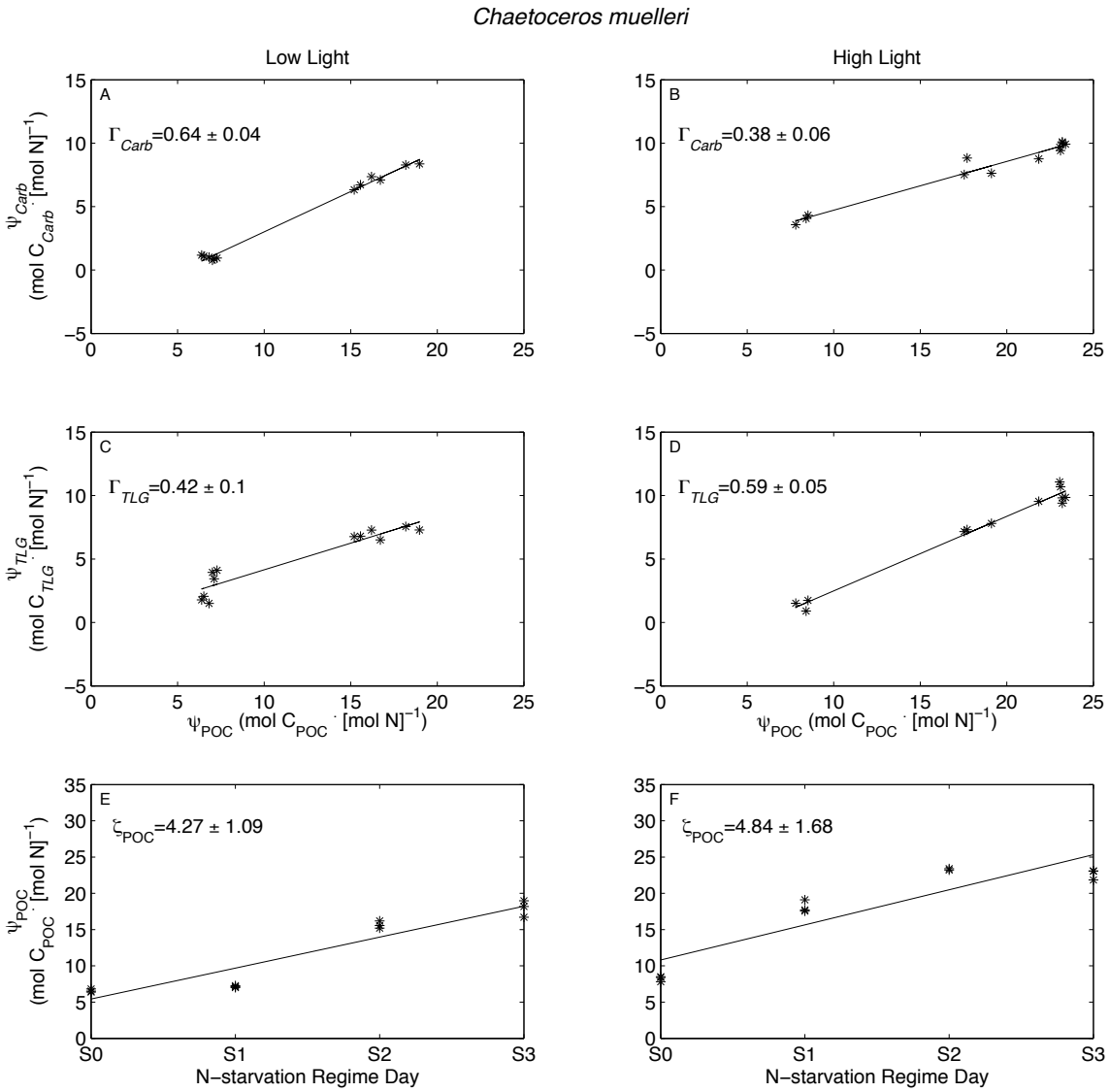

Figure 3.4. The proportion of carbon allocated between non-nitrogenous compounds and the rate of change of accumulation of energy storage carbon for the diatom *Chaetoceros muelleri*, acclimated to LL (175 µmol quanta m^{-2} s^{-1}) and HL (600 µmol quanta m^{-2} s^{-1}), during periods of increasing nitrogen-starvation (S0 – S3). The proportion of carbon allocated toward (A, B) carbohydrate (Γ_{Carb}, mol C_{Carb} · [mol C]$^{-1}$) and (C, D) gravimetric total lipid (Γ_{TLG} ,mol C_{TLG} · [mol C]$^{-1}$) during N-starvation, is indicated by the slope of ψ_i vs. ψ_{POC}. (E, F) The rate of carbon allocation toward energy stores (ζ_{POC}, mol C · [mol N]$^{-1}$ · d^{-1}) is the slope of ψ_{POC} vs. time, as indicated by N-starvation day.

3.3 Changes in Chemical Composition and Physiological Status for Different Species and Light Regimes

Changes in the chemical composition and physiological status for the LL treatment of *Chaetoceros muelleri* were described in section 3.1. Results for each of the four species, grown in low (LL) and high (HL) light are compared for five key chemical composition and physiological status measurements in sections 3.3.1 – 3.3.4. Acclimated N-replete values from sampling day R3 are presented in Table 3.1. These values are used for comparison between the N-replete treatments and as the S0 baseline for calculating changes during N-starvation. Mean values for the N-replete regime (R1 – R3), are presented in Appendix A.2.

Table 3.1. Chemical composition and physiological status for four species of microalgae acclimated to N-replete growth at 30°C at two different light levels (LL = 175 μmol quanta m^{-2} s^{-1} PAR, HL = 600 μmol quanta m^{-2} s^{-1} PAR) on a 12h:12h light:dark cycle: measurements for the final day, R3/S0, of a 3 day N-replete regime. Growth rate ($\mu_{F'}$), F'_v/F'_m, chlorophyll *a*:PON, carbon:chlorophyll *a*, POC:PON, carbon content of carbohydrate and gravimetrically-determined total lipid normalized to PON (ψ_{Carb} and ψ_{TLG}). Error ± SE for n = 3 independent cultures, unless otherwise indicated.

Species	Light Level	$\mu_{F'}$ (d^{-1})	F'_v/F'_m (dimensionless)	Chl *a*:N (g · [mol N]$^{-1}$)	C:Chl *a* (g:g)	ψ_{POC} (mol C · [mol N]$^{-1}$)	ψ_{Carb} (mol C_{Carb} · [mol N]$^{-1}$)	ψ_{TLG} (mol C_{TLG} · [mol N]$^{-1}$)
Chaetoceros muelleri	LL	1.46 (0.02)	0.64 (0.003)	6.67 (0.11)	11.85 (0.41)	6.57 (0.13)	1.09 (0.05)	1.78 (0.16)
	HL	2.47 (0.02)	0.59 (0.01)	4.15 (0.01)	23.85 (0.87)	8.24 (0.22)	3.99 (0.22)	1.38 (0.25)
Dunaliella salina	LL	0.81 (0.01)	0.54 (0.003)	5.32 (0.17)	11.31 (0.2)	5.00 (0.08)	1.15 (0.02)	1.35 (0.18)
	HL	1.46 (0.004)	0.56 (0.003)	3.79 (0.01)	25.61 (0.49)	8.09 (0.23)	3.64 (0.14)	1.62 (0.48)
Thalassiosira pseudonana	LL	1.11 (0.01)	0.54 (0.01)	5.04 (0.13)	17.09 (0.56)	7.16 (0.12)	2.26 (0.09)	1 (0.55)
	HL	1.76 (0.00)	0.52 (0.01)	3.33 (0.1)	38.51 (1.12)	10.66 (0.17)	5.8 (0.15)	2.19 (0.09)
Tetraselmis sp.	LL	0.59 (0.02)	0.57 (0.003)	7.87 (2.01)	13.96 (1.83)	9.57 (3.10)	2.59[a]	8.77 (2.85)[b]
	HL	1.70 (0.01)	0.51[a]	4.83 (0.01)	28.17 (1.43)	11.35 (0.67)	8.33 (1.52)	11.7 (0.73)

[a] n = 1
[b] n = 2 (± range)

3.3.1 Chaetoceros muelleri

Nutrient-replete growth – During the N-replete regime (R1 – R3, Figure 3.5), individual measurements, with the exception of ψ_{TLG}, were nearly constant day to day, indicating that the LL and HL treatments of *Chaetoceros muelleri* were in balanced growth, consistent with the assumptions of the Brand *et al.* (1981) method. Variation in ψ_{TLG} was greater than 30% for both LL and HL treatments (Figure 3.4 G, H). N-replete growth rates were the highest of all treatments, with the S0 values of 1.44 d^{-1} for LL and 2.40 d^{-1} for HL (Table 3.1). F_v'/F_m' (dimensionless) was 8% higher for the LL treatment of *C. muelleri* compared to the HL treatment: LL = 0.64 ± 0.003 (mean±SE, n = 3, Table 3.1, Figure 3.5 I) and HL = 0.59 ± 0.01 (mean±SE, n = 3, Table 3.1, Figure 3.5 J), consistent with the findings of Parkhill *et al*. (2001).

Chemical composition differed between light levels. For example, PON-specific chlorophyll *a* (g chl *a* · [mol N]$^{-1}$) in the LL treatment was approximately 50% higher than in the HL treatment (Table 3.1). This is similar to trends shown by Chan (1978) for congeneric *Chaetoceros* sp. (Singapore), in which chl *a*:protein (µg:µg) concentration at low light (~ 20 µmol quanta m^{-2} s^{-1}) was approximately 2-fold higher than at a higher light level (250 µmol quanta m^{-2} s^{-1}). Although Chan (1978) did not report PON values, the near constancy of PON-specific protein quotas (Geider & La Roche, 2002, Lourenço *et al.*, 2004) allows the comparison.

Both PON-specific POC, ψ_{POC}, and carbohydrate-carbon, ψ_{Carb}, were higher in the HL treatments, by 25% (Figure 3.5 C, D) and 260% (Figure 3.5 E, F), respectively, consistent with enhanced accumulation in energy storage compounds at high irradiance (Terry *et al.*, 1983, Renaud *et al.*, 1991, Geider *et al.*, 1996). Consequently, while the LL

treatment values for ψ_{POC} were similar to those of the Redfield Ratio (6.57 ± 0.07 vs. 6.625 mol C · [mol N]$^{-1}$ (Redfield, 1958), the HL treatment values of ψ_{POC} were 24% higher (8.24 ± 0.13 mol C · [mol N]$^{-1}$). The difference in ψ_{POC} , between HL and LL ($\psi_{POC}HL - \psi_{POC}LL$ = 1.67 mol C · [mol N]$^{-1}$) can be largely explained by the higher carbohydrate carbon content ($\psi_{Carb}HL - \psi_{Carb}LL$ = 2.89 mol C_{Carb} · [mol N]$^{-1}$). Unlike ψ_{Carb} , ψ_{TLG} was not significantly different between the light treatments (Table 3.1, Figure 3.5 G, H), although a modest shift would have been masked by analytical error.

Response to nitrogen-starvation – Once dilution was stopped, the responses to N-starvation described in section 3.1 for the LL treatment also occurred in the HL treatment, but with a more rapid onset. Changes in F_v'/F_m' , ψ_{POC} , ψ_{Carb} and ψ_{TLG} in the HL treatment were evident on S1, a day earlier than in the LL treatments (Figure 3.5). In the LL treatment, NO_3^- was being depleted during the first day of the N-starvation regime, S1, and the chemical composition on S1was still relatively similar to the S0 N-replete values as the treatment had been growing during day S1, rather than adjusting to N-stress (Figure 3.1). In both LL (Figure 3.5 I) and HL (Figure 3.5 J) treatments, F_v'/F_m' (dimensionless), showed a rapid response to N-starvation and the beginning of unbalanced growth. As NO_3^- was depleted in the HL treatment a day sooner than in the LL treatment (see Appendix A.1), responses were more pronounced than in the LL

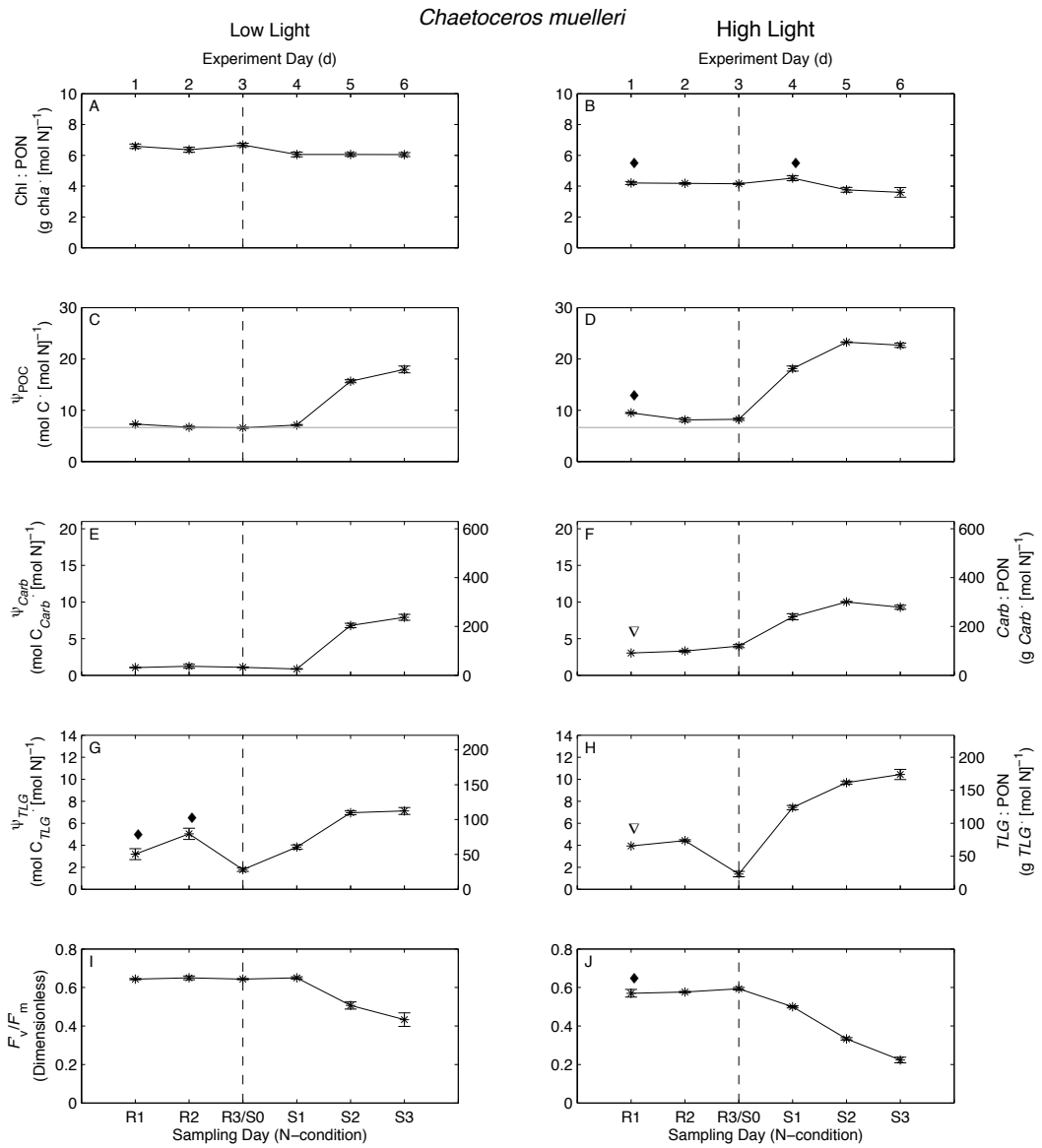

Figure 3.5. Changes in the chemical composition and physiological status of the diatom *Chaetoceros muelleri* acclimated to LL (175 µmol quanta m^{-2} s^{-1}) and HL (600 µmol quanta m^{-2} s^{-1}), during periods of nutrient replete growth (R1 – R3) and increasing nutrient starvation (S1 – S3). (A, B) Chlorophyll *a,* normalized to PON (g chl *a* · [mol N]$^{-1}$), (C, D) Particulate C, normalized to PON (ψ_{POC}, mol C · [mol N]$^{-1}$), (E, F) Carbohydrate-carbon normalized to PON (ψ_{Carb}, mol C_{Carb} · [mol N]$^{-1}$), with a scale for carbohydrate by weight, (G, H) Gravimetric lipid-carbon normalized to PON (ψ_{TLG}, mol C_{TLG} · [mol N]$^{-1}$) with a scale for *TLG* by weight, (I, J) Photochemical efficiency (F_v'/F_m', dimensionless). Error bars indicate standard error (n = 3), range (♦, n = 2) for independent cultures. The absence of error bars indicates a single determination (▽). Vertical bars represent the beginning of the N-starvation regime. i.e., one day after the final dilution. The horizontal bar in E represents the Redfield Ratio of ψ_{POC} = 6.625 mol C · [mol N]$^{-1}$ (Redfield, 1958).

treatment. F_v'/F_m' decreased by about 0.2 in the LL treatment (Figure 3.5 I) and by about 0.35 in the HL treatment (Figure 3.5 J), indicating that the HL treatment experienced greater N-stress, in large part because it was stressed for an extra day.

When a response to N-starvation became observable, ψ_{POC} increased as a result of carbon being allocated toward non-nitrogenous compounds (Figures 3.5 C). Coinciding with this were slight decreases in chl *a*:PON (Figures 3.5 A), confirming that the net synthesis of chl *a* had stopped (Geider *et al.*, 1998) concurrent with the cessation of nitrogen uptake. The changes in carbon allocated toward non-nitrogenous compounds shortly after N-depletion are commonly observed; for example Gosselin *et al.* (1990) and Richardson and Cullen (1995) reported on the increase in carbohydrate:protein (g:g) in response to N-starvation in sea-ice microalgae and the diatom *Thalassiosira weissflogii*, respectively.

As the HL treatment was subjected to N-stress for a day longer than the LL treatment (as explained above), the magnitude of changes during the N-starvation regime differed between the treatments. The increase in carbon allocated toward non-nitrogenous compounds, $\Delta\psi_{POC}$, between S0 – S3 was lower in the LL treatment than the HL treatment: 11.38 vs. 14.42 mol C · [mol N]$^{-1}$ (Figure 3.5 C, D). Carbon was possibly lost from the HL treatment as there was a decrease in $\Delta\psi_{POC}$ of 0.61 mol C · [mol N]$^{-1}$ between S2 and S3. The allocation of carbon between the non-nitrogenous compounds additionally varied between the LL and HL light treatments for Γ_{Carb}: 0.64 vs. 0.38 mol C_{Carb} · [mol C]$^{-1}$ (Figure 3.6 A, B, Table 3.2), Γ_{TLG}: 0.42 vs. 0.59 mol C_{TLG} · [mol C]$^{-1}$ (Figure 3.6 C, D, Table 3.2), and Γ_{TLI}: 0.36 vs. 0.62 mol C_{TLI} · [mol C]$^{-1}$ (Figure 3.6 E, F, Table 3.2). The rate of carbon allocated toward non-nitrogenous compounds during the

N-starvation regime, ζ_{POC} (mol C · [mol N]$^{-1}$ · d^{-1}), was relatively high for both the *C. muelleri* treatments, and higher for HL: 4.27 vs. 4.84 mol C · [mol N]$^{-1}$ d^{-1} (Figure 3.6 G, H, Table 3.2). Nonlinearity in the $\Delta\psi_{POC}$ vs. time relationship (e.g. Figure 3.6 G, H) will be discussed in section 4.1.2.

Table 3.2. Summary of the proportional allocation of carbon to the non-nitrogenous compounds carbohydrate (Γ_{Carb}), gravimetric total lipid (Γ_{TLG}) and inferred total lipid (Γ_{TLI}), in addition to the rate of increase of all non-nitrogenous compounds during N-starvation (ζ_{POC}). Values are linear regression slopes ± 95 % CI.

Species	Light Level	Γ_{Carb} (mol C_{Carb} · [mol C]$^{-1}$	Γ_{TLG} (mol C_{TLG} · [mol C]$^{-1}$	Γ_{TLI} (mol C_{TLI} · [mol C]$^{-1}$	ζ_{POC} (mol C · [mol N]$^{-1}$ d^{-1}
Chaetoceros	LL	0.64 ±0.04	0.41 ± 0.1	0.36 ± 0.04	4.27 ± 1.09
muelleri	HL	0.38 ± 0.06	0.59 ± 0.05	0.62 ±0.05	4.84 ± 1.68
Dunaliella	LL	0.83 ± 0.07	0.25 ± 0.2	0.17 ± 0.07	4.02 ± 1.27
salina	HL	0.76 ± 0.08	0.27 ± 0.12	0.24 ± 0.08	3.06 ± 1.38
Thalassiosira	LL	0.73 ± 0.12	0.17 ± 0.45	0.27 ± 0.11	2.66 ± 0.57
pseudonana	HL	0.53 ± 0.08	0.12 ± 0.31	0.47 ± 0.08	2.24 ± 0.54
Tetraselmis	LL	-	-	-	-
sp.	HL	0.54 ± 0.26	-0.35 ± 0.3	0.46 ± 0.26	5.16 ± 1.43

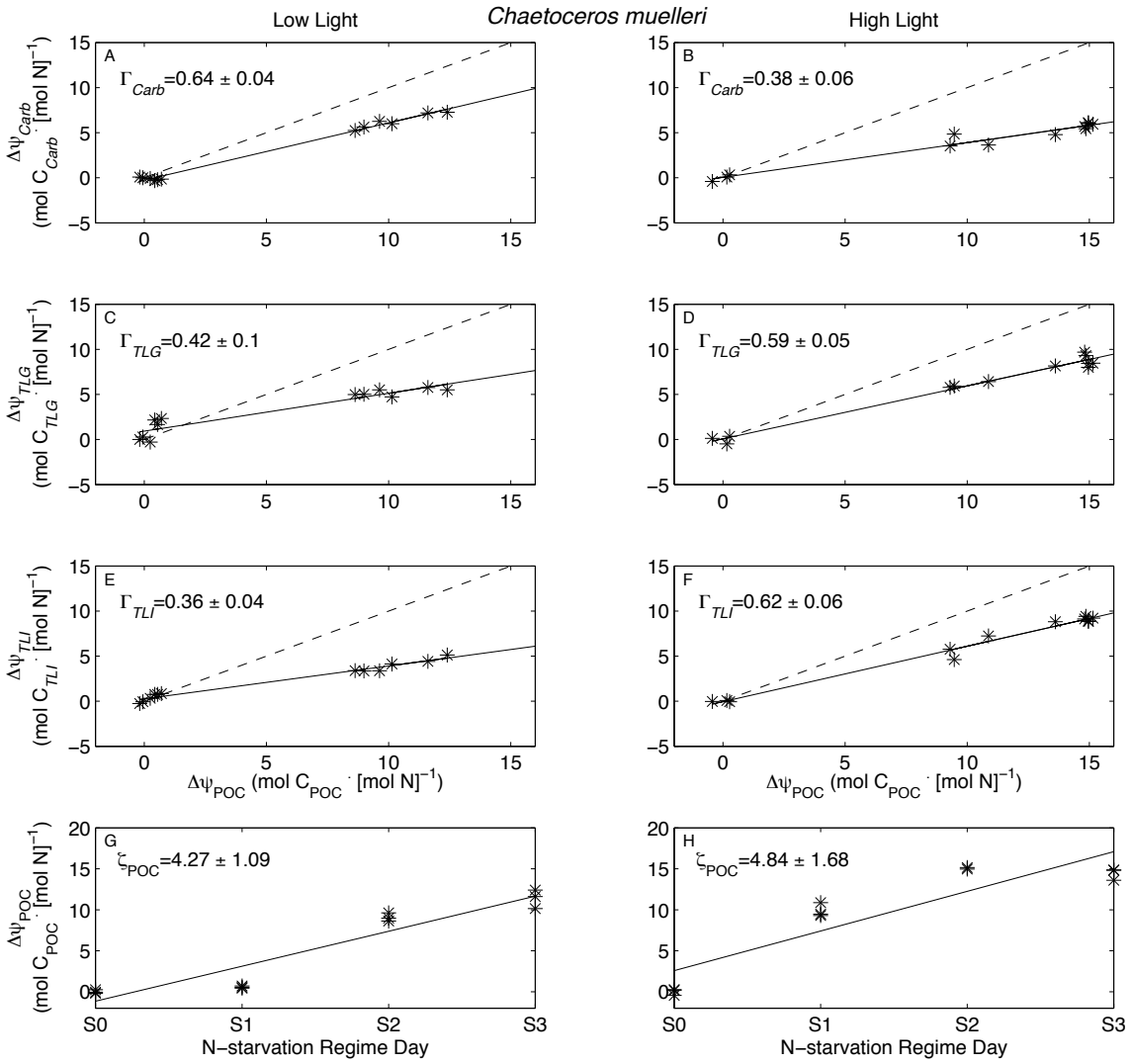

Figure 3.6. The relative change in the N-specific carbon content for: (A, B) carbohydrate ($\Delta\psi_{Carb}$), (C, D) gravimetric total lipid ($\Delta\psi_{TLG}$), (E, F) inferred total lipid ($\Delta\psi_{TLI}$), and (G, H) the temporal change in POC ($\Delta\psi_{POC}$) in *Chaetoceros muelleri.* Cultures were acclimated to LL (175 µmol quanta m^{-2} s^{-1}) and HL (600 µmol quanta m^{-2} s^{-1}) during increasing N-starvation, as indicated by increasing $\Delta\psi_{POC}$. The carbon content of carbohydrate, gravimetric total lipid and inferred total lipid described in Section 2.4.1. The dashed lines represents $\Gamma_i = 1$, i.e. the theoretical maximum allocation of carbon to compound *i*, whereas the solid lines represents the linear regressions (Γ_i , mol C_i · [mol C]$^{-1}$) for each treatment and compound, see Section 3.3.3 – 3.2.4. Errors associated with Γ_i and ζ_{POC} are the 95% CI of the slopes.

3.3.2 Dunaliella salina

Nutrient-replete growth – During the N-replete regime, measurements of chemical composition were generally consistent with balanced growth, varying less than 10% over days R1 – R3, with the exception of chl *a*:PON in the LL treatment. This varied by about 20%, suggesting a problem with chlorophyll analysis rather than the cultures not being in balanced growth. Variation of ψ_{TLG} in both light treatments could not be assessed with confidence because values for R2 were excluded due to contamination of the samples during lipid extraction.

On S0, growth rate ($\mu_{F'}$, d^{-1}) in the HL treatment was about twice that in the LL treatment, 1.39 d^{-1} vs. 0.71 d^{-1} (Table 3.1). F_v'/F_m' (dimensionless) on S0 was slightly lower in the LL treatment, (Figure 3.7 I) than in the HL treatment (Table 3.1, Figure 3.7 J).

The effects of growth irradiance on chemical composition were similar to those observed in *Chaetoceros muelleri*. On S0, chl *a*:PON (g chl *a* · [mol N]$^{-1}$) was approximately 40% higher in the LL treatment than in the HL treatment (Table 3.1, Figure 3.7 A, B). This is comparable to the differences in chl *a*:protein reported between light levels reported by Renaud *et al.* (1991), on the assumption that protein:PON ratios are constant (Lourenço *et al.*, 2004). N-specific chl *a* quotas were lower in *D. salina* than in *C. muelleri* in both light treatments. As observed for *C. muelleri*, ψ_{POC} for *D. salina* was higher in the HL treatment than in the LL. In contrast to *C. muelleri,* the LL treatment was lower than the Redfield Ratio of 6.625 mol C · [mol N]$^{-1}$ (Redfield, 1958) by 1.6 mol C · [mol N]$^{-1}$ whereas the HL treatment was greater than Redfield by 1.4 mol C · [mol N]$^{-1}$ (Table 3.1). These results suggest that carbon was being allocated

preferentially toward nitrogenous compounds at low light and that non-nitrogenous compounds were accumulated in high light, matching expectations based on Geider *et al*. (1996). Further supporting this interpretation is the significantly higher ψ_{Carb} in the HL treatment, which was 2.49 mol C_{Carb} · [mol N]$^{-1}$ higher than in the LL treatment (Figure 3.7 E, F). As with the *C. muelleri* treatments, there was no significant difference between the LL and HL treatments for ψ_{TLG} (mol C_{TLG} · [mol N]$^{-1}$): the value in the LL treatment was 1.35 ± 0.18 (mean±SE, n = 3, Table 3.1, Figure 3.7 G) and the value in the HL treatment was 1.62 ± 0.48 (mean±SE, n = 3, Table 3.1, Figure 3.7 H), an interpretation compromised by analytical uncertainty.

Response to nitrogen starvation – As in *Chaetoceros muelleri,* the response of *Dunaliella salina* to N-starvation was observed sooner in the HL treatment than in the LL treatment. F_v'/F_m' (dimensionless) decreased during the N-starvation regime for both LL and HL treatments; by about 0.15 to 0.4 for the LL treatment (Figure 3.7 I) while the HL treatment decreased by about 0.27 to 0.3 (Figure 3.7 J). The greater response to N-starvation in the HL treatment was largely associated with a more rapid onset of N-stress. When the N-starvation response became observable, ψ_{POC} increased as a result of carbon being allocated primarily toward non-nitrogenous compounds. However, the LL *D. salina* treatment showed a continual increase in chl *a*:PON throughout the N-starvation regime, with a total increase of 3.19 g chl *a* · [mol N]$^{-1}$ between S0 and S3 (Figure 3.4 A). This indicates that some carbon was still being allocated toward the synthesis of light-harvesting compounds during N-starvation in the LL treatment, which must have required remobilization of cellular N (Boussiba *et al.*, 1999). This was not the case in the HL

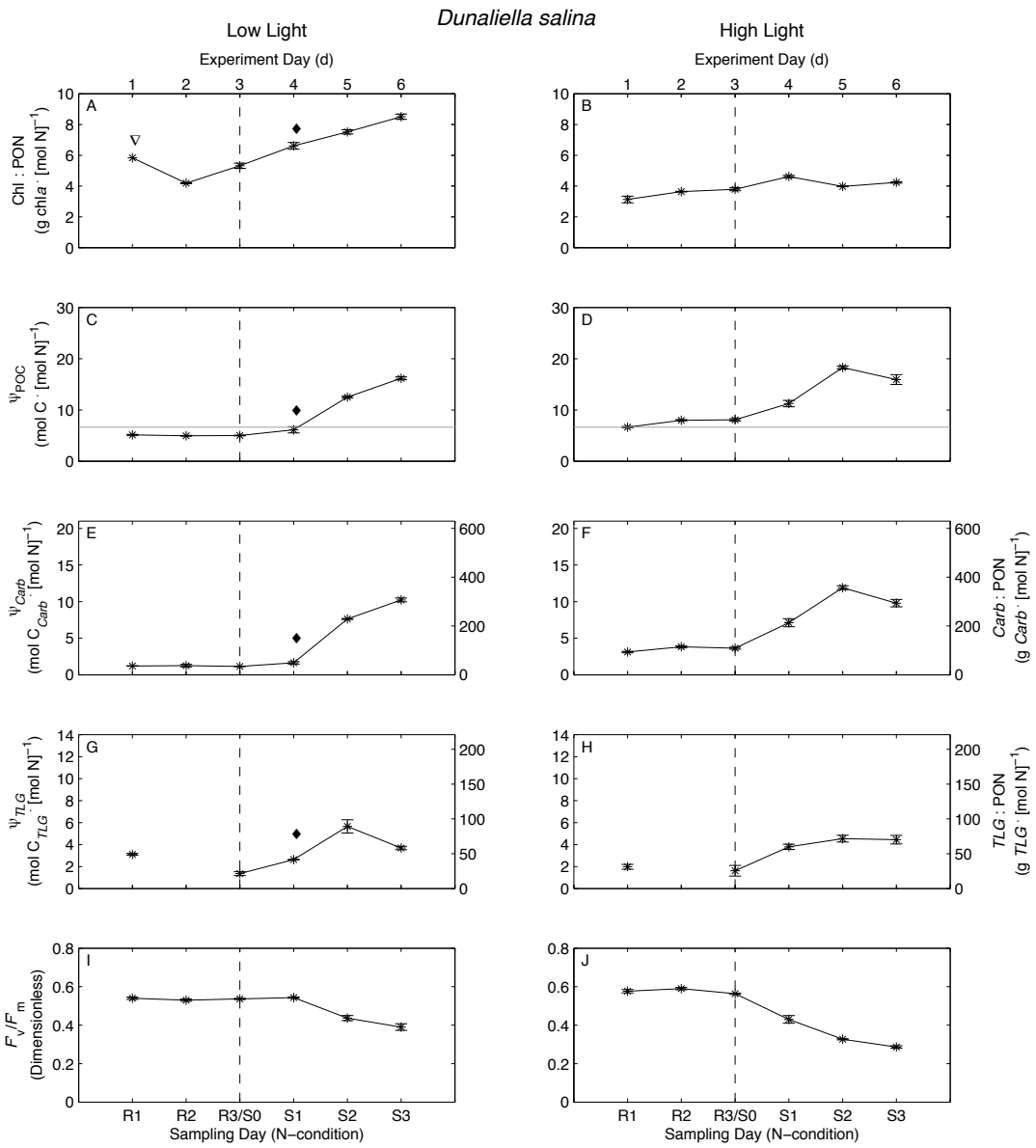

Figure 3.7. Changes in the chemical composition and physiological status of the chlorophyte *Dunaliella salina* acclimated to LL (175 µmol quanta m^{-2} s^{-1}) or HL (600 µmol quanta m^{-2} s^{-1}), during periods of nutrient replete growth (R1 – R3) and increasing nutrient starvation (S1 – S3). (A, B) Chlorophyll *a,* normalized to PON (g chl *a* · [mol N]$^{-1}$), (C, D) Particulate C, normalized to PON (ψ_{POC}, mol C · [mol N]$^{-1}$), (E, F) Carbohydrate-carbon normalized to PON (ψ_{Carb}, mol C_{Carb} · [mol N]$^{-1}$), with a scale for carbohydrate by weight, (G, H) Gravimetric lipid-carbon normalized to PON (ψ_{TLG}, mol C_{TLG} · [mol N]$^{-1}$) with a scale for *TLG* by weight, (I, J) Photochemical efficiency (F_v'/F_m', dimensionless). Symbols are as presented in Figure 3.4.

treatment, which, like *C. muelleri*, ceased net synthesis of chl *a* during N-starvation (Figure 3.5 B) (Geider *et al.*, 1998).

The HL treatment of *D. salina* responded to N-starvation a day earlier than the LL treatment, on S1 vs. S2, as it did for *Chaetoceros muelleri*. Unlike *C. muelleri*, the maximum change in carbon content, $\Delta\psi_{POC}$, was slightly greater in the LL treatment: 11.17 mol C · [mol N]$^{-1}$ on S3 in LL (Figure 3.6 C) vs. 10.20 mol C · [mol N]$^{-1}$, which occurred on S2 in HL (Figure 3.6 D). Observation of the maximum $\Delta\psi_{POC}$ on S2 in the HL treatment is most likely explained by carbon loss between S2 and S3.

In both treatments, the majority of the increase in $\Delta\psi_{POC}$ could be attributed to the increase in carbohydrate: Γ_{Carb} = 0.83 mol C_{Carb} · [mol C]$^{-1}$ in the LL treatment (Figure 3.8 A) and 0.76 mol C_{Carb} · [mol C]$^{-1}$ in the HL treatment (Figure 3.8 B). Both gravimetric and inferred total lipid contributed less to the increase in $\Delta\psi_{POC}$ for both light treatments: at LL Γ_{TLG} = 0.25 mol C_{TLG} · [mol C]$^{-1}$ (Figure 3.8 C) and Γ_{TLI} = 0.17 mol C_{TLI} · [mol C]$^{-1}$ (Figure 3.8 E); and at HL Γ_{TLG} = 0.27 mol C_{TLG} · [mol C]$^{-1}$, (Figure 3.8 D) and Γ_{TLI} = 0.24 mol C_{TLI} · [mol C]$^{-1}$ (Figure 3.8 F). The larger contribution of carbohydrates to $\Delta\psi_{POC}$ in LL was similar to the LL treatment of *C. muelleri* (Table 3.2). However for the HL treatments, the two species differed in the predominant compound that contributed more toward $\Delta\psi_{POC}$: in *Chaetoceros muelleri* it was lipids but in *D. salina* it was carbohydrate (Table 3.2). The summation of the non-nitrogenous compounds, $\Delta\widehat{\psi}_{POC}$, came closest to matching $\Delta\psi_{POC}$ (102%) in the LL treatment but over-estimated it (114%) in the HL treatment.

A noticeable difference between the two light treatments was that $\Delta\psi_{POC}$ and $\Delta\psi_{Carb}$ both decreased in the HL treatment on the final day of N-starvation (Figure 3.7 D, F). Excretion of carbohydrate might account for this loss (Myklestad, 2000, Granum *et al.*, 2002), as the loss of this carbon-rich compound would not change PON, which did not decline (see Appendix A.1), but would reduce ψ_{Carb} and ψ_{POC}. The loss of carbon on S3 may also account for the differences in ζ_{POC} between the light treatments (Figure 3.8 G, H). Unlike the differences between the light treatments for *Chaetoceros muelleri*, there was a greater rate of carbon accumulation in non-nitrogenous compounds for the LL treatment for *Dunaliella salina*, ζ_{POC} = 4.02 mol C · [mol N]$^{-1}$ · d^{-1}, than in the HL treatment ζ_{POC} = 3.06 mol C · [mol N]$^{-1}$ · d^{-1} (Figure 3.6 G, H, Table 3.2). Had only S0 - S2 data been used in the regression to determine the rate of increase, HL ζ_{POC} would have been 5.10 mol C · [mol N]$^{-1}$ · d^{-1} (data not shown).

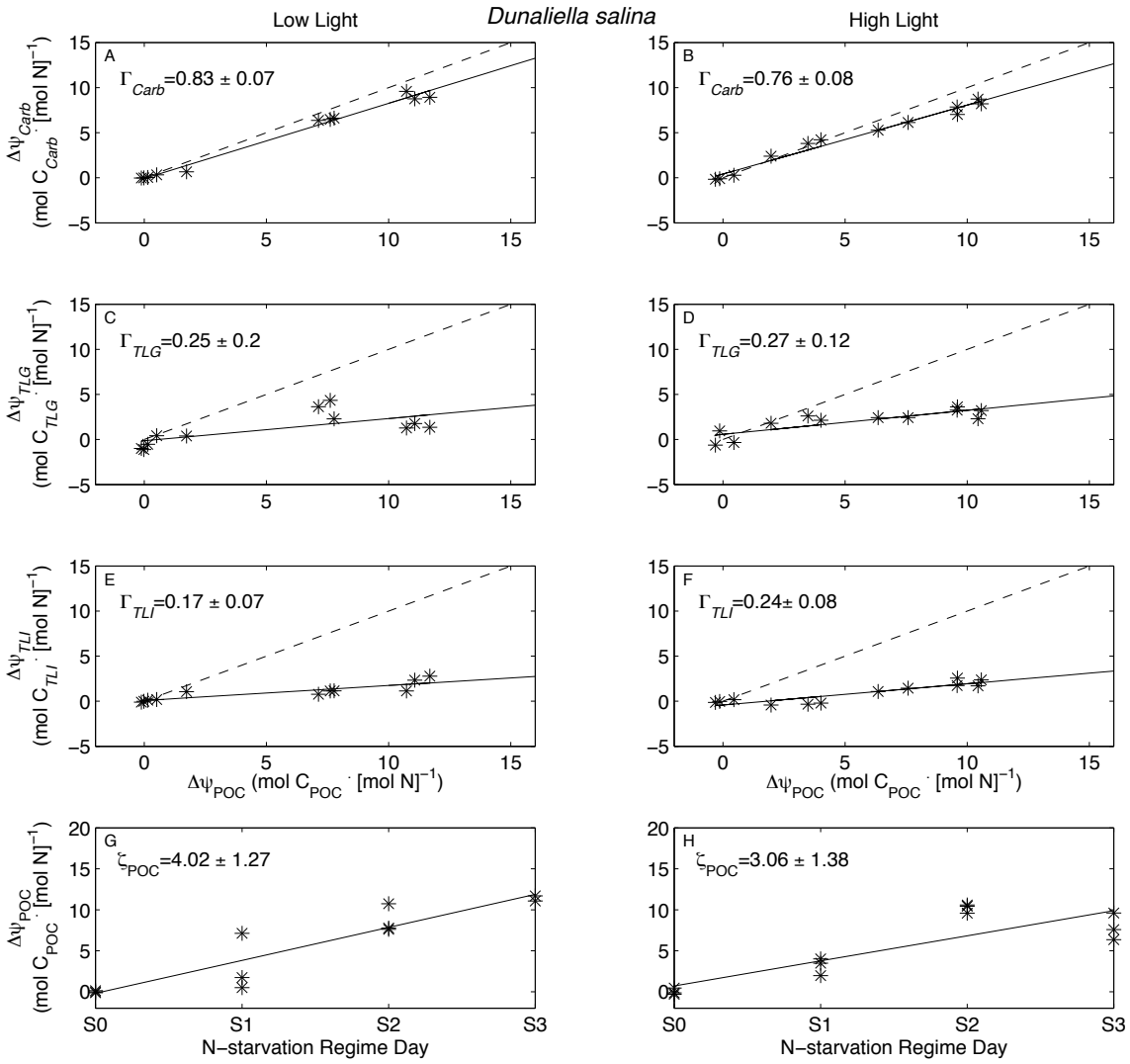

Figure 3.8. The relative change in the N-specific carbon content for: (A, B) carbohydrate ($\Delta\psi_{Carb}$), (C, D) gravimetric total lipid ($\Delta\psi_{TLG}$), (E, F) inferred total lipid ($\Delta\psi_{TLI}$), and (G, H) the temporal change in POC ($\Delta\psi_{POC}$) in *Dunaliella salina.* Cultures were acclimated to LL (175 µmol quanta m^{-2} s^{-1}) and HL (600 µmol quanta m^{-2} s^{-1}) during increasing N-starvation, as indicated by increasing $\Delta\psi_{POC}$. The carbon content of carbohydrate, gravimetric total lipid and inferred total lipid described in Section 2.4.1. The dashed lines represents $\Gamma_i = 1$, i.e. the theoretical maximum allocation of carbon to compound *i*, whereas the solid lines represents the linear regressions (Γ_i , mol C_i · [mol C]$^{-1}$) for each treatment and compound, see Section 3.3.3 – 3.2.4. Errors associated with Γ_i and ζ_{POC} are the 95% CI of the slopes.

3.3.3 Thalassiosira pseudonana

Nutrient-replete growth – There was variation of > 10% for all of the chemical composition measurements, with the exception of ψ_{Carb}, during N-replete growth in the LL and HL treatments of *Thalassiosira pseudonana* (Figure 3.9). For example, chl *a*:PON varied by more than 20% in the LL treatment and 10% in the HL treatment. However, given the consistency in the physiological status measurements, it was presumed that treatments were close to balanced growth (Eppley & Renger, 1974).

The growth rates ($\mu_{F'}$, d^{-1}) for LL and HL treatments on S0 were less than for the other diatom, *C. muelleri* (Table 3.1) but higher for HL as compared to LL, similar to data reported by Geider *et al.* (1985). Similarly, F_v'/F_m' (dimensionless) values were lower than for *C. muelleri* (Table 3.1, Figure 3.9 I, J), most likely due to difference in species (Suggett *et al.*, 2009). For example, in the LL treatments of *C. muelleri* and *T. pseudonana*, F_v'/F_m' was 0.64 vs. 0.54, respectively.

The effect of light level on chemical composition followed the same pattern in *T. pseudonana* as in the other species studied. On S0, the ratio of chl *a*:PON (g chl *a* · [mol N]$^{-1}$) was approximately 50% higher for the LL treatment than the HL treatment (Geider *et al.*, 1985) (Table 3.1, Figure 3.9 A, B). Measures of ψ_{POC}, ψ_{Carb} and ψ_{TLG} were significantly higher in the HL treatments: by 62% (Figure 3.9 C, D), 217% (Figures 3.9 E, F) and 219% (Figure 3.9 G, H), respectively, consistent with carbon primarily being allocated toward energy storage compounds at high-light levels (Geider *et al.*, 1996). However, both the LL and HL ψ_{POC} were statistically greater than the Redfield Ratio of 6.625 mol C · [mol N]$^{-1}$ (Redfield, 1958), by 0.54 mol C · [mol N]$^{-1}$ and 4.04 mol C · [mol N]$^{-1}$, respectively. The differences for ψ_{POC}, ψ_{Carb} and ψ_{TLG} between HL and LL

($\psi_i HL - \psi_i LL$) additionally indicated the higher concentration at high light: 3.08 mol C · [mol N]$^{-1}$, 2.49 mol C_{Carb} · [mol N]$^{-1}$ and 0.26 mol C_{TLG} · [mol N]$^{-1}$, respectively.

Response to nitrogen starvation – The trends in biochemical composition during N-starvation of *T. pseudonana* were similar to what has presented above. Over the duration of the N-starvation regime, F_v'/F_m' (dimensionless) decreased by about 0.17, with the LL F_v'/F_m' = 0.37 (Figure 3.9 I) and the HL F_v'/F_m' = 0.35 (Figure 3.9 J) on day S3. However, the decrease in F_v'/F_m', for *T. pseudonana* was less than for *C. muelleri*, and the HL treatment of *D. salina*.

Responses in chemical compositions to N-starvation occurred a day earlier for the HL treatment than for the for the LL treatment, S1 vs. S2. There was little change in chl *a*:PON (g chl *a* · [mol N]$^{-1}$) throughout the N-starvation regime (Figure 3.9 A, B). The small increase in chl *a*:PON in the LL treatment indicated that some carbon was still being allocated toward the pigment synthesis, as in the LL treatment of *D. salina* (Figure 3.7 A), but the changes were small. As available nitrate was depleted, it was assumed that net synthesis of nitrogenous compounds had ceased. Between S0 and S3, $\Delta\psi_{POC}$ (mol C · [mol N]$^{-1}$) increased for both treatments, with LL having a slightly larger increase: LL = 7.43 (Figure 3.9 C) and HL = 7.01 (Figure 3.9 D). In contrast to the other HL treatments, $\Delta\psi_{POC}$ did not decrease on S3 in the HL treatment of *T. pseudonana*, indicating that there was no net loss of carbon (Figure 3.9 D). However, on S3 there was a decrease in

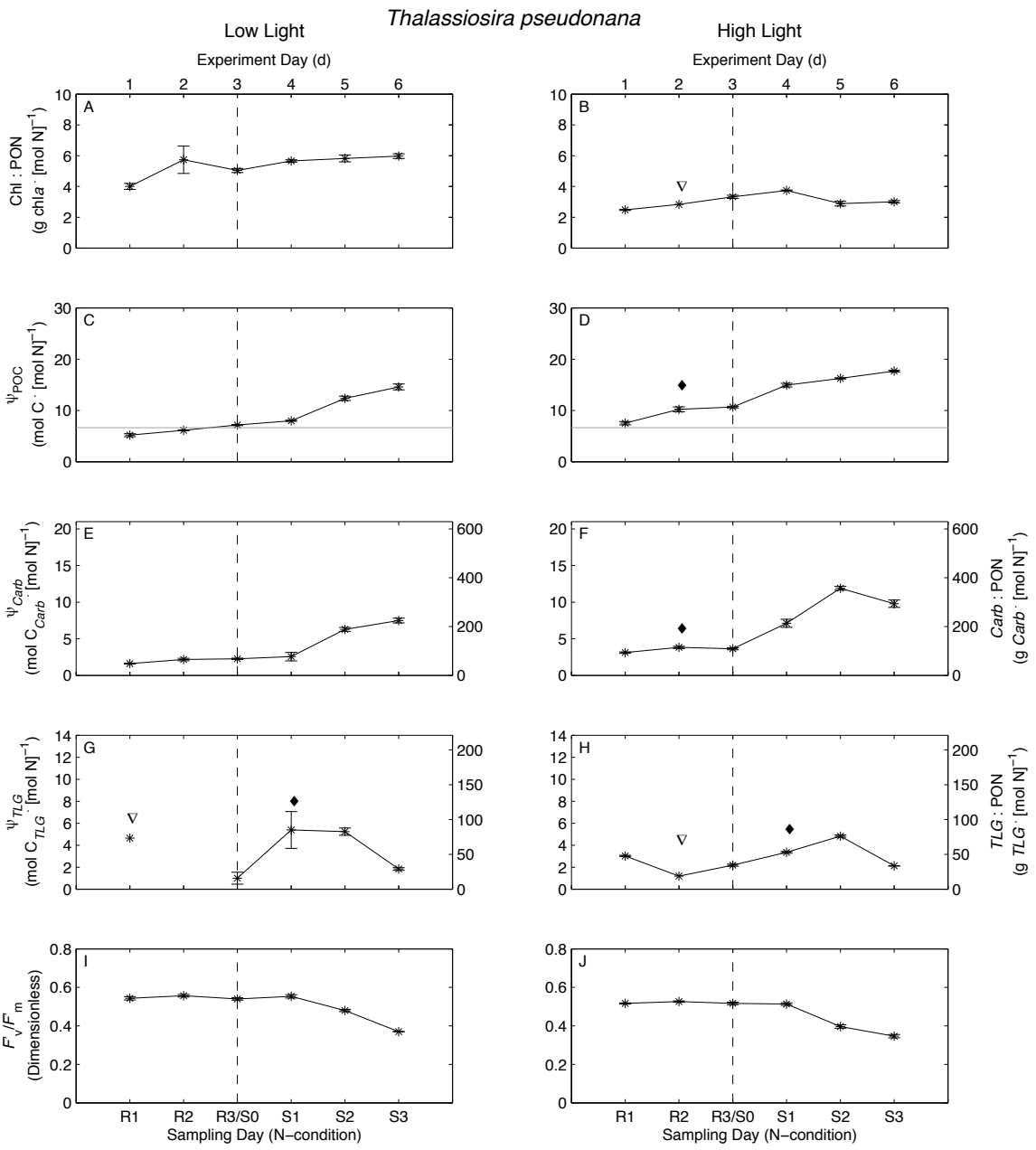

Figure 3.9. Changes in the chemical composition and physiological status of the diatom *Thalassiosira pseudonana* acclimated to LL (175 µmol quanta m^{-2} s^{-1}) or HL (600 µmol quanta m^{-2} s^{-1}), during periods of nutrient replete growth (R1 – R3) and increasing nutrient starvation (S1 – S3). (A, B) PON-specific chlorophyll *a* (g chl *a* · [mol N]$^{-1}$), (C, D) PON-specific particulate C (ψ_{POC}, mol C · [mol N]$^{-1}$), (E, F) PON-specific carbohydrate (ψ_{Carb}, mol C_{Carb} · [mol N]$^{-1}$), (G, H) PON-specific gravimetric lipid (ψ_{TLG}, mol C_{TLG} · [mol N]$^{-1}$), (I, J) Photochemical efficiency (F_v'/F_m', dimensionless). Symbols are as presented in Figure 3.4.

both ψ_{Carb} and in ψ_{TLG}, inconsistent with POC measurements, suggesting at a minimum that there were errors in determination of *TLG*.

The majority of the LL $\Delta\psi_{POC}$ increase was likely due to an increase in carbohydrate, Γ_{Carb} = 0.73 mol C_{Carb} · [mol C]$^{-1}$ (Figure 3.10 A). The increase in gravimetric total lipid was considerably less; Γ_{TLG} = 0.17 mol C_{TLG} · [mol C]$^{-1}$ (Figure 3.10 C). As $\Delta\psi_{Carb}$ decreased on S3, it was inferred that total lipid attributed more to the increase in $\Delta\psi_{POC}$ than was observed; Γ_{TLI} = 0.27 mol C_{TLI} · [mol C]$^{-1}$ (Figure 3.10 E). The increase in $\Delta\psi_{POC}$ in the HL treatment was believed to be due more to carbohydrate (Γ_{Carb} = 0.53 mol C_{Carb} · [mol C]$^{-1}$, Figure 3.20 B), than gravimetric total lipid (Γ_{TLG} = 0.12 mol C_{TLG} · [mol C]$^{-1}$, Figure 3.10 D). The measured change in lipid was considerably less than what was inferred by difference (Γ_{TLI} = 0.47 mol C_{TLI} · [mol C]$^{-1}$, Figure 3.10 F).

Unlike *Dunaliella salina*, *Thalassiosira pseudonana* had a similar rate of carbon allocation toward non-nitrogenous carbon compounds in the HL treatment (ζ_{POC} = 2.24 ± 0.54 mol C · [mol N]$^{-1}$ · d^{-1}) and the LL treatment (ζ_{POC} = 2.66 ± 0.57 mol C · [mol N]$^{-1}$ · d^{-1}). Of the four species studied, *T. pseudonana* had the lowest ζ_{POC}, regardless of light level (Figure 3.12, Table 3.2).

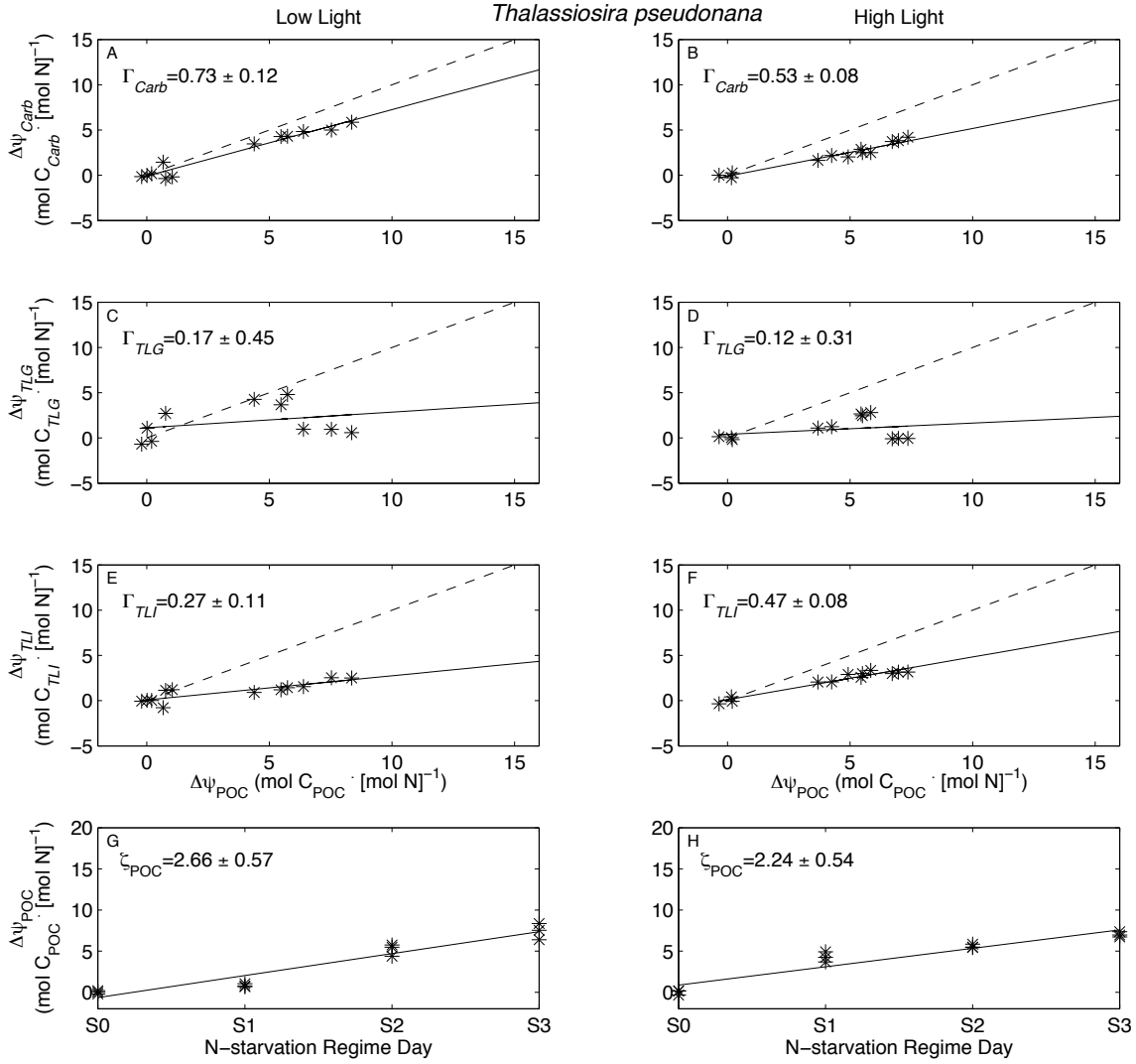

Figure 3.10. The relative change in the N-specific carbon content for: (A, B) carbohydrate ($\Delta\psi_{Carb}$), (C, D) gravimetric total lipid ($\Delta\psi_{TLG}$), (E, F) inferred total lipid ($\Delta\psi_{TLI}$), and (G, H) the temporal change in POC ($\Delta\psi_{POC}$) in *Thalassiosira pseudonana.* Cultures were acclimated to LL (175 µmol quanta m^{-2} s^{-1}) and HL (600 µmol quanta m^{-2} s^{-1}) during increasing N-starvation, as indicated by increasing $\Delta\psi_{POC}$. The carbon content of carbohydrate, gravimetric total lipid and inferred total lipid described in Section 2.4.1. The dashed lines represents $\Gamma_i = 1$, i.e. the theoretical maximum allocation of carbon to compound *i*, whereas the solid lines represents the linear regressions (Γ_i , mol C_i · [mol C]$^{-1}$) for each treatment and compound, see Section 3.3.3 – 3.2.4. Errors associated with Γ_i and ζ_{POC} are the 95% CI of the slopes.

3.3.4 Tetraselmis sp.

Of the four species studied, *Tetraselmis* sp. was the most difficult to monitor because of its tendency to stick to the walls of containers, compromising the assumption of the Brand *et al.* (1981) dilution method and leading to uneven subsampling. Consequently, some results for *Tetraselmis* sp. were discarded and the remainder should be treated with caution.

Nutrient-replete growth – The LL *Tetraselmis* sp. light treatments showed consistent values during the first two days of the N-replete regime whereas the HL treatment showed an increase in the four measures of chemical composition shown in Figure 3.11, similar to the *D. salina* HL treatment (Figure 3.7). On the third N-replete day, there was an anomalous increase for all PON-specific measurements (Figure 3.11) that was not explained by anomalously low PON (see Appendix A.1). This microalga stuck to culture vessels during sampling, removing biomass from suspension and influencing results. Growth rate ($\mu_{F'}$, d^{-1}), on S0 at both light levels, were the lowest of all treatments (Table 3.1). At the same time, F_v'/F_m' (dimensionless) for the LL treatment was relatively high, 0.57 (Table 3.1, Figure 3.11 I), while the HL treatment was relatively low, 0.51 (Table 3.1, Figure 3.10 J), when compared to the other treatments for each light level.

The majority of biochemical parameters did not show a significant difference between the LL and HL treatments; however, this was in part due to the large variance, often greater than 20%, present in the LL treatment. Chl *a*:PON (g chl *a* · $[\text{mol N}]^{-1}$) was relatively high in both treatments, with the LL treatment not significantly different from the *C. muelleri* LL treatment (Table 3.1, Figure 3.11 A). Chl *a*:PON in the HL treatment was the highest of the HL treatments at 4.83 ± 0.01 g chl *a* · $[\text{mol N}]^{-1}$ (mean±SE, n = 3,

Table 3.1, Figure 3.11 B), but was not significantly different from the LL treatment. On S0, ψ_{POC} in the LL treatment was not significantly different from the Redfield Ratio of 6.625 mol C · [mol N]$^{-1}$ (Redfield, 1958) due to the large variance in the measurement: ψ_{POC} = 9.57 ± 3.10 mol C · [mol N]$^{-1}$ (Table 3.1, Figure 3.10 C). However, the ratio in the HL treatment was significantly higher than the Redfield Ratio, by approximately 5 mol C · [mol N]$^{-1}$ (Table 3.1, Figure 3.6 D), ψ_{POC} = 11.35 ± 0.67 mol C · [mol N]$^{-1}$. Within each light treatment, *Tetraselmis* sp. had the highest ψ_{Carb} and ψ_{TLG} of all species tested, with ψ_{Carb} being significantly higher in the HL treatment (Table 3.1, Figure 3.11 E, G, F).

Due to the anomalous increase on S0, the changes that occurred during the N-starvation regime could not be defined with the same degree of certainty as in the other species tested, as outlined in section 3.1.

Response to nitrogen-starvation – Once NO_3^- was depleted, changes in chemical composition and physiological status became observable. As NO_3^- was not depleted until S3 for the LL treatment, observable changes in chemical composition and physiological status were limited to a single day compared to three days for the HL treatment. As such, the LL treatment will not be discussed here. Measurements of F_v'/F_m' (dimensionless) were not available on S3, however S2 values showed that the HL treatment had decreased by about 0.27 to 0.24 (Figure 3.11 J) during N-starvation.

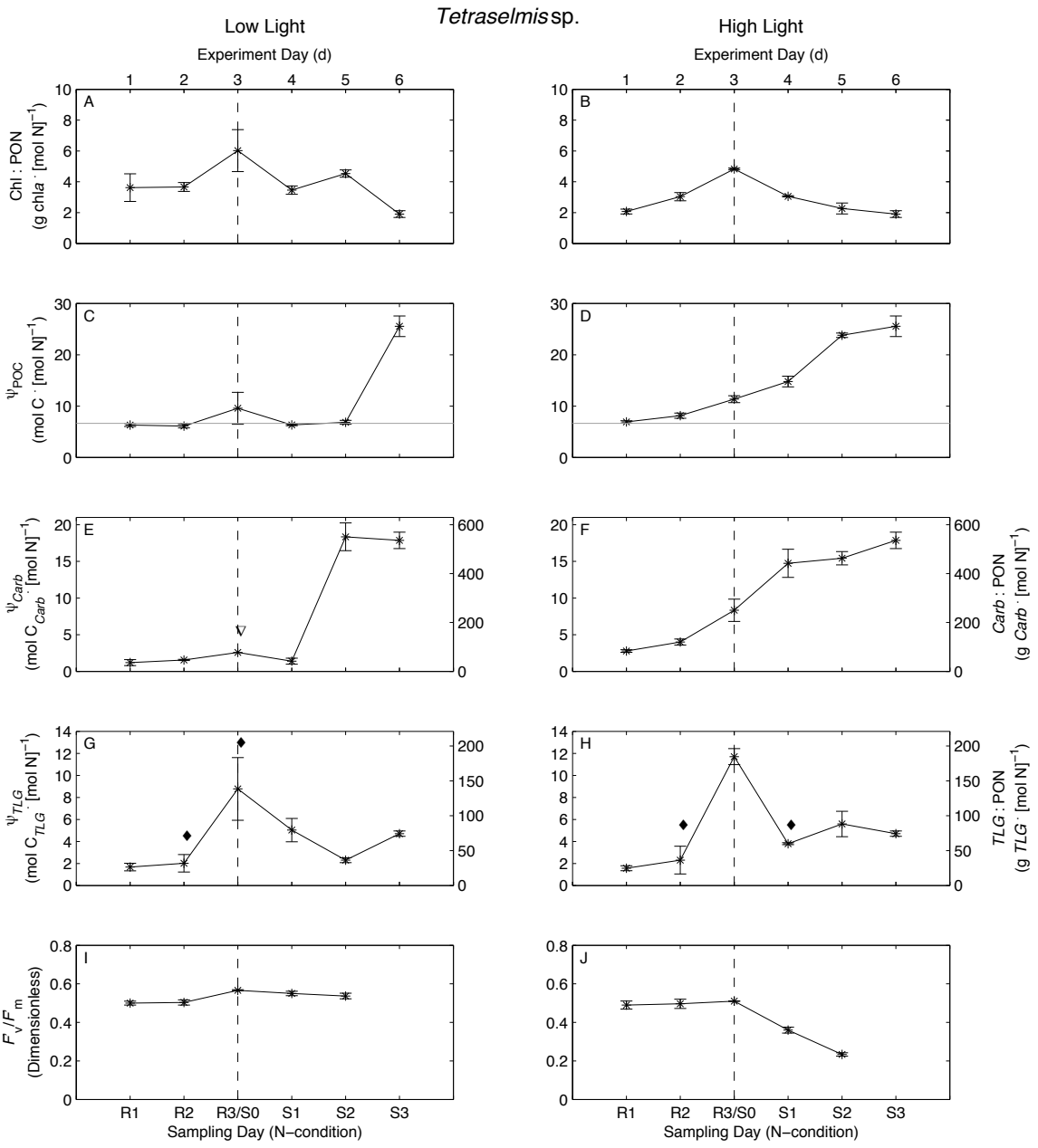

Figure 3.11. Changes in the chemical composition and physiological status of the green *Tetraselmis* sp. acclimated to LL (175 µmol quanta m^{-2} s^{-1}) or HL (600 µmol quanta m^{-2} s^{-1}), during periods of nutrient replete growth (R1 – R3) and increasing nutrient starvation (S1 – S3). (A, B) PON-specific chlorophyll *a* (g chl *a* · [mol N]$^{-1}$), (C, D) PON-specific particulate C (ψ_{POC}, mol C · [mol N]$^{-1}$), (E, F) PON-specific carbohydrate (ψ_{Carb}, mol C_{Carb} · [mol N]$^{-1}$), (G, H) PON-specific gravimetric lipid (ψ_{TLG}, mol C_{TLG} · [mol N]$^{-1}$), (I, J) Photochemical efficiency (F_v'/F_m', dimensionless). Symbols are as presented in Figure 3.4.

Unlike the other species, chl *a*:PON (g chl *a* · [mol N]$^{-1}$) in the HL treatment decreased during the N-starvation regime by 39.4% (Figure 3.11 B). This decrease suggested the down-regulation of light-harvesting complexes to match the reduced potential for protein synthesis (Geider *et al.*, 1998). During the N-starvation regime (S0 – S3), the HL treatment increased the amount of carbon allocated toward non-nitrogenous compounds: $\Delta\psi_{POC}$ = 14.21 mol C · [mol N]$^{-1}$ (Figure 3.11 D). Of the HL increase in $\Delta\psi_{POC}$, the small majority was attributed toward the increase in carbohydrate; Γ_{Carb} = 0.54 mol C_{Carb} · [mol C]$^{-1}$ (Figure 3.12 A, Table 3.2) so that Γ_{TLI} = 0.46 mol C_{TLI} · [mol C]$^{-1}$ (Figure 3.12 B). Gravimetric total lipid indicated a relatively large loss, Γ_{TLG} = -0.35 mol C_{TLG} · [mol C]$^{-1}$ (Figure 3.12 C) although the value should be treated with caution given the increase in $\Delta\psi_{POC}$ and the known issues with the gravimetric total lipid method (see section 3.2.2). The most likely explanation for this negative value was that on S0 there was an unexpected large peak in ψ_{TLG} (Figure 3.11 J), making the reference point greater than the measures of ψ_{TLG} made during N-starvation. This resulted in negative $\Delta\psi_{TLG}$ values, which then was translated into a negative Γ_{TLG} (Figure 3.12 B).

Of all species and treatments, the HL treatment of *Tetraselmis* sp. had the highest rate of carbon allocation toward non-nitrogenous compounds, ζ_{POC} = 5.16 mol C · [mol N]$^{-1}$ · d^{-1} (Figure 3.11 D). Presumably, this was driven by the large increase in carbohydrate in response to N-starvation.

Data for the *Tetraselmis* sp. LL treatment was compromised by slow growth, sampling and analysis error and inadequate time under N-starvation. It will be excluded from subsequent analyses.

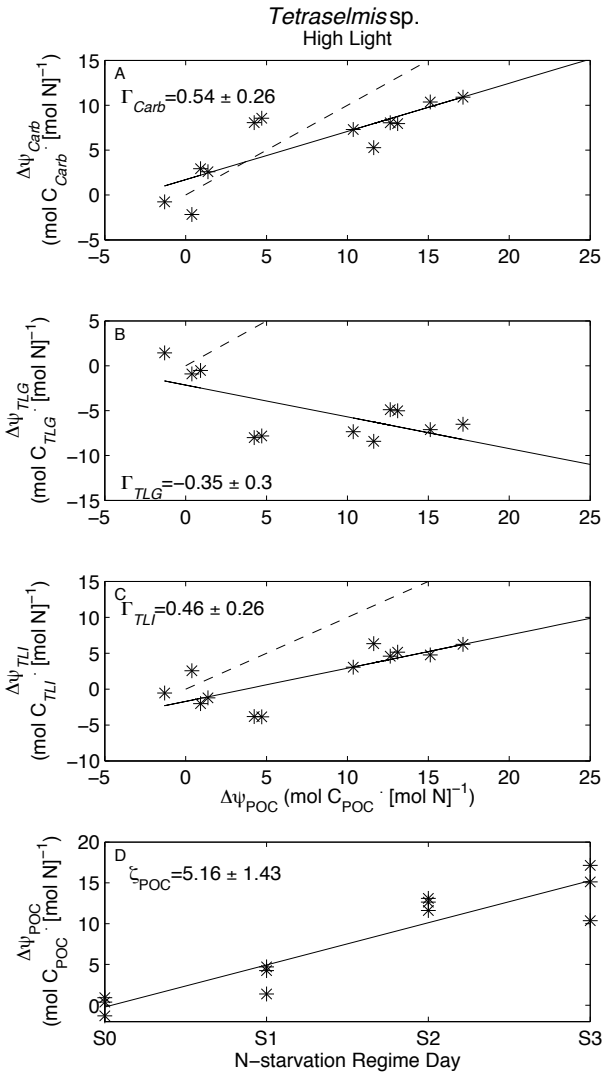

Figure 3.12. The relative change in the N-specific carbon content for: (A, B) carbohydrate ($\Delta\psi_{Carb}$), (C, D) gravimetric total lipid ($\Delta\psi_{TLG}$), (E, F) inferred total lipid ($\Delta\psi_{TLI}$), and (G, H) the temporal change in POC ($\Delta\psi_{POC}$) in *Tetraselmis* sp. Cultures were acclimated HL (600 µmol quanta m^{-2} s^{-1}) during increasing N-starvation, as indicated by increasing $\Delta\psi_{POC}$. The carbon content of carbohydrate, gravimetric total lipid and inferred total lipid described in Section 2.4.1. The dashed lines represents $\Gamma_i = 1$, i.e. the theoretical maximum allocation of carbon to compound *i*, whereas the solid lines represents the linear regressions (Γ_i , mol C_i · [mol C]$^{-1}$) for each treatment and compound, see Section 3.3.3 – 3.2.4. Errors associated with Γ_i and ζ_{POC} are the 95% CI of the slopes.

3.4 Influence of Genotype and Irradiance on the Allocation of Carbon to Carbohydrate vs. Lipid

The parameter Γ_i describes the relative contribution of carbohydrate vs. total lipid to the increase of non-nitrogenous carbon biomass during N-starvation. Γ_{Carb} was determined directly as the slope of the regression between $\Delta\psi_{Carb}$ and $\Delta\psi_{POC}$ for the combined results of three replicates during four days of N-starvation. Because gravimetric determinations of lipid were unreliable, Γ_{TLI} was calculated as 1 - Γ_{Carb}, assuming that only carbohydrate and lipid contributed to the accumulation of particulate carbon during N-starvation. Consequently, the figure summarizing results for the effects of genotype and irradiance on the allocation of carbon to carbohydrate vs. lipid (Figure 3.13) shows measured results for carbohydrate complemented with inferred results for lipid.

The responses to N-starvation varied between treatments, but there were consistent patterns. For the three LL cultures that could be assessed, photosynthate was allocated primarily toward carbohydrate during N-starvation: Γ_{Carb} (±95% CI) was greater than 50% for each (Figure 3.13). Lipid synthesis contributed more to the accumulation of carbon in HL treatments, but only one treatment had a Γ_{TLI} (±95% CI) clearly greater than 50%: *Chaetoceros muelleri* (Figure 3.13, Table 3.2). However, the 95% CI for both HL treatments of *Thalassiosira pseudonana* and *Tetraselmis* sp. did include 50% (Figure 3.13, Table 3.2). *Dunaliella salina* accumulated particulate carbon primarily as carbohydrate, with consistently high Γ_{Carb} between light treatments (Figure 3.13). A comparison between light treatments could not be made for *Tetraselmis* sp. because the LL treatment was excluded due to NO_3^- not being depleted until S3. Only

Chaetoceros muelleri showed a large change in Γ_i in response to light levels, switching between producing carbohydrate in LL and lipid in HL.

The values of Γ_{Carb} are slopes of regression. The effects of species and irradiance on Γ_{Carb} were tested for significant difference using 1-way Analysis of Covariance (ANCOVA) using $\Delta\psi_{Carb}$ as the dependent variable, $\Delta\psi_{POC}$ as the covariate and treatment (e.g. *C. muelleri* LL) as the categorical factor. Assumptions for ANCOVA were that 1) measurements were randomly sampled and independent of each other, 2) the dependent variables had normal distribution, 3) the variances of the dependent variables were homoscedastic, and 4) the regression slopes of individual treatments were homogeneous. The null hypotheses tested was that treatment (i.e. species cultured at a given light level) did not have an effect on the allocation of carbon between carbohydrate vs. lipid during N-starvation. Tukey's HSD post-hoc test was used to identify which treatments had significantly different Γ_{Carb}, as indicated by lower-case letters above the bars in Figure 3.13.

Tetraselmis sp. treatments were excluded from statistical analyses as the LL treatment had not become N-starved until S3 and the HL treatment violated at least one assumption of ANCOVA, while the other treatments had passed the assumptions of ANCOVA. The slopes of Γ_{TLI} were not tested for significant difference as they were calculated by difference from carbohydrate and contain no extra information.

The null hypothesis was rejected as treatment was shown to have a significant effect on the allocation of carbon to carbohydrate vs. lipid during N-starvation (1-way ANCOVA, $p < 0.05$, Table 3.3). Tukeys-HSD post-hoc test revealed that the LL

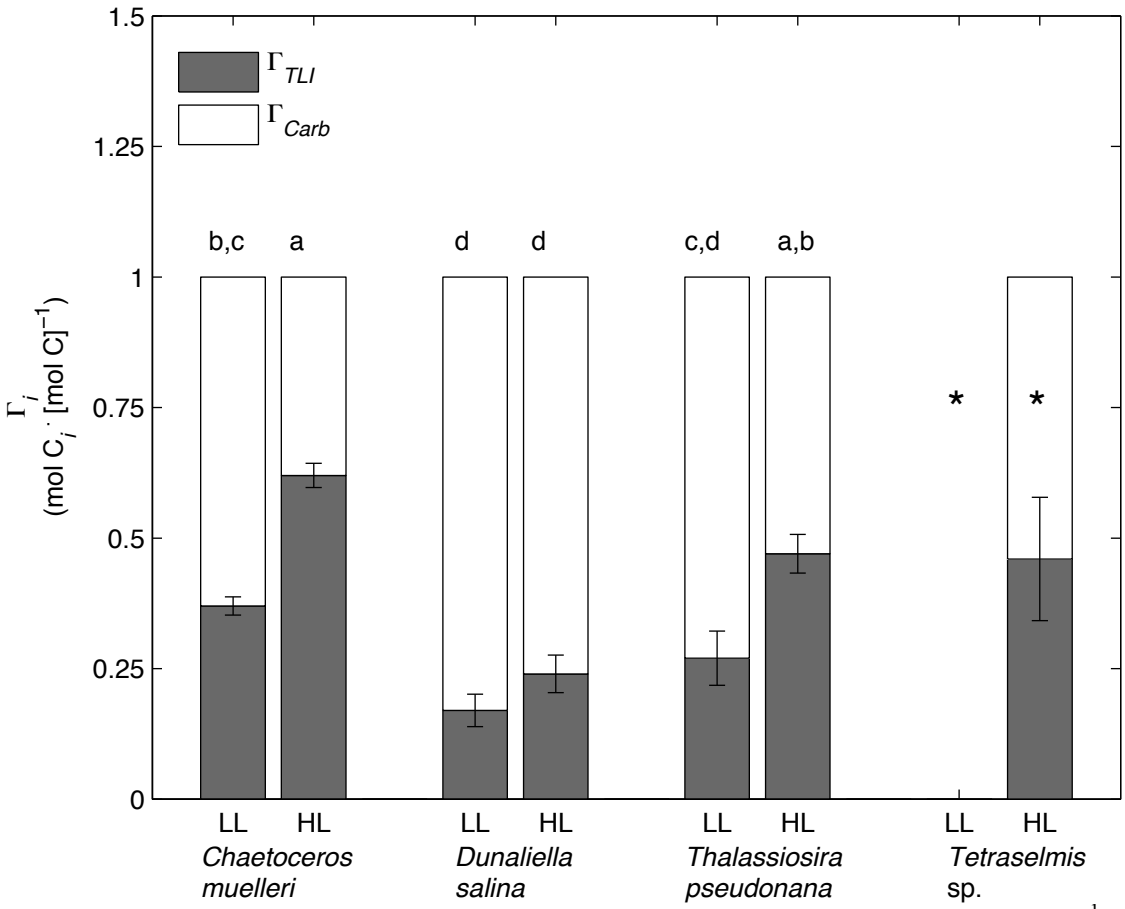

Figure 3.13. Relative contributions of carbohydrate-carbon, Γ_{Carb} (mol C_{Carb} · [mol C^{-1}) and inferred total lipid-carbon Γ_{TLI} (mol C_{TLI} · [mol C]$^{-1}$), to the increase in non-nitrogenous carbon stores during N-starvation. Error bars represent ± SE (n = 9) of the slope, Γ_i. Asterisk (*) for the *Tetraselmis* sp. treatments represents data excluded from 2-way ANCOVA due to lack of pairing. Letters over bars indicate statistically homogeneous groups as determined with Tukey's HSD.

treatment of *C. muelleri* was significantly lower than the HL treatment of *C. muelleri*, as expected, and both light treatments of *D. salina* (Figure 3.13). Similarly, the HL treatment of *C. muelleri* was significantly higher than the LL treatment of *C. muelleri* and the *D. salina* treatments as well as the LL treatment of *T. pseudonana*. There was no significant difference between the light treatments of *D. salina* (Figure 3.13). The HL treatment of *T. pseudonana* was significantly higher than the LL treatment of *T. pseudonana* and both light treatments of *D. salina* (Figure 3.13).

3.5 Influence of Genotype and Irradiance on the Rate of Carbon Allocated to Non-nitrogenous Compounds

The metric ζ_{POC} (mol C · [mol N]$^{-1}$ · d^{-1}) is the slope of a regression of $\Delta\psi_{POC}$ vs. time during N-starvation for the three replicates within each treatment. It is the rate of carbon allocation toward energy stores in cultures with the same nitrogen content; high rates are desirable for biofuels production. The effect of species and irradiance on ζ_{POC} was tested using 1-way ANCOVA using $\Delta\psi_{POC}$ as the dependent variable, time as the covariate and treatment (e.g. *C. muelleri* LL) as the categorical factor. Assumptions are as above. The null hypotheses tested was that treatment (i.e. species cultured at a given light level) did not have an effect on the rate of carbon allocated to energy stores during N-starvation. Tukey's HSD post-hoc test was used to identify which treatments had significantly different ζ_{POC}, as indicated by lower-case letters above the bars in Figure 3.14.

Tetraselmis sp. treatments were excluded from statistical analyses as the LL treatment had not become N-starved until S3 and the HL treatment violated at least one

assumption of ANCOVA, while the other treatments had passed the assumptions of ANCOVA.

The null hypothesis was rejected as it was shown that treatment had a significant effect on the rate of carbon allocation to energy stores during N-starvation (1-way ANCOVA, $p < 0.05$, Table 3.4). However, Tukeys-HSD post-hoc test showed that the there was no significant difference between light treatments for each species (Figure 3.14). The rate of carbon allocated toward energy stores for the LL *C. muelleri* treatment was significantly higher than the HL treatment of *T. pseudonana.* Additionally, the HL treatment of *C. muelleri* was shown to be significantly higher than both light treatments of *T. pseudonana* (Figure 3.14). Both light treatments of *D. salina* were not significantly different from the other treatments.

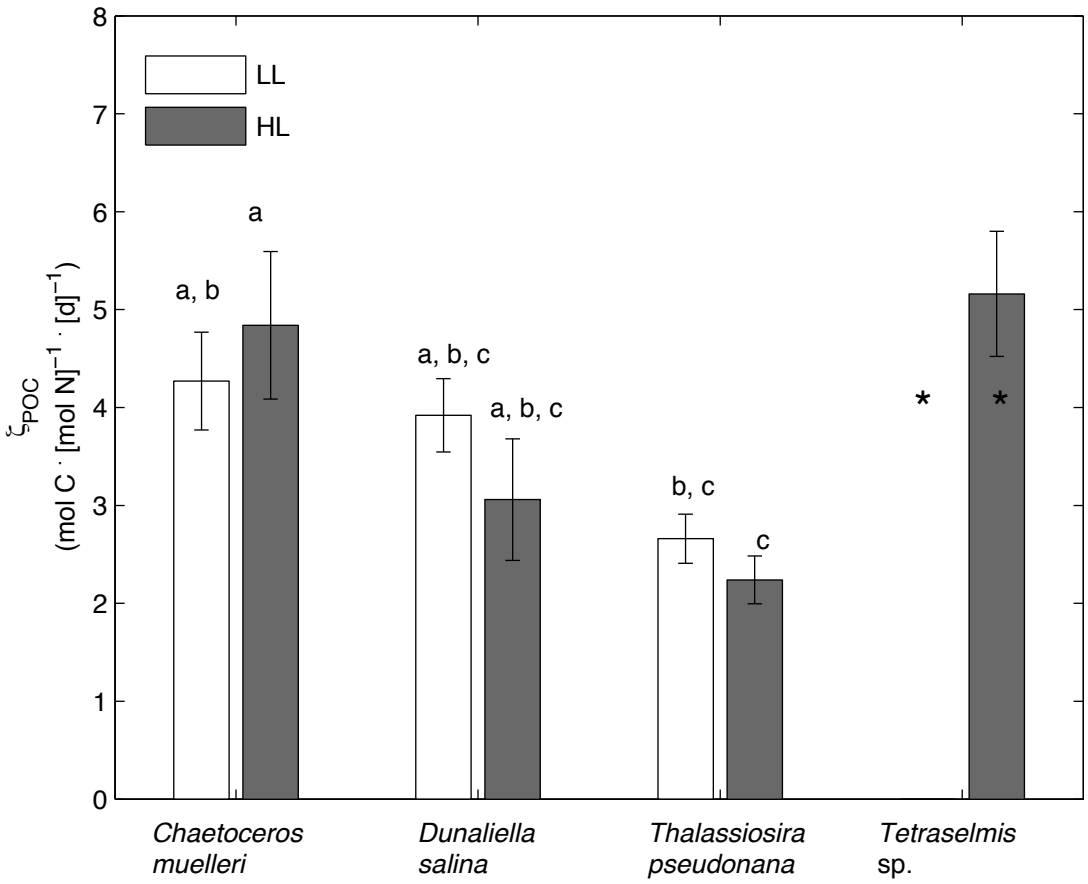

Figure 3.14. Rate of carbon allocation toward energy stores during N-starvation in cultures, ζ_{POC} (mol C · [mol N]$^{-1}$ · d^{-1}). Error bars represent ± SE (n = 9) of the slope, ζ_{POC}. Asterisk (*) for the *Tetraselmis* sp. treatments represents data excluded from ANCOVA due to lack of pairing. Letters over bars indicate statistically homogeneous groups as determined with Tukey's HSD.

Table 3.3. Effect of treatment (i.e. species cultured at a given light level) on the allocation of carbon toward carbohydrate (Γ_{Carb}) during N-starvation using 1-way ANCOVA.

Source	d.f.	Sum Squares	Mean Squares	F	Prob>F
Treatment	5	83.57	16.71	81	<<0.001
POC	1	515.14	515.14	2496.47	<<0.001
Treatment*POC	5	41.41	8.28	40.13	<<0.001
Error	59	12.17	0.21		

Table 3.4. Effect of treatment (i.e. species cultured at a given light level) on the rate of carbon allocation toward energy stores (ζ_{POC}) during N-starvation using 1-way ANCOVA.

Source	d.f.	Sum Squares	Mean Squares	F	Prob>F
Treatment	5	302.22	60.44	17.04	<<0.001
Date	1	1097.08	1097.08	309.23	<<0.001
Treatment*Date	5	75.84	15.17	4.28	<0.01
Error	59	209.32	3.55		

Chapter 4: Discussion

Changes in the allocation of carbon between the major classes of biological compounds are influenced by environmental conditions such as irradiance and ambient nutrient concentrations (Shifrin & Chisholm, 1981, Geider *et al.*, 1996, Hu *et al.*, 2008). This phenotypic response differs between species (Ben-Amotz *et al.*, 1985, Wilhelm *et al.*, 2006), demonstrating the influence of genotype. One focus of microalgal biofuel research is on finding a combination of genotypically-determined phenotypic responses that will maximize neutral lipid concentrations in response to an environmental stimulus, typically nitrogen starvation (Sheehan *et al.*, 1998, Hu *et al.*, 2008). During nitrogen starvation, carbon is allocated toward non-nitrogenous compounds such as carbohydrate and neutral lipid, while synthesis of nitrogenous compounds, for example proteins, RNA and DNA, is limited (Morris, 1981, Geider *et al.*, 1998). An ideal strain for biofuel production would continue photosynthesis during initial nutrient starvation, while allocating the majority of carbon toward the production of neutral lipid, maximizing returns on the resources provided (Hu *et al.*, 2008). With ongoing nutrient starvation, carbon could be catabolized from nitrogenous compounds and/or carbohydrate to form neutral lipid (Larson & Rees, 1996, Brown *et al.*, 1996, Hu, 2006), further improving yields. The main goal of this thesis was to show the influence that genotype and light level have on the change in carbon allocation during ongoing nitrogen starvation. This goal was addressed by developing metrics of the rate of synthesis of energy stores during N-starvation and the allocation of carbon toward lipid vs. carbohydrate. This enabled comparisons of experimental results and the development of criteria for choosing optimal strains and culture conditions for the commercial production of lipid by algae.

4.1 Growth and Chemical Composition as Influenced by Light and N-starvation

4.1.1 Nitrogen Replete Growth

Prior to the N-replete regime, cultures were acclimated for a minimum of 8 generations to consistent day-to-day environmental conditions. Once the 8 generations had passed, it was expected that cultures were in balanced growth and that the "internal adjustments of metabolic pathways have ceased so the rate of change of all cellular components is the same" (MacIntyre & Cullen, 2005), establishing the conditions for characterizing growth and chemical composition during N-replete growth. As these experiments used a photoperiod of 12h:12h light:dark, and measurements were made at the same time in the photoperiod, it was assumed that rates of increase of all cellular components were the same, day to day, even though the proportions of those components might change during the day (Eppley, 1981, MacIntyre & Cullen, 2005). During the N-replete regime, R1 – R3 measurements should have been consistent had cultures been in balanced growth, which was mostly the case. There were a few treatments, e.g. *Thalassiosira pseudonana* LL that appeared to be close to balanced growth (see Figure 3.8), but not fully acclimated. Nonetheless, measurements of growth rate, physiological status and chemical composition (except for gravimetric lipid) varied little, < 10%, during the N-replete phase, and measurements at R3 (Table 3.1) can be considered representative of balanced N-replete growth.

Responses to irradiance in carbon allocation levels are species specific (Terry *et al.*, 1983, Claustre & Gostan, 1987, Harrison *et al.*, 1990, Renaud *et al.*, 1991, Fabregas *et al.*, 2004), however generalizations can be made for nutrient-replete cultures. Geider *et al*. (1996) provide a model describing the changes in carbon allocation in response to

different irradiance levels. Briefly, carbon can be partitioned into three categories: those that are light-regulated (e.g. light harvesting compounds), not light-regulated (e.g. cellular structure), or energy stores (e.g. non-polar lipid and carbohydrate). Low irradiances stimulate the synthesis of light-regulated compounds, in order to maximize the light harvesting at the cost of synthesizing energy storage compounds. When exposed to high irradiance, the cellular response is similar to that when cells become nutrient starved; synthesis of light regulated compounds is down-regulated while synthesis of energy storage compounds is increased (Terry *et al.*, 1983, Geider *et al.*, 1996).

Our results, presented in Table 3.1, matched these expectations, as well as one outlined by Laws and Chalup (1990): low light levels resulted in carbon being allocated toward nitrogenous compounds, leading to low C:N and C:Chl *a* ratios, whereas at high light, carbon was being allocated toward non-nitrogenous compounds, high C:N and C:Chl *a* ratios.

Additionally, irradiance level can influence lipid composition. Polar lipids, which can be incorporated into the photosynthetic machinery, are synthesized at low-irradiance where light-regulated compounds are favoured over energy-storage compounds (Sukenik *et al.*, 1989, Geider *et al.*, 1996). At high-irradiance, fewer light-harvesting components are produced, lowering the requirement for polar lipid and resulting in increased synthesis of non-polar lipids for energy storage (Fabregas *et al.*, 2004).

4.1.2 Nitrogen Starvation

When daily dilutions were stopped, continued growth depleted the nitrate remaining in the cultures and metabolic pathways were forced to change, resulting in unbalanced growth (Eppley, 1981, MacIntyre & Cullen, 2005). Under nitrogen depletion,

net synthesis of nitrogenous compounds including those required for light harvesting, is slowed or stopped (Gosselin *et al.*, 1990, Richardson & Cullen, 1995); repair or replacement of important compounds, such as the D1 protein in the PSII reaction center is restricted (Geider *et al.*, 1993) and carbon is allocated primarily toward non-nitrogenous compounds, increasing both the C:N and C:Chl *a* ratios (Moal *et al.*, 1987, Larson & Rees, 1996). These changes were typically more pronounced for the high-light treatments than for the low-light treatments (see Section 3.3).

Between light levels, the high-light treatments generally depleted nitrate earlier than their low-light counterparts, resulting with greater changes in chemical composition. An exact time point for nitrate depletion could not be determined given the sampling design utilized here. A possible loss of carbon was noted for the high-light treatments as carbohydrate and particulate organic carbon often decreased on the third day of N-starvation, indicating possible extracellular release (Myklestad, 1995, Granum *et al.*, 2002). Of the different treatments, only the high-light treatment of *Chaetoceros muelleri* expressed continual increase of gravimetric total lipid during N-starvation (see Section 3.3), indicating continued synthesis, even with ambient nitrogen depleted. Gravimetric measurements of total lipid must be treated with caution, but those made when concentrations were highest are most reliable because the amounts were well above limits of quantification (see Appendix A.4).

4.2 Irradiance, Nitrogen Stress and the Photosynthetic Apparatus

Treatments under balanced growth expressed differences between the low- and high-irradiances: typically the low-irradiance treatments had a lower C:chl *a* and higher F_v'/F_m' than the high-irradiance treatments (see Section 3.3 and Table 3.1). At high-

irradiances, the synthesis of light harvesting compounds is down-regulated (Geider *et al.*, 1996), increasing C:chl *a* (Table 3.1). The lower F_v'/F_m' values observed in the high-light treatments were consistent with growth rates becoming light saturated (Kolber *et al.*, 1988, Parkhill *et al.*, 2001). Differences in F_v'/F_m' between treatments within a light level (Table 3.1) must be attributed to genotype (Suggett *et al.*, 2009), but it cannot be assumed that the relative differences between species would be the same for other combinations of irradiance and temperature.

During unbalanced growth induced by N-starvation, synthesis of the D1 protein was likely slowed, decreasing the proportion of functional reaction centers, which in turn would result in a decrease in F_v'/F_m' for all treatments (Geider *et al.*, 1993). The rate of decrease in F_v'/F_m' in response to N-starvation, differed between treatments as species (Suggett *et al.*, 2009) and irradiance level (Parkhill *et al.*, 2001) played an influence. For example, the decrease in F_v'/F_m' for the high-light treatments was greater than the low-light treatments, but the magnitude of the difference varied between species.

Declines in F_v'/F_m' can be used as a measure of nutrient stress (Parkhill *et al.*, 2001). Microalgal species that maintain a high F_v'/F_m' during N-starvation are more likely to produce more photosynthate than species that exhibit a decline in F_v'/F_m' (J. Cullen, personal comm.), making them an ideal candidate for biofuel screening.

4.3 Quantifying Production of Lipid and Carbohydrate

The primary focus of this research was on the production of lipids, and how it can be optimized for biofuel production. However, our capabilities for analyzing lipid were limited to gravimetric determinations that were relatively insensitive (see Appendix A.4) and so better suited to larger sample volumes than could be produced using the

experimental design (Brand *et al.*, 1981) employed here. Although measurements of gravimetric lipid for N-starved cultures with high lipid contents were consistent with expectations based on the assumption that carbon in energy stores comes from lipid and carbohydrate (for example see Figure 3.3), analyses had to be developed to provide consistent metrics of lipid accumulation during all stages of N-starvation.

It was assumed that during nitrogen starvation, new photosynthate accumulated by the cells was solely allocated toward the energy stores, carbohydrate and lipid. Additionally, the proportional allocation of photosynthate between these compounds was assumed to remain constant as nitrogen-starvation progressed. This allowed for a mass balance equation to be established: the summation of carbon accumulated in carbohydrate and gravimetric total lipid should be equivalent to the measured accumulation of particulate organic carbon (POC) during nitrogen starvation. However, this was not the case for the majority of replicates. Instead, the calculated summation of carbon was greater than the measured accumulation, the difference in which was attributed to questionable gravimetric total lipid values (see Section 3.2.2). Using the mass balance assumption, an inferred total lipid value could be calculated, which was used to show the change in carbon allocation in response to nitrogen-starvation.

Organic matter could have been released from the cells during N-starvation (Myklestad, 1995, Granum *et al.*, 2002). Extracellular polymeric carbohydrates could have been retained on the filters and counted as carbohydrate whereas low molecular weight compounds such as glucan (Myklestad, 2000) would not be measured. Neither occurrence would influence the assumption that the carbon accumulated during N-starvation and measured on filters is made up of carbohydrates and lipids.

4.3.1 Total Lipid

One of the primary problems with gravimetric determination of lipid was that the low biomass collected on each filter results in correspondingly low lipid weights. For example, the mass of a typical vial is approximately 25.5 g whereas the mass of lipid can be well under 2 mg, i.e. four orders of magnitude lower. Gravimetric determinations by difference are thus susceptible to contamination and uncertainties due to small differences in calibration that might have occurred when the semi-microbalance had to be moved between pre- and post-extraction measurements (C. Rafuse, personal comm.). If a smaller extraction vial could successfully be used by the Dionex ASE 350 solvent extraction system, the relative significance of error, due to the vial itself could be reduced.

More commonly-reported analytical issues with the gravimetric methodology are reported by Smedes and Thomasen (1996), Iverson *et al*. (2001), Inoue and Lotufo (2006) and Xiao *et al*. (2012). Briefly, the issues that may have influenced results are incomplete lipid extraction (Smedes & Thomasen, 1996, Iverson *et al.*, 2001, Xiao *et al.*, 2012) and inclusion of non-lipid material, such as pigment, in the extract (Wood, 1985, Inouye & Lotufo, 2006). Bligh and Dyer (1959) reported an optimal lipid extraction solvent of 1:2 w/w methanol:chloroform. Since then, it has been reported that this ratio is not fully effective in the extraction of neutral lipids (Smedes & Thomasen, 1996), which are soluble in methanol. As was done for these experiments, increasing the proportion of methanol in the extraction solvent (1:1.85 v/v methanol:chloroform) presumably resulted in an increase in the recovery of neutral lipid (Smedes & Askland, 1999), but this was not tested against other methanol:chloroform ratios.

Due to the uncertainty in the gravimetric determination of lipid, the variable *TLI* (inferred total lipid) was introduced to provide a more accurate estimate of lipid production during N-starvation. It was assumed that during N-starvation all newly fixed particulate carbon was allocated only towards non-nitrogenous compounds, either carbohydrate or lipid. While other non-nitrogenous compounds, such as glycolate, were likely synthesized during N-starvation it was assumed that these compounds were excreted from the cell (Mague *et al.*, 1980, Wood & van Valen, 1990), limiting impact on the observed metrics. Inferred total lipid was considered here to be a more valid approximation of lipid content than the gravimetrically determined total lipid content.

Similar to gravimetric lipid measurements, Nile Red measurements were considered too inconsistent to be reliable (see Appendix A.3). Concern about the Nile Red fluorochrome being able to permeate the cell wall have been addressed by Chen *et al.* (2011) where culture samples were subjected to microwaves prior to and after the addition of Nile Red. By lysing the cells, Chen *et al*. (2011) showed a 10 times increase in Nile Red fluorescence over cells that were not lysed. Caution must be noted here as Nile Red fluorescence has been shown to be temperature dependent (Deye *et al.*, 1990) so the difference between the microwave and plate reader may influence measurements.

4.3.2 Allocation to Carbohydrate vs. Lipid During N-starvation

The linear regression used to fit the allocation of carbon toward carbohydrate (Γ_{Carb}, mol C_{Carb} · [mol C]$^{-1}$) and lipid (Γ_{TLG}, mol C_{TLG} · [mol C]$^{-1}$), and the rate of carbon allocation toward energy storage pools (ζ_{POC}, mol C · [mol N]$^{-1}$ d^{-1}), due to N-starvation, was shown to be a poor fit for gravimetric total lipid, due to variance in the data. For our work, it was assumed that the allocation of carbon between carbohydrate

and lipids did not vary during N-starvation, allowing for a linear fit of the data. However this may not be an accurate assumption. Hu *et al*. (2008) proposed that the majority of diatoms are capable of accumulating lipid to a maximum lipid content of *c.* 44% of dry weight, while green algae could accumulate *c*. 46% of dry weight under nutrient stressed conditions. If this is generally true, it suggests that the allocation ratio between lipid and carbohydrate could be variable during initial nutrient starvation. Data collected here and elsewhere, suggest that the assumption that the proportion of carbon allocated to carbohydrate (Γ_{Carb}) and lipid (Γ_{TLI}) does not change appears to be incorrect, suggesting that a non-linear model would better fit the data. Regardless, a linear model shows first-order trends between treatments. A more complicated model would have at least one more parameter, with associated increases in statistical uncertainty.

One issue with the data was that the linear regression for both $\Delta\psi_{Carb}$ vs. $\Delta\psi_{POC}$ and $\Delta\psi_{POC}$ vs. *t*, had an intercept (± 95% CI) that differed from the expected value for some treatments. As the linear regressions were calculated for changes that occurred between the N-replete and N-starvation regimes (see Section 3.2.1), the calculated intercept (± 95% CI) should have included 0 (see Section 3.2.3, Figure 3.4). For those treatments that did not it was assumed that nonlinearities due to either the delayed response to N-starvation, typically in the low-light treatments, or the possible excretion of carbon, typically in the high-light treatments, was responsible.

The data showed that carbon allocation (Γ_i , mol $C_i \cdot$ [mol C]$^{-1}$) to carbohydrate vs. lipid during nutrient starvation was not determined by a single factor. 1-way Analysis of Covariance (ANCOVA) showed that there were significant differences due to treatment (Figure 3.13, Table 3.3). Tukeys HSD post-hoc test identified that both diatom species

showed a significant difference in the allocation of carbon between carbohydrate vs. lipid in response to light level: more carbon was allocated toward lipid under increased irradiance. Additionally, significant difference existed between most species, regardless of light level, indicating that both light level and genotype played a role in carbon allocation between carbohydrate vs. lipid Similarly, 1-way ANCOVA results for the rate of carbon allocation to non-nitrogenous compounds (ζ_{POC}, mol C · [mol N]$^{-1}$ · d^{-1}) showed difference between some treatments, but Tukeys HSD results showed that differences in ζ_{POC} between light-level for each species were not significant, suggesting that genotype is the primary factor in determining the rate of carbon allocation towards non-nitrogenous compounds during N-starvation.

Shifrin and Chisholm (1981) reported changes in lipid concentration for multiple marine and freshwater diatom and chlorophytic species before and after 7 – 9 days of N-starvation. To compare their results with those reported here, the metric $\hat{\Gamma}_{TLG}$ (mol C_{TLG} · [mol C]$^{-1}$) was calculated for all species reported in the study:

$$\hat{\Gamma}_{TLG} = \frac{\Delta\psi_{TLG}}{\Delta\psi_{POC}} \tag{4.1}$$

where the proportion of carbon allocated toward lipid ($\hat{\Gamma}_{TLG}$, mol C_{TLG} · [mol C]$^{-1}$) is calculated from the change in lipid ($\Delta\psi_{TLG}$, mol C_{TLG} · [mol N]$^{-1}$) and POC ($\Delta\psi_{POC}$, mol C · [mol N]$^{-1}$) in response to N-starvation (Figure 4.1). Of the 26 species reported, half had a $\hat{\Gamma}_{TLG}$ greater than 0.5 (mol C_{TLG} · [mol C]$^{-1}$), indicating that the majority of carbon was being allocated towards lipid during N-starvation. Comparatively, results from our experiments showed that only a single treatment, *Chaetoceros muelleri* acclimated to high-light, allocated the majority of carbon toward lipid during N-starvation. The

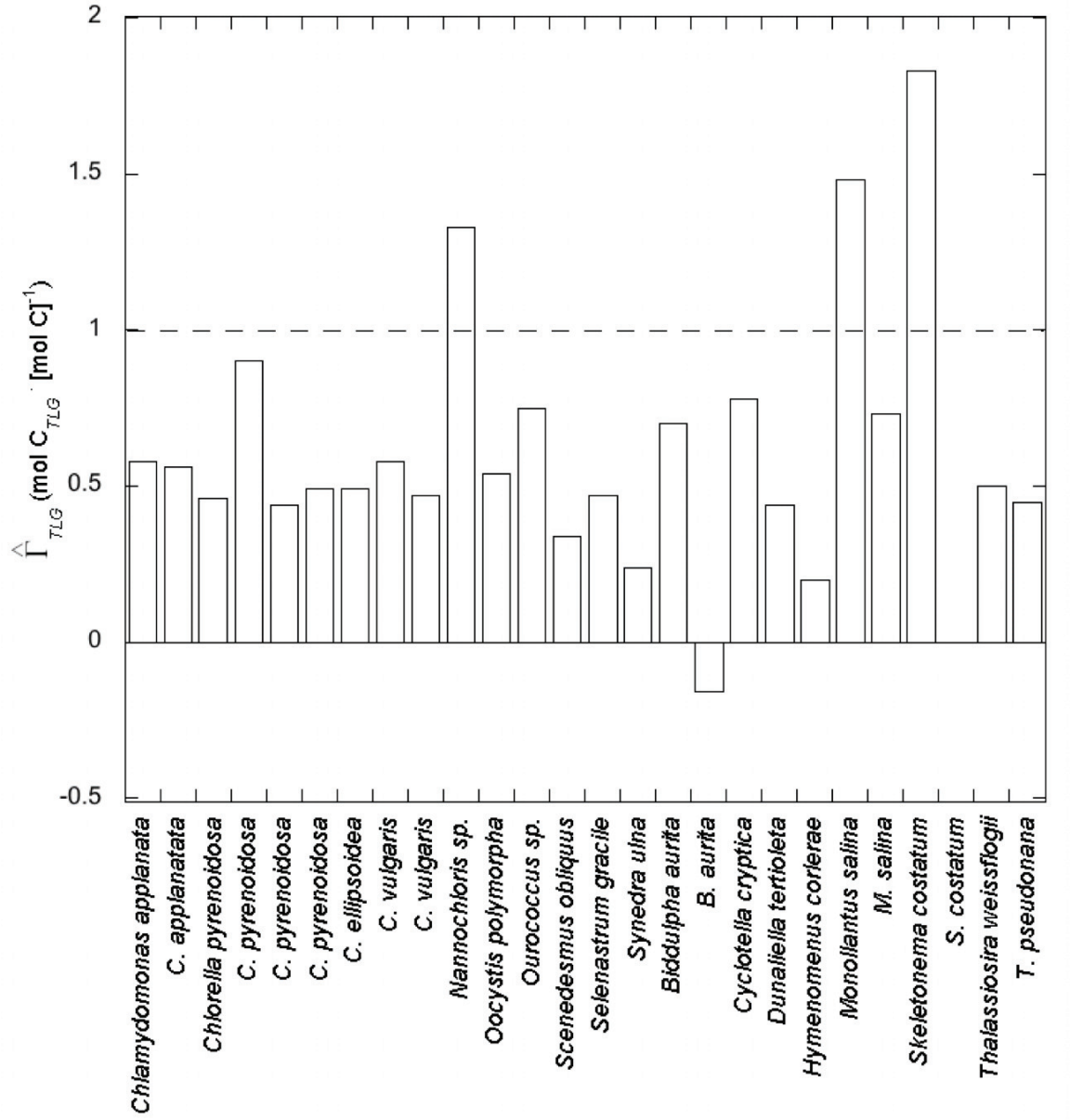

Figure 4.1. Calculated allocation of carbon to lipid as a proportion of carbon accumulated during N-starvation ($\hat{\Gamma}_{TLG}$, mol C_{TLG} · [mol C]$^{-1}$) for multiple microalgae species assessed after 7 – 9 days of N-starvation. Dashed horizontal line represents the theoretical maximum of carbon that could be allocated toward $\hat{\Gamma}_{TLG}$. Values greater than 1 are believed to be resultant from faulty gravimetric measurements. Values less than 0 are believed to be either a result of faulty gravimetric measurements or a loss of lipid from the cell during N-starvation. Data from Shifrin and Chisholm (1981).

estimate of $\hat{\Gamma}_{TLG}$ for *Thalassiosira pseudonana*, the only species present for both studies, was higher for Shifrin and Chisholm's (1981) study than in our low-light treatment (0.47 vs. 0.17 mol $C_{TLG} \cdot$ [mol C]$^{-1}$). The longer duration of N-stress for Shifrin and Chisholm's (1981) experiments may have resulted in a higher proportion of carbon being allocated toward lipid. The low-light level used here, 175 µmol quanta m^{-2} s^{-1} was only slightly less than the light-level used by Shifrin and Chisholm (1981), 190 µmol quanta m^{-2} s^{-1}, so was probably not the cause of the difference.

Larson and Rees (1996) reported the carbon:nitrogen ratio for the diatom *Phaeodactylum tricornutum,* acclimated to 175 µmol quanta m^{-2} s^{-1}, during ongoing N-starvation. ζ_{POC}, calculated from their data was 5.4 ± 0.4 mol C $\cdot$ [mol N]$^{-1}$ $\cdot$ d^{-1} (mean±SE, n = 5), which was significantly higher than the LL treatments reported here, further supporting the idea that genotype influences the rate of carbon allocation towards non-nitrogenous compounds during N-starvation. A review of the literature did not produce a suitable comparison for testing the influence of light level on the rate of carbon allocation to non-nitrogenous compounds during N-starvation.

Excretion – Excreted carbon was not assessed in the experiments reported here, as the focus was solely on particulate pools of carbohydrate, lipid and carbon, so it is useful to consider the influence that excretion might have had on the interpretation of results. Regardless of the physiological state of the microalgae, it is well established that organic products are excreted from the cell (Hellebust, 1965, Mague *et al.*, 1980, Granum *et al.*, 2002). Myklestad (2000) provided a summary of these products and the variables that influenced their release. The predominant form excreted was carbohydrate, followed by amino acids and proteins, lipids and fatty acids, vitamins and others. Algal species,

temperature, irradiance and nutrient status influence both the percent of photosynthate being excreted and its composition. $\Delta\psi_{POC}$ (mol C · [mol N]$^{-1}$) measurements showed decrease on the final day of N-starvation for some high-light treatments. To account for this, more carbon than was accumulated would have to be excreted from the cell. As the carbon allocation ratios used here were normalized to particulate organic nitrogen, any decrease would result from a decrease in carbon, specifically in lipid and carbohydrate, or increasing nitrogen. As nitrate was already depleted, inferring that PON could not increase further, it is likely that carbon was being lost from these pools. As observable excretion from the carbon pool was apparently limited to a single day, it is believed that excretion could have influenced the interpretation of results; however, as the focus was on the accumulation of particulate material during N-starvation, excretion could be excluded from consideration.

The re-mobilization of carbon away from the lipid pool to carbohydrate may explain why the lipid-carbon allocation in the high-irradiance treatment of *Tetraselmis* sp. was consistently lower than under nutrient-replete conditions. As with the other treatments, it was expected that nitrogen starvation would increase the carbon allocated toward lipid, but this was not observed. D'Souza and Kelly (2000) reported a nutrient-starvation response in *Tetraselmis suecica* in which lipid decreased, however this appears to occur in the minority of cases studied (Shifrin & Chisholm, 1981, Thomas *et al.*, 1984b, Rodolfi *et al.*, 2009). Phosphate starvation has also been shown to decrease lipid content in *Tetraselmis* sp. (Molina *et al.*, 1991, Guschina & Harwood, 2006), but phosphate was not limiting during these experiments.

It was assumed that during N-starvation, carbon was allocated solely toward particulate pools of carbohydrate and lipid, and that the proportion at which this was done remained constant. As a result of these assumptions, metrics were developed to describe the proportional allocation of carbon to carbohydrate vs. lipid (Γ_i, mol C_i · [mol C]$^{-1}$) during N-starvation. Species and light level were tested to determine genotypic and phenotypic influence on Γ_i. As expected, carbon was allocated more toward lipid at high-light, however this varied by species and the increase from the low-light treatment was not always significant (Figure 3.13).

4.4 Influence of Species and Irradiance on Carbon Accumulation

On average green algae have higher lipid content than diatoms under nutrient-replete conditions (Shifrin & Chisholm, 1981, Sheehan *et al.*, 1998, Scott *et al.*). However, polar lipids are accumulated under nutrient-replete conditions, whereas neutral lipids are accumulated during nutrient-starvation (Singh & Kumar, 1992, Yu *et al.*, 2009). Lipid-rich species typically have a lower growth rate than those with less cellular lipid (Griffiths & Harrison, 2009, Rodolfi *et al.*, 2009). Lipid data presented here did not match this "typical" description. At both irradiances, and under nutrient-replete and nutrient-starved growth, the mean lipid concentration (mg L^{-1}) in the diatoms, which had a higher mean growth rate, was greater than that for green alga. Rodolfi *et al*. (2009) showed similar results for nutrient-replete conditions; the mean lipid content for the diatoms *Chaetoceros muelleri* and *Thalassiosira pseudonana* was greater than for *Tetraselmis* sp.. *Dunaliella salina* was not included in the comparison (Rodolfi *et al.*, 2009).

There was a significant difference in the carbon allocation between carbohydrate and lipid due to the treatment, i.e. species and irradiance, used for these experiments (Table 3.2, Figure 3.13). During N-starvation, the treatment that had less than half of new carbon allocated toward carbohydrate, Γ_{Carb} (mol C_{Carb} · [mol C]$^{-1}$), thus more than half of new carbon was allocated toward lipid, Γ_{TLI} (mol C_{TLI} · [mol C]$^{-1}$), was the high-light culture of *Chaetoceros muelleri,* indicating that this species synthesized primarily lipid when under nitrogen-stress at high irradiance. The proportion of carbon allocated toward lipid during N-starvation, showed slight increase at high light for all treatments, albeit in most cases the increase between light levels was not significant (Figure 3.13).

Irradiance and species were shown to have a significant effect on the rate of carbon allocation toward the energy storage pool, ζ_{POC} (mol C · [mol N]$^{-1}$), using 2-way ANCOVA (Table 3.3, Figure 3.14). However, Tukeys HSD did not establish significant difference between light treatments for any species (Figure 3.14). During N-starvation, the high-light treatment of *Chaetoceros muelleri* had the highest rate of carbon allocation toward energy stores, however was not significantly higher than the low-light treatment of *C. muelleri*.

The two metrics used for this thesis describe the proportion of carbon allocated towards non-nitrogenous compounds, Γ_i (mol C_i · [mol C]$^{-1}$), and the rate at which carbon was allocated toward these compounds, ζ_{POC} (mol C · [mol N]$^{-1}$ d^{-1}). Combining the two metrics provides a description on how microalgae allocate carbon in response to N-starvation. For this thesis, the highest lipid production was in the high-light culture *C. muelleri*. This preferentially accumulated lipids during N-starvation, and had the highest

rate of carbon allocated toward the energy storage pool. Simply put, this treatment accumulated lipids quickly.

4.5 Influence of Bacteria

Cultures used for these experiments were not axenic, introducing the possibility that the presence of bacteria could have influenced values of particulate organic carbon (POC) and particulate organic nitrogen (PON) (Danger et al., 2007), thereby altering the calculated rate of carbon allocation toward energy stores (ζ_{POC} , mol C · [mol N]$^{-1}$ · d^{-1}). Under nutrient-replete conditions, the C:N ratio for bacteria is lower than the Redfield Ratio of 6.625 mol C · [mol N]$^{-1}$ (Redfield, 1958), commonly observed for the microalgal cultures (Vrede et al., 2002). In response to nitrogen-starvation, bacterial C:N increases (Vrede *et al.*, 2002), however the increase is much smaller than what was observed for the microalgal cultures. If enough bacteria biomass were present to influence results, the calculated rate of POC being allocated toward energy stores would be underestimated. To correct this rate, a bacterial population would have to be determined (e.g. Coulter-Counter) with bacterial POC and PON being estimated using reported cellular content (fg · [cell]$^{-1}$) (Vrede *et al.*, 2002). Removing the estimated bacterial POC and PON from the measured POC and PON values would result with microalgal POC and PON, which can then be used to re-calculate the rate of carbon allocation toward energy stores. Bacteria contribution to POC and PON were not determined for these experiments, as the size range utilized on the Coulter-Counter was greater than bacterial cell size. Contamination cannot be conclusively excluded as a factor in our analyses, but it should be recognized that the cultures had been growing for many daily transfers at growth rates

of 0.59 - 2.47 d^{-1}, and a significant bacterial component could have persisted only if bacterial growth rates were nearly as high. This is unlikely in healthy cultures.

4.6 Conclusion

This research focused on finding a microalga that produces large quantities of lipid under nutrient starvation, and the optimum conditions for this production. The key question was: what influences do species and light level have on the accumulation of lipid by microalgae during nutrient starvation? To answer this question, experiments were conducted on four species of microalgae, grown at two light levels and developing comparable metrics, ultimately identifying the best performance and providing a tool for screening other species of microalgae. These metrics quantified the change in carbon allocation to carbohydrate (Γ_{Carb}) and inferred total lipid (Γ_{TLI}) under nutrient-starvation, as well as the rate at which the energy storage pool increased (ζ_{POC}). Through these metrics, it was determined that a combination of high-light and an appropriate species, in this case *Chaetoceros muelleri*, led to more than half of the carbon accumulated during three days of N-starvation being allocated toward lipids.

The use of quantitative metrics of lipid production, determined in a highly repeatable experimental regime, provides rapid, comparable parameters that can be utilized in high-throughput algal screening for biofuel purposes.

Appendix A

A.1 Raw Data

Data presented in this thesis were mostly normalized to particulate organic nitrogen (PON, μmol N L^{-1}) to remove biases due to differences in biomass as cellular nitrogen. Normalization facilitates the comparison of chemical composition of algae during and between treatments; however experimental results for individual chemical compounds are not reported. For completeness, and to make it easier to evaluate variation in normalized results, measurements of chemical composition prior to normalization are presented in Figures A.1 – A.8. Physiological status measurements were not normalized to PON. Sample analyses are described in section 2.3.

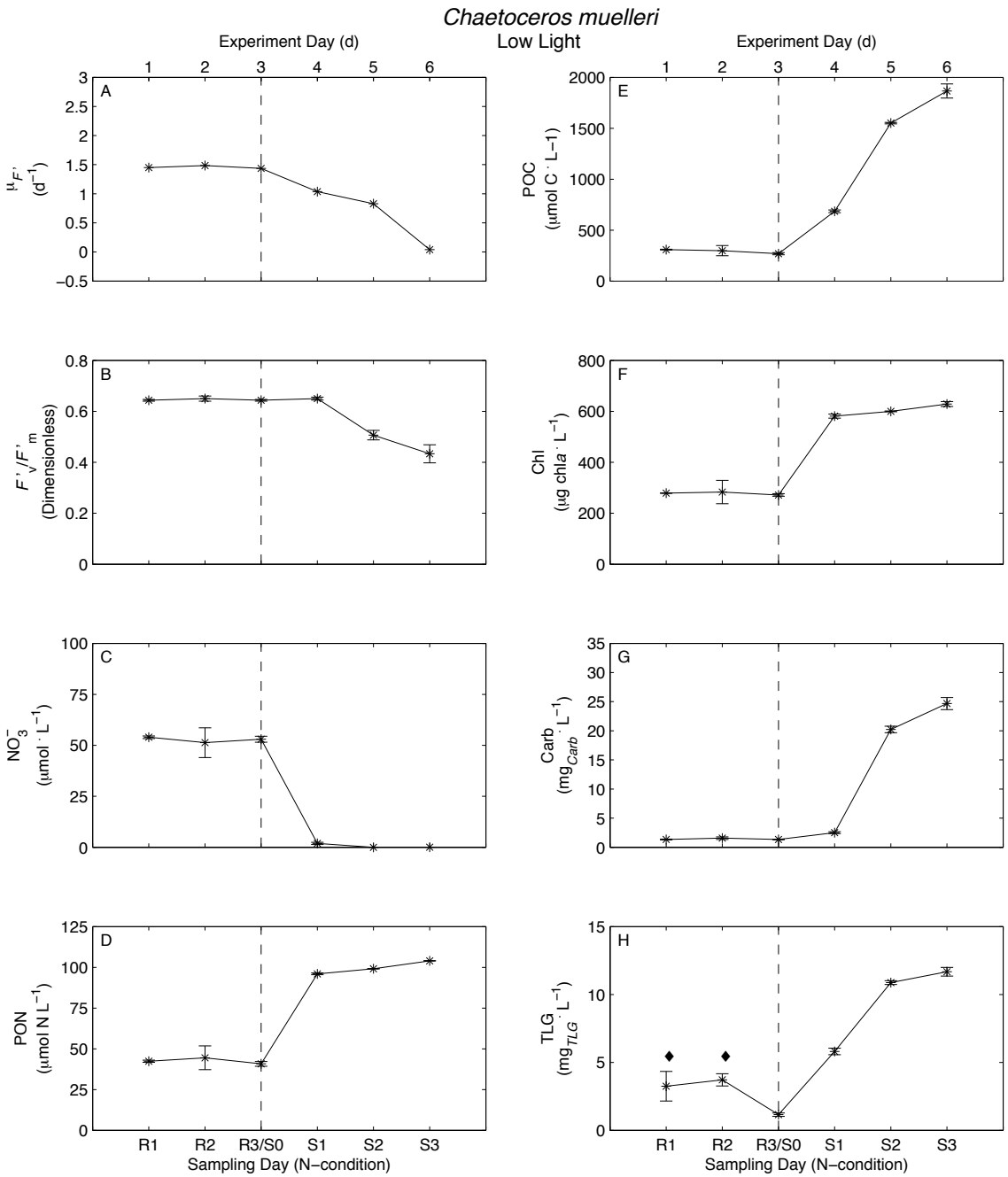

Figure A.1. Physiological status and cellular composition of the low light treatment of *Chaetoceros muelleri*. (A) growth rate ($\mu_{F'}$, d^{-1}) based on non-dark adapted *in vivo* fluorescence, (B) non-dark adapted F_v'/F_m' (dimensionless), (C) Residual nitrate (NO_3^-, µmol L^{-1}) of the media (D) particulate organic nitrogen (PON, µmol N L^{-1}), (E) particulate organic carbon (POC, µmol C L^{-1}), (F) chlorophyll *a* (µg chl *a* L^{-1}), (G) carbohydrate (mg_{Carb} L^{-1}) and (H) gravimetric total lipid (mg_{TLG} L^{-1}). Error bars indicate standard error (n = 3), unless otherwise indicated: ♦ range (n = 2) shown or ∇ no error bars (n = 1).

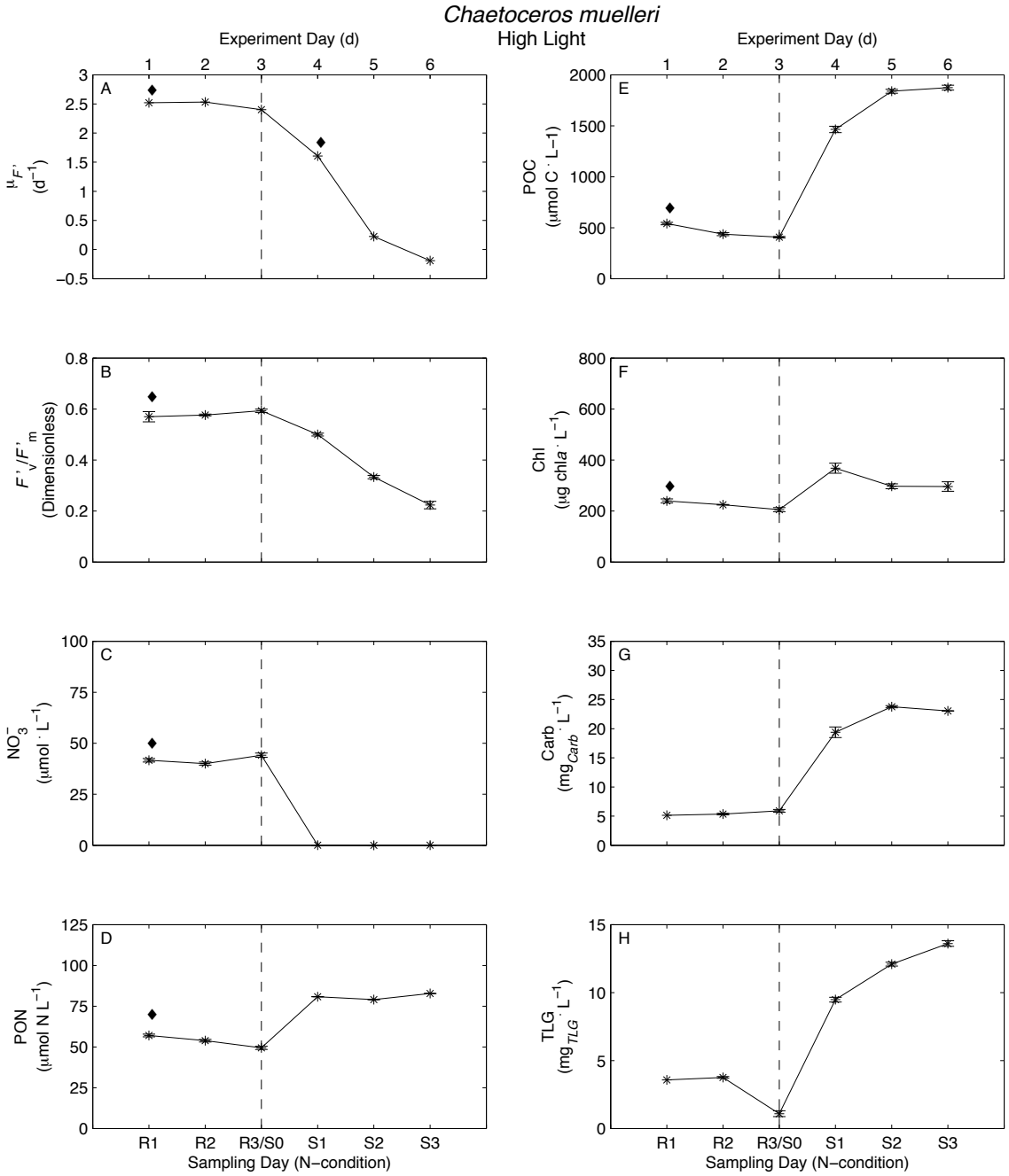

Figure A.2. Physiological status and cellular composition of the high light treatment of *Chaetoceros muelleri*. (A) growth rate ($\mu_{F'}$, d^{-1}) based on non-dark adapted *in vivo* fluorescence, (B) non-dark adapted F_v'/F_m' (dimensionless), (C) Residual nitrate (NO_3^-, $\mu mol\ L^{-1}$) of the media (D) particulate organic nitrogen (PON, $\mu mol\ N\ L^{-1}$), (E) particulate organic carbon (POC, $\mu mol\ C\ L^{-1}$), (F) chlorophyll *a* ($\mu g\ chl\ a\ L^{-1}$), (G) carbohydrate ($mg_{Carb}\ L^{-1}$) and (H) gravimetric total lipid ($mg_{TLG}\ L^{-1}$). Symbols as shown in Figure A.1

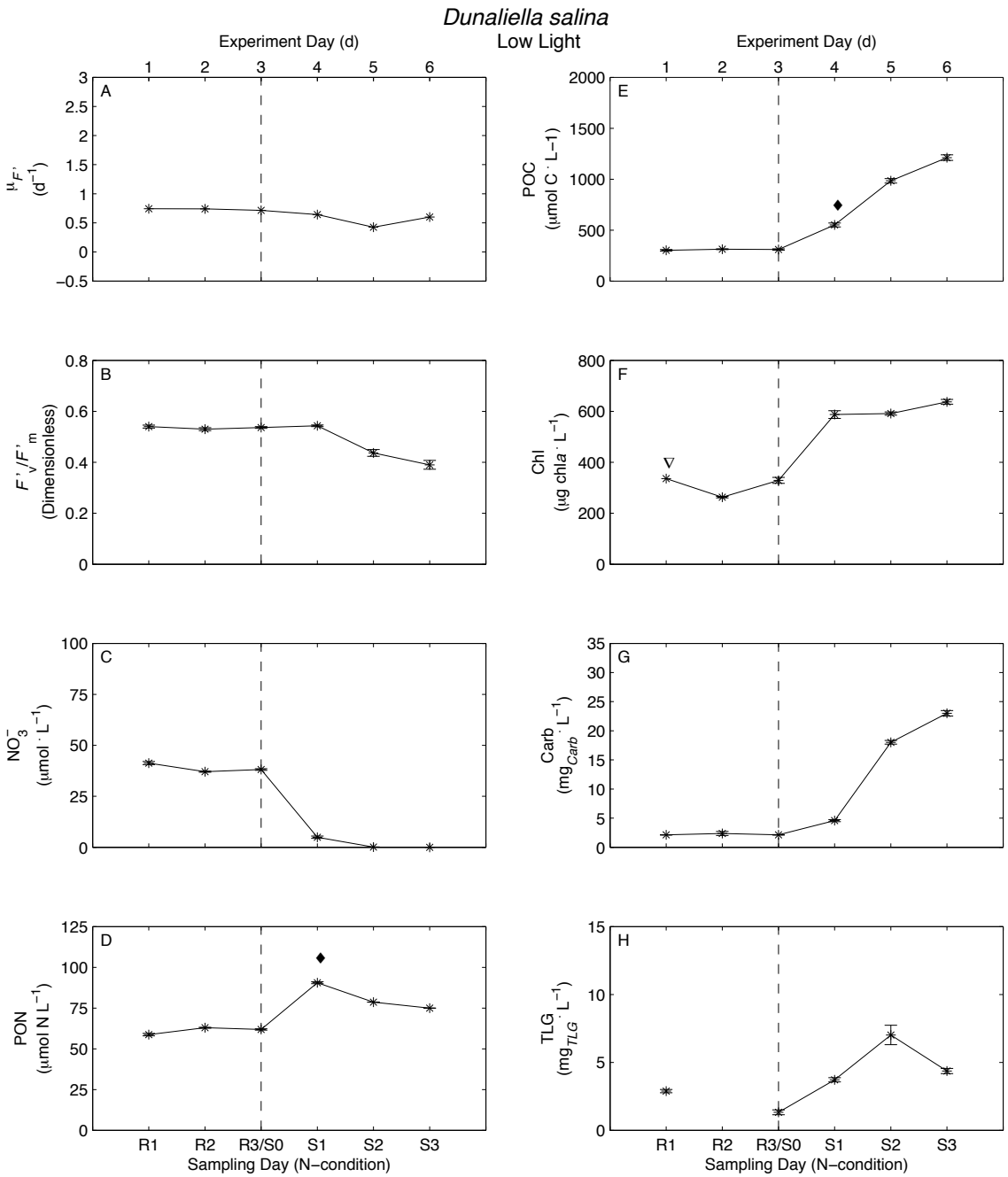

Figure A.3. Physiological status and cellular composition of the low light treatment of *Dunaliella salina*. (A) growth rate ($\mu_{F'}$, d^{-1}) based on non-dark adapted *in vivo* fluorescence, (B) non-dark adapted F_v'/F_m' (dimensionless), (C) Residual nitrate (NO_3^-, µmol L^{-1}) of the media (D) particulate organic nitrogen (PON, µmol N L^{-1}), (E) particulate organic carbon (POC, µmol C L^{-1}), (F) chlorophyll *a* (µg chl *a* L^{-1}), (G) carbohydrate (mg_{Carb} L^{-1}) and (H) gravimetric total lipid (mg_{TLG} L^{-1}). Symbols as shown in Figure A.1

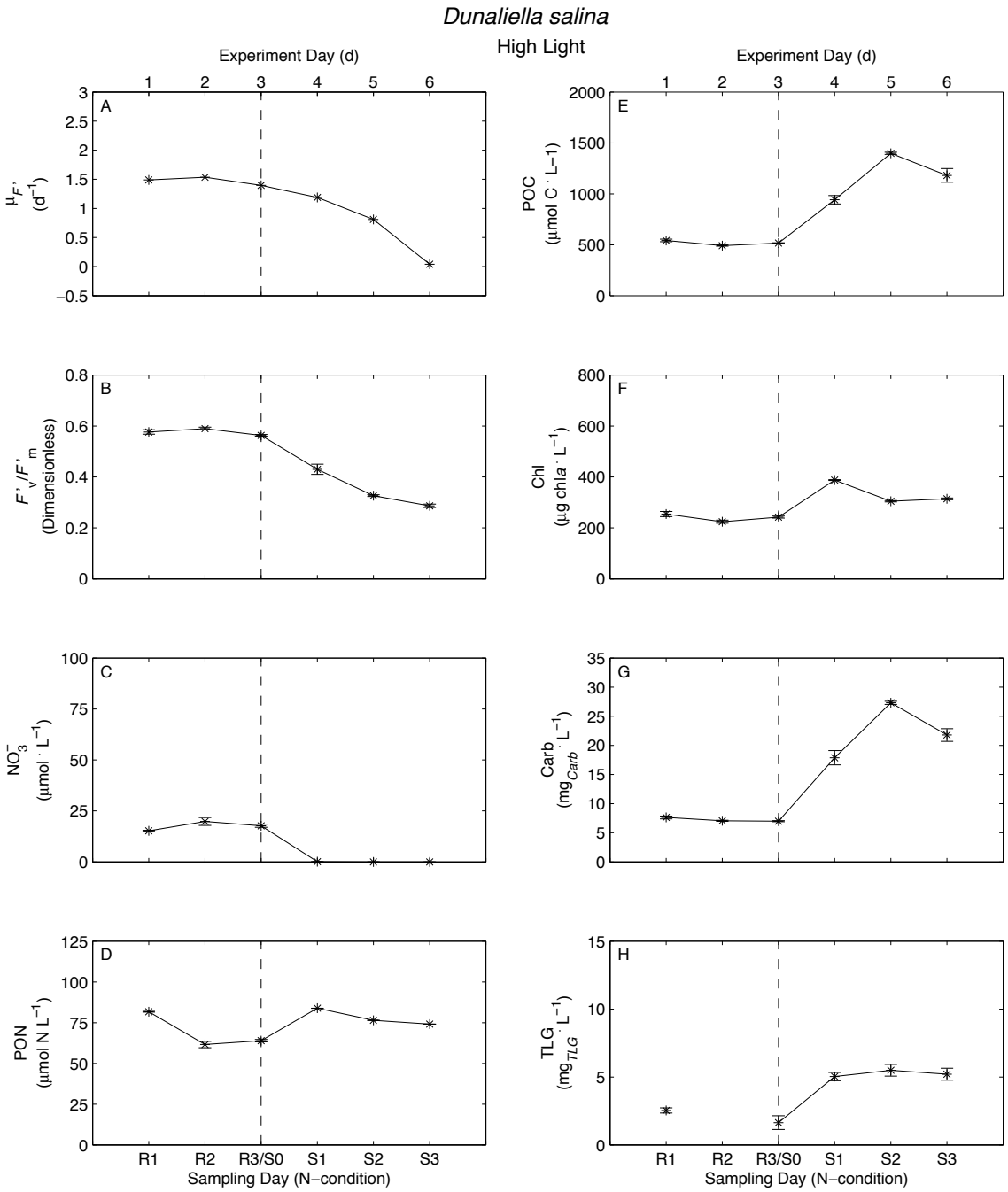

Figure A.4. Physiological status and cellular composition of the high light treatment of *Dunaliella salina*. (A) growth rate ($\mu_{F'}$, d^{-1}) based on non-dark adapted *in vivo* fluorescence, (B) non-dark adapted F_v'/F_m' (dimensionless), (C) Residual nitrate (NO_3^-, µmol L^{-1}) of the media (D) particulate organic nitrogen (PON, µmol N L^{-1}), (E) particulate organic carbon (POC, µmol C L^{-1}), (F) chlorophyll *a* (µg chl *a* L^{-1}), (G) carbohydrate (mg_{Carb} L^{-1}) and (H) gravimetric total lipid (mg_{TLG} L^{-1}). Symbols as shown in Figure A.1

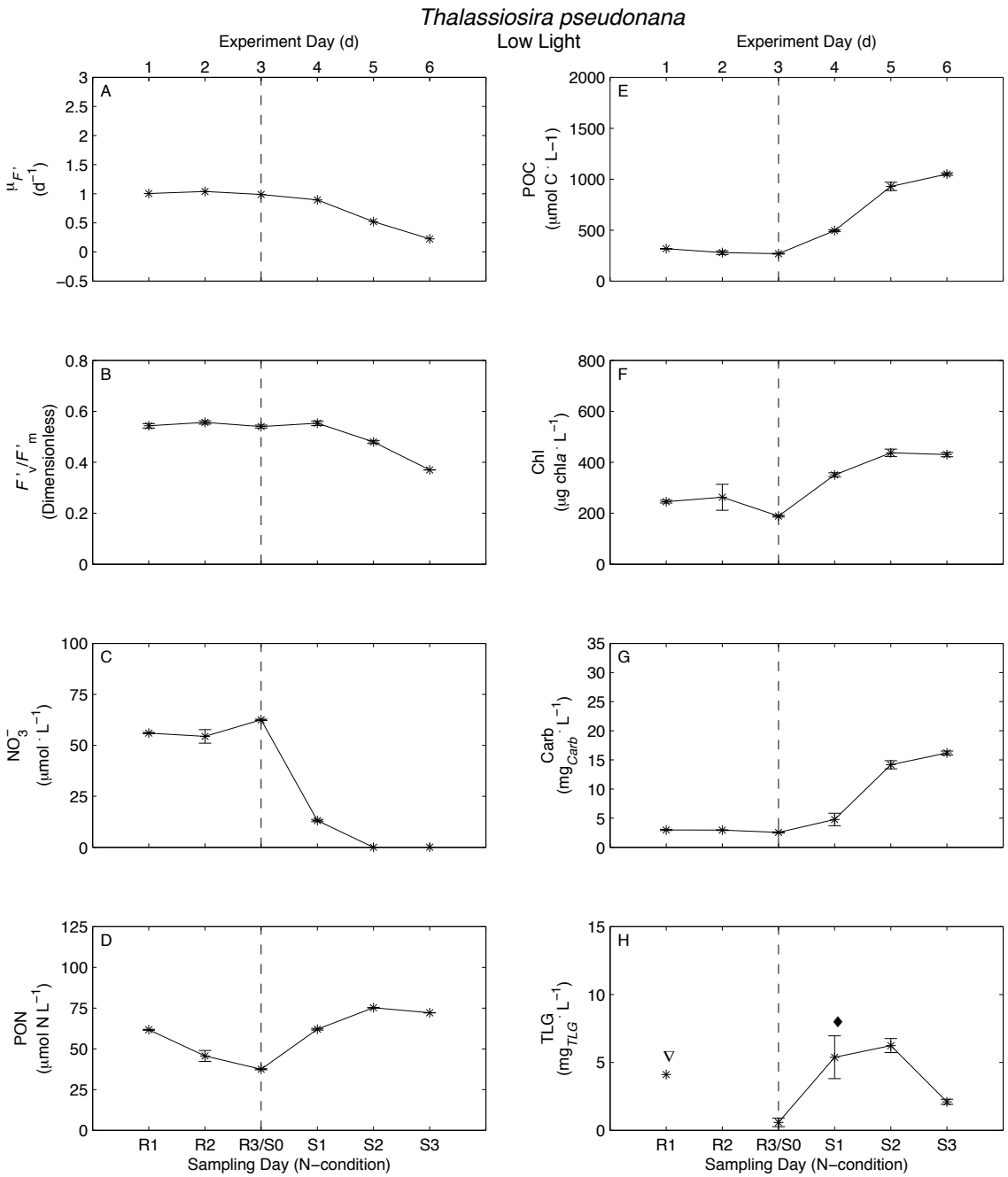

Figure A.5. Physiological status and cellular composition of the low light treatment of *Thalassiosira pseudonana*. (A) growth rate ($\mu_{F'}$, d^{-1}) based on non-dark adapted *in vivo* fluorescence, (B) non-dark adapted F_v'/F_m' (dimensionless), (C) Residual nitrate (NO_3^-, µmol L^{-1}) of the media (D) particulate organic nitrogen (PON, µmol N L^{-1}), (E) particulate organic carbon (POC, µmol C L^{-1}), (F) chlorophyll *a* (µg chl *a* L^{-1}), (G) carbohydrate (mg_{Carb} L^{-1}) and (H) gravimetric total lipid (mg_{TLG} L^{-1}). Symbols as shown in Figure A.1

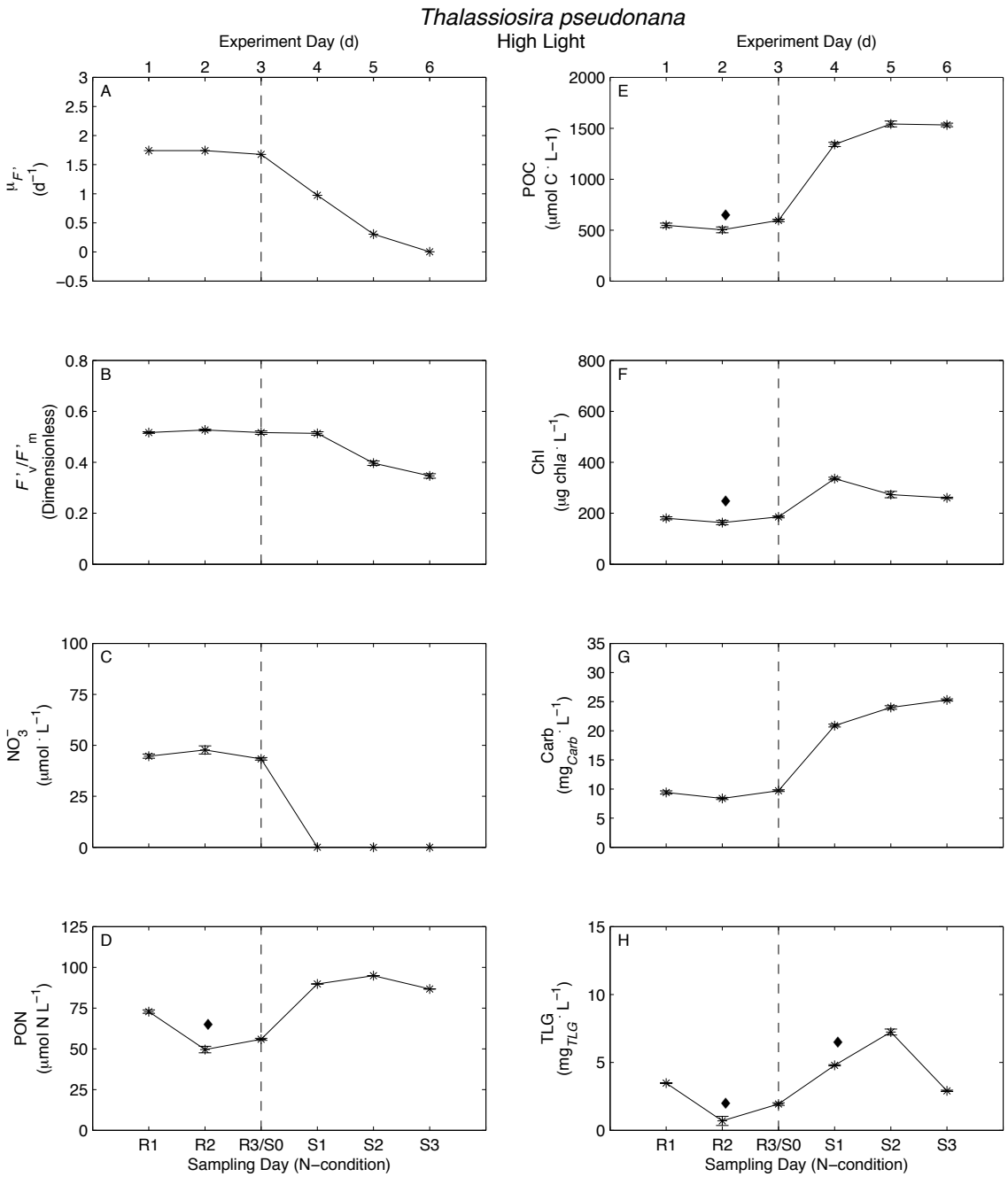

Figure A.6. Physiological status and cellular composition of the high light treatment of *Thalassiosira pseudonana*. (A) growth rate ($\mu_{F'}$, d^{-1}) based on non-dark adapted *in vivo* fluorescence, (B) non-dark adapted F_v'/F_m' (dimensionless), (C) Residual nitrate (NO_3^-, $\mu mol\ L^{-1}$) of the media (D) particulate organic nitrogen (PON, $\mu mol\ N\ L^{-1}$), (E) particulate organic carbon (POC, $\mu mol\ C\ L^{-1}$), (F) chlorophyll *a* (μg chl *a* L^{-1}), (G) carbohydrate ($mg_{Carb}\ L^{-1}$) and (H) gravimetric total lipid ($mg_{TLG}\ L^{-1}$). Symbols as shown in Figure A.1

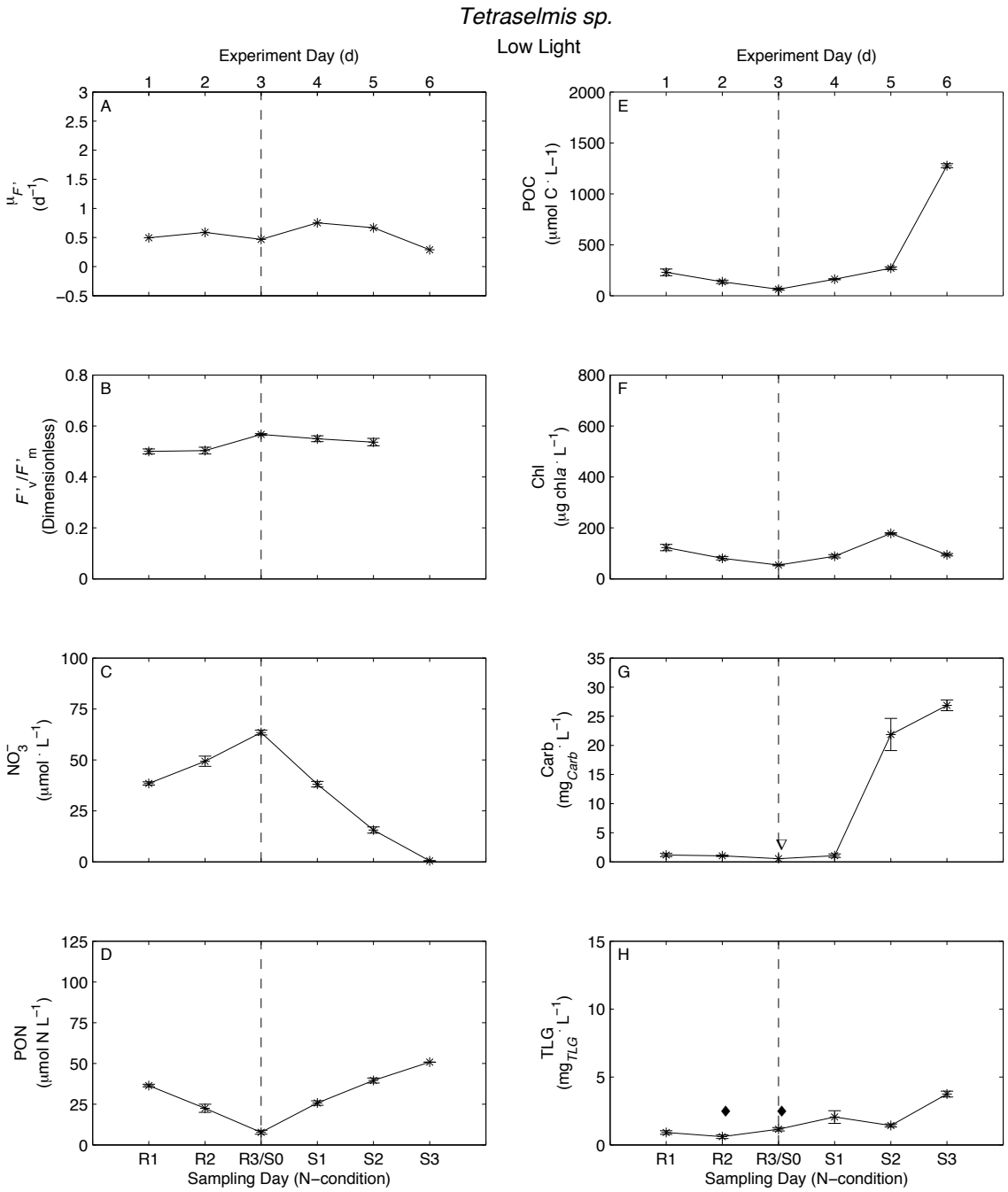

Figure A.7. Physiological status and cellular composition of the low light treatment of *Tetraselmis* sp. (A) growth rate ($\mu_{F'}$, d^{-1}) based on non-dark adapted *in vivo* fluorescence, (B) non-dark adapted F_v'/F_m' (dimensionless), (C) Residual nitrate (NO_3^-, µmol L^{-1}) of the media, (D) particulate organic nitrogen (PON, µmol N L^{-1}), (E) particulate organic carbon (POC, µmol C L^{-1}), (F) chlorophyll *a* (µg chl *a* L^{-1}), (G) carbohydrate (mg_{Carb} L^{-1}) and (H) gravimetric total lipid (mg_{TLG} L^{-1}). Symbols as shown in Figure A.1

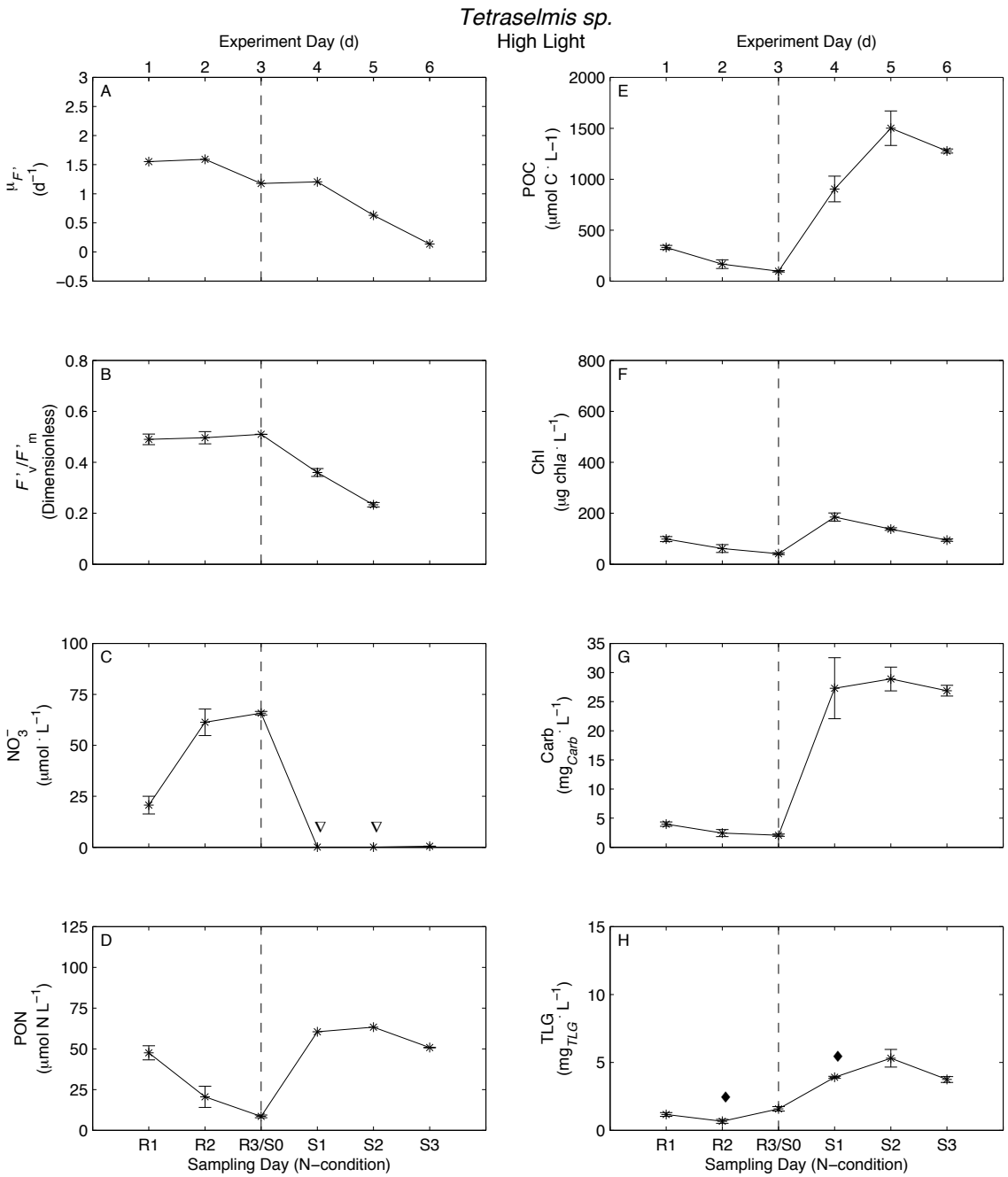

Figure A.8. Physiological status and cellular composition of the high light treatment of *Tetraselmis* sp. (A) growth rate ($\mu_{F'}$, d^{-1}) based on non-dark adapted *in vivo* fluorescence, (B) non-dark adapted F_v'/F_m' (dimensionless), (C) Residual nitrate (NO_3^-, µmol L^{-1}) of the media, (D) particulate organic nitrogen (PON, µmol N L^{-1}), (E) particulate organic carbon (POC, µmol C L^{-1}), (F) chlorophyll *a* (µg chl *a* L^{-1}), (G) carbohydrate (mg_{Carb} L^{-1}) and (H) gravimetric total lipid (mg_{TLG} L^{-1}). Symbols as shown in Figure A.1

A.2 Mean N-replete Values

Data presented in Table 3.1 were based on the third day of the N-replete regime, chosen as the N-replete reference relative to which changes due to N-starvation were compared to. Means, ±SE ($n > 3$), for the duration of the N-replete regime (R1 – R3) are an alternate measure of N-replete results. These are presented in Table A.1 for comparison.

Table A.1. Chemical composition and physiological status for four species of microalgae acclimated to N-replete growth at 30°C at two different light levels (LL = 175 μmol quanta m^{-2} s^{-1} PAR, HL = 600 μmol quanta m^{-2} s^{-1} PAR) on a 12h:12h light:dark cycle: measurements for the final day, R3/S0, of a 3 day N-replete regime. Growth rate ($\mu_{F'}$), F'_v/F'_m, chlorophyll *a*:PON, carbon:chlorophyll *a*, POC:PON, carbon content of carbohydrate and gravimetrically-determined total lipid normalized to PON (ψ_{Carb} and ψ_{TLG}). Error ± SE for n = 3 independent cultures, unless otherwise indicated.

		$\mu_{F'}$ (d^{-1})	F'_v/F'_m (dimensionless)	Chl *a*:N (g · [mol N]$^{-1}$)	C:Chl *a* (g:g)	ψ_{POC} (mol C · [mol N]$^{-1}$)	ψ_{Carb} (mol C_{Carb} · [mol N]$^{-1}$)	ψ_{TLG} (mol C_{TLG} · [mol N]$^{-1}$)
Chaetoceros muelleri	LL	1.46 (0.01)	0.65 (0.003)	6.54 (0.08)	12.61 (0.31)	6.85 (0.13)	1.13 (0.08)	3.77 (0.82)
	HL	2.48 (0.04)	0.58 (0.01)	4.17 (0.03)	24.47 (0.7)	8.50 (0.25)	3.56 (0.18)	3.05 (0.60)
Dunaliella salina	LL	0.73 (0.01)	0.54 (0.003)	4.91 (0.27)	12.48 (0.64)	5.04 (0.05)	1.20 (0.05)	2.23 (0.40)
	HL	1.47 (0.04)	0.58 (0.01)	3.52 (0.12)	25.89 (0.47)	7.57 (0.25)	3.52 (0.13)	1.8 (0.25)
Thalassiosira pseudonana	LL	1.01 (0.02)	0.55 (0.004)	4.93 (0.37)	15.36 (0.8)	6.16 (0.30)	2.02 (0.12)	1.91 (0.99)
	HL	1.72 (0.02)	0.52 (0.003)	2.89 (0.17)	33.27 (4.82)	9.37 (0.57)	5.21 (0.28)	2.40 (0.26)
Tetraselmis sp.	LL	0.52 (0.04)	0.52 (0.01)	5.05 (0.95)	19.21 (0.08)	7.33 (1.06)	1.55 (0.24)	3.8 (1.44)
	HL	1.44 (0.13)	0.5 (0.01)	3.31 (0.41)	33.61 (1.90)	8.80 (0.71)	5.04 (0.96)	5.55 (1.84)

A.3 Estimation of Lipid Concentration Using a Nile Red Assay

Fluorescence of the dye Nile Red has been used for an *in vivo* estimation of lipid concentration in an algal culture (Dempster & Sommerfeld, 1998). During this thesis research, the methods of Elsey *et al.* (2007) and Chen *et al.* (2009) were applied (see Section 2.3.6). However, complications encountered during experiments as well as known issues with this methodology allowed for only a qualitative assessment.

Standard solution – During this research a standard Chemically Defined Lipid Concentrate (CDLC, Invitrogen, Carlsbad, CA, USA), did not stain consistently throughout experiments, preventing a repeatable dilution series from being established. For example, when CDLC was stained with Nile Red and observed using fluorescence microscopy, staining did not appear homogenous throughout the different observable particles, nor within subsamples of the same aliquot (not reported). Instead, following each run, the lipid fluorescence values were normalized to the fluorescence signal of a standard plate supplied by BioTek. The normalized lipid fluorescence values were then used as a qualitative indicator of lipid concentration, used in the evaluation of apparent outliers in gravimetric lipid measurements.

Effects of assay conditions – Nile Red fluorescence has been shown to be influenced by temperature (Deye *et al.*, 1990, Chen *et al.*, 2009), staining time (Priscu *et al.*, 1990) and species (Chen *et al.*, 2009). During experiments, both ambient and plate reader temperatures were not controlled for, nor recorded, possibly influencing fluorescence readings. It was noted, however, that large changes in the ambient room temperature were reflected in the plate reader temperature. Coinciding experiments, using the microalgae *Nanofrustulum shiloi,* confirmed that the initial temperature of the sample

and Nile Red dye influenced the kinetics of the reaction, ultimately altering the fluorescence values obtained (Figure A.9).

Cultures of *Nanofrustulum shiloi* were cultured at 25°C, 30°C or 35°C for a minimum of 8 generations prior to assessment under N-replete and N-starved conditions. To determine the effect of temperature on the reaction kinetics, aliquots of Nile Red dye were placed in an incubator with a temperature matching that of the *N. shiloi* cultures (i.e. 25°C, 30°C or 35°C) for 30 min. prior to analysis. The results obtained here were similar to Chen *et al.* (2009), who reported that Nile Red fluorescence values increased roughly 50% between 20°C - 40°C, decreasing at greater temperatures, with rapid decrease occurring at temperatures greater than 50°C. It should be noted that Chen *et al.* (2009) incubated the stained cultures at each temperature for 10 min. after they had been stained with Nile Red, whereas the unstained culture and Nile Red was incubated at each temperature for 30 min. prior to staining for these experiments. As fluorescence was read over a 30 min. interval, staining time was not believed to be a concern. Species was shown to have an effect on fluorescence values (Figures A.10, A.11) however, without a robust lipid standard or accurate measure of *TLG*, this could not be controlled for here.

There were concerns regarding the lipid composition of the samples, as Nile Red indiscriminately stained both polar and non-polar lipid (Chen *et al.*, 2009). The excitation (540 ± 12.5 nm) and emission (590 ± 10 nm) wavelengths of the filter set used were more specific for neutral lipids; however overlap with polar lipids did exist (BioTek Instruments Inc. Winooski, VT, USA.). Without knowing the specific lipid composition of individual treatments, it cannot be determined if shifts observed in Nile Red fluorescence, without corresponding changes in gravimetric lipid, were due to

measurement error or changes in the polar vs. non-polar lipid composition. However, results obtained during these experiments suggested that Nile Red, and the appropriate filter set, could be used to determine the increase in neutral lipid during N-starvation. For example, during nitrogen-starvation, the increase in particulate organic carbon (POC) normalized to particulate organic nitrogen (PON), $\Delta\psi_{POC}$ (mol C $\cdot$ [mol N]$^{-1}$), increased as a result of carbon being allocated toward non-nitrogenous compounds. In some cases, most notably *Chaetoceros muelleri*, there was a corresponding increase in Nile Red fluorescence (Figure A.10). To ensure that the increase in Nile Red fluorescence was not due to the fluorochrome bonding to other chemical compounds, Nile Red fluorescence was compared to the gravimetric total lipids (*TLG*), present per sample. In the case of *C. muelleri*, there was a corresponding increase for both Nile Red fluorescence and *TLG*, which was above the L.O.Q. (10 SE of the blank, where $SE = SD/\sqrt{n}$, n = 3). Increases in Nile Red fluorescence exist for all taxa other than *Dunaliella salina,* which remained constant throughout (Figure A.11).

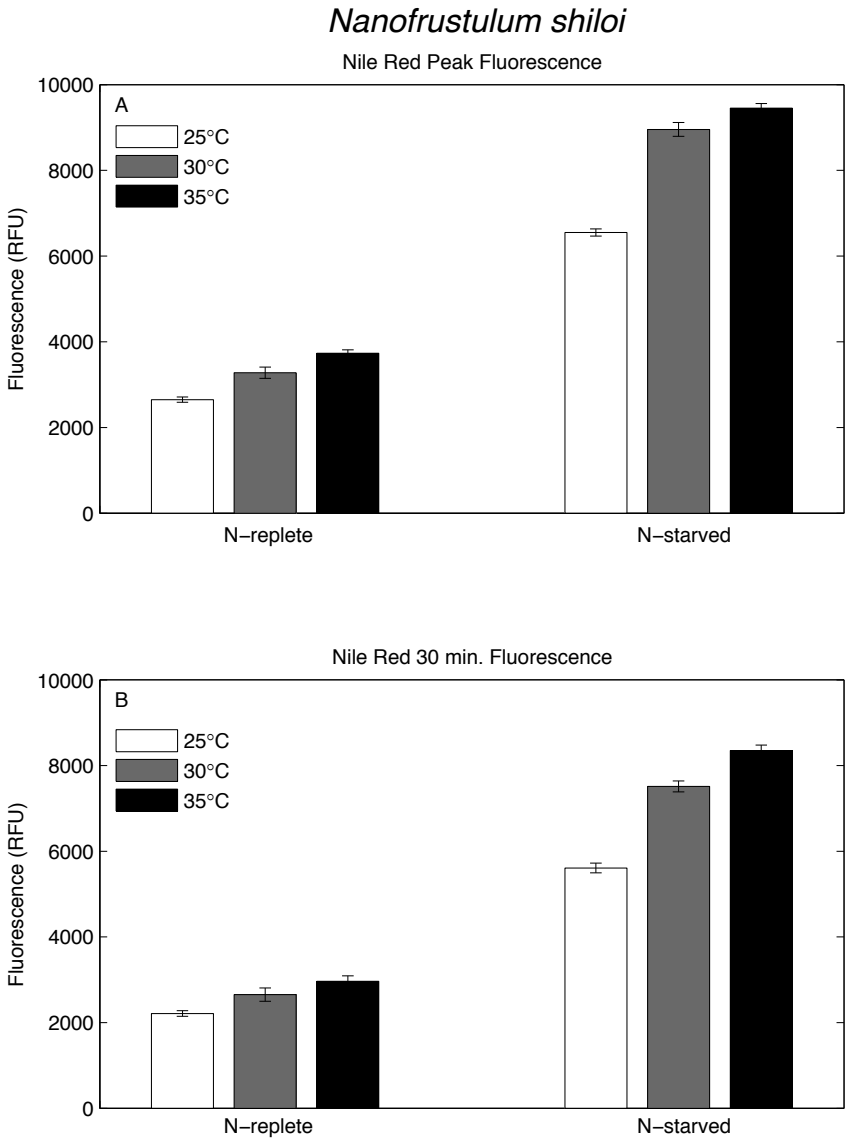

Figure A.9. Influence of temperature and physiological state of the microalgae *Nanofrustulum shiloi* on Nile Red fluorescence (RFU) values. Measurements were made on cultures during nutrient replete (N-replete) and nutrient starved (N-starved) conditions. Samples were incubated at 25°C, 30°C or 35°C, for 30 min. prior to being measured on a plate reader every 30 s. for 10 min, then every 2 min. for another 20 min. (A) Nile Red fluorescence peak values from the time series. (B) Nile Red fluorescence values from the final point of the time series (t = 30 min.). Shaded bars indicate individual temperatures with errorbars representing standard error (n = 3) of the measurements.

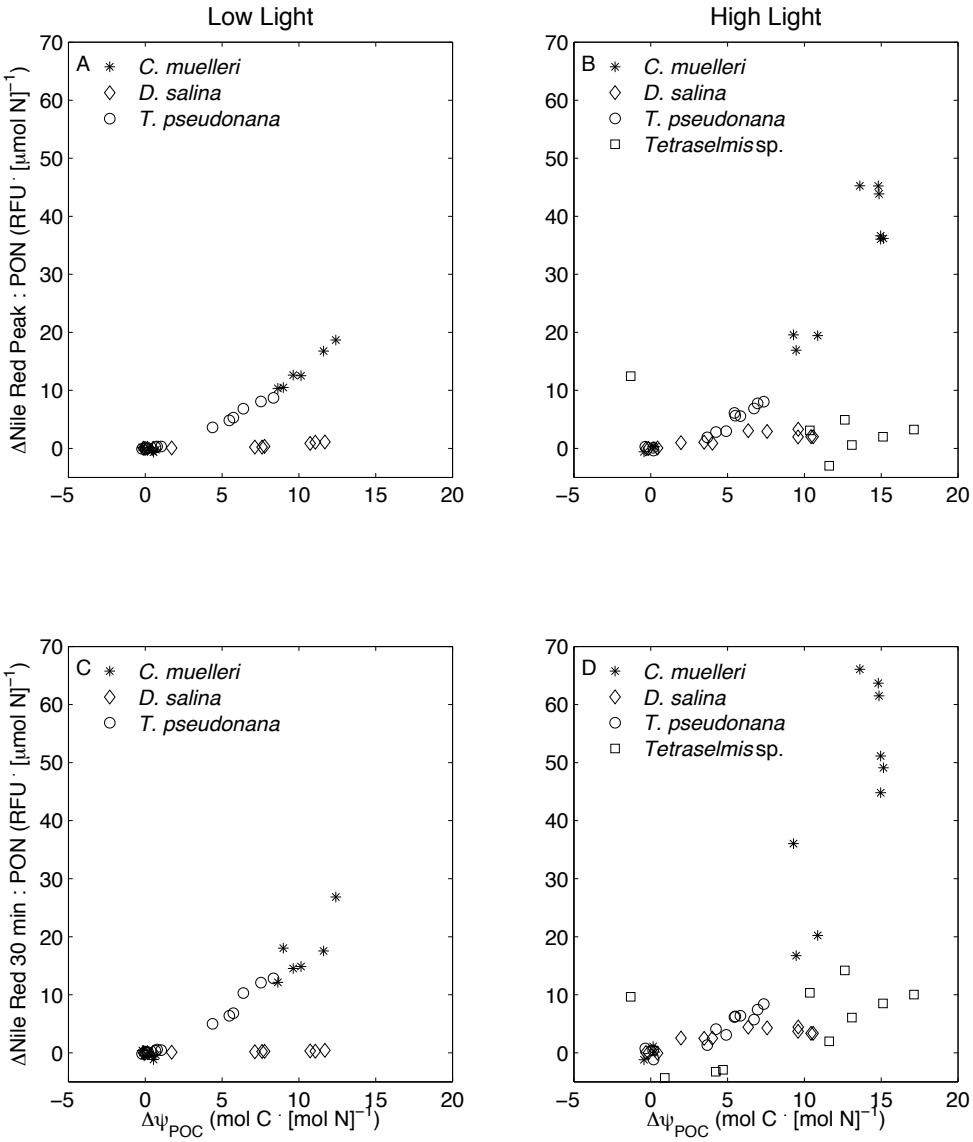

Figure A.10. The relative change in Nile Red fluorescence, compared to the relative change in carbon allocated toward non-nitrogenous compounds ($\Delta\psi_{POC}$, mol C · [mol N]$^{-1}$), during increasing N-starvation, for four species of microalgae acclimated to either low (left panes) or high (right panes) light. Nile Red measurements reported were either the (A, B) peak or (C, D) 30 min. values. The low light values for *Tetraselmis* sp. were excluded.

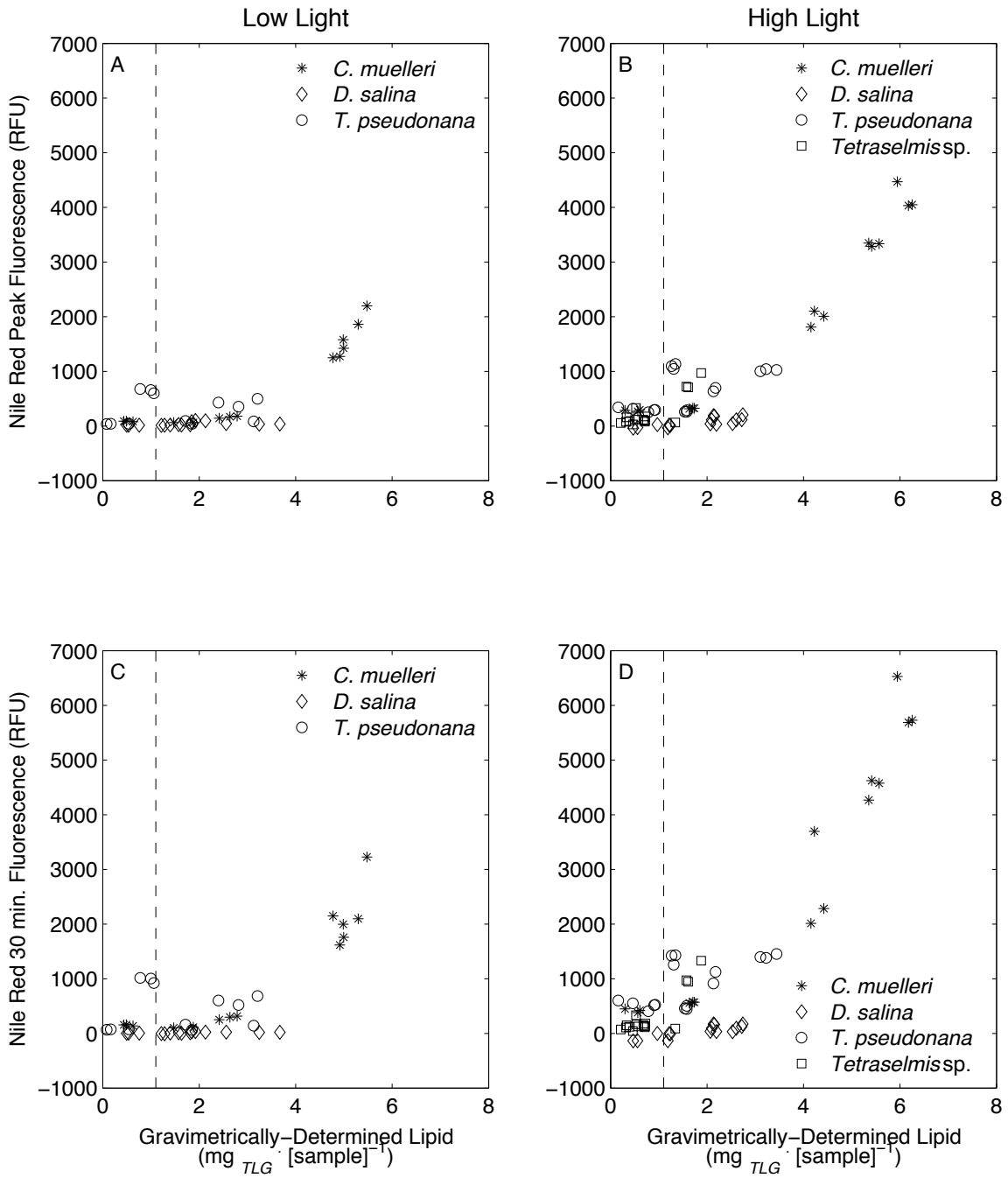

Figure A.11. The relative change in Nile Red fluorescence, compared to the relative change in carbon allocated toward gravimetric total lipid, during increasing N-starvation, for four species of microalgae acclimated to either low (left panes) or high (right panes) light. Nile Red measurements reported were either (A, B) the peak or (C, D) 30 min. values. The low light values for *Tetraselmis* sp. were excluded. Dashed line represents the limit of quantification for gravimetric lipid (L.O.Q. = 10 SE of the blank, where $SE = SD/\sqrt{n}$, n = 3).

A.4 Gravimetric Lipid Quantification

One of the main concerns for these experiments was the small amounts of lipid present on sample filters, during the N-replete regime and the start of the N-starvation regime, for some treatments. When the N-replete samples are compared to the N-starvation samples, it was observed that the majority of the N-replete samples were less than, or close to the limit of quantification (L.O.Q.), which was based on the mean blank value + 10 SE ($SE = SD/\sqrt{n}$, n = 3), while the majority of the N-starvation regime samples were greater than the L.O.Q. (L.O.Q. = 1.1 mg) (Figure A.12). Because many N-replete samples fell short of the L.O.Q., a more accurate alternate estimate of total lipid had to be developed as the reference point, to which changes due to N-starvation were compared. This estimate, inferred total lipid ($\Delta\psi_{TLI}$, mol C_{TLI} · [mol N]$^{-1}$), was dependent on measurements of POC and *Carb* (equation 2.5) and was considered to be more accurate than *TLG*, but which depends on the assumption that the non-nitrogenous particulate carbon that accumulates during N-starvation is composed solely of carbohydrate and lipid.

Variation in the ratio of $\Delta\psi_{TLG}/\Delta\psi_{TLI}$ (mol C_{TLG} · [mol C_{TLI}]$^{-1}$) can be due to errors in the determination of *TLG* or in the measurement (POC, *Carb*) or assumptions in the calculation of *TLI*. When the amount of lipid on filters is high, errors in *TLG* should decrease, so if the change in *TLI* is a good measure of the change in *TLG* during N-starvation, the ratio of the two should converge to 1.0 for weights of lipid that exceed the L.O.Q., as is the case. At higher lipid concentrations, the $\Delta\psi_{TLG}/\Delta\psi_{TLI}$ ratio approaches 1.0 (Figure A.13) consistent with *TLG* becoming more reliable when there is higher biomass present per sample and $\Delta\psi_{TLI}$ being a good measure of $\Delta\psi_{TLG}$.

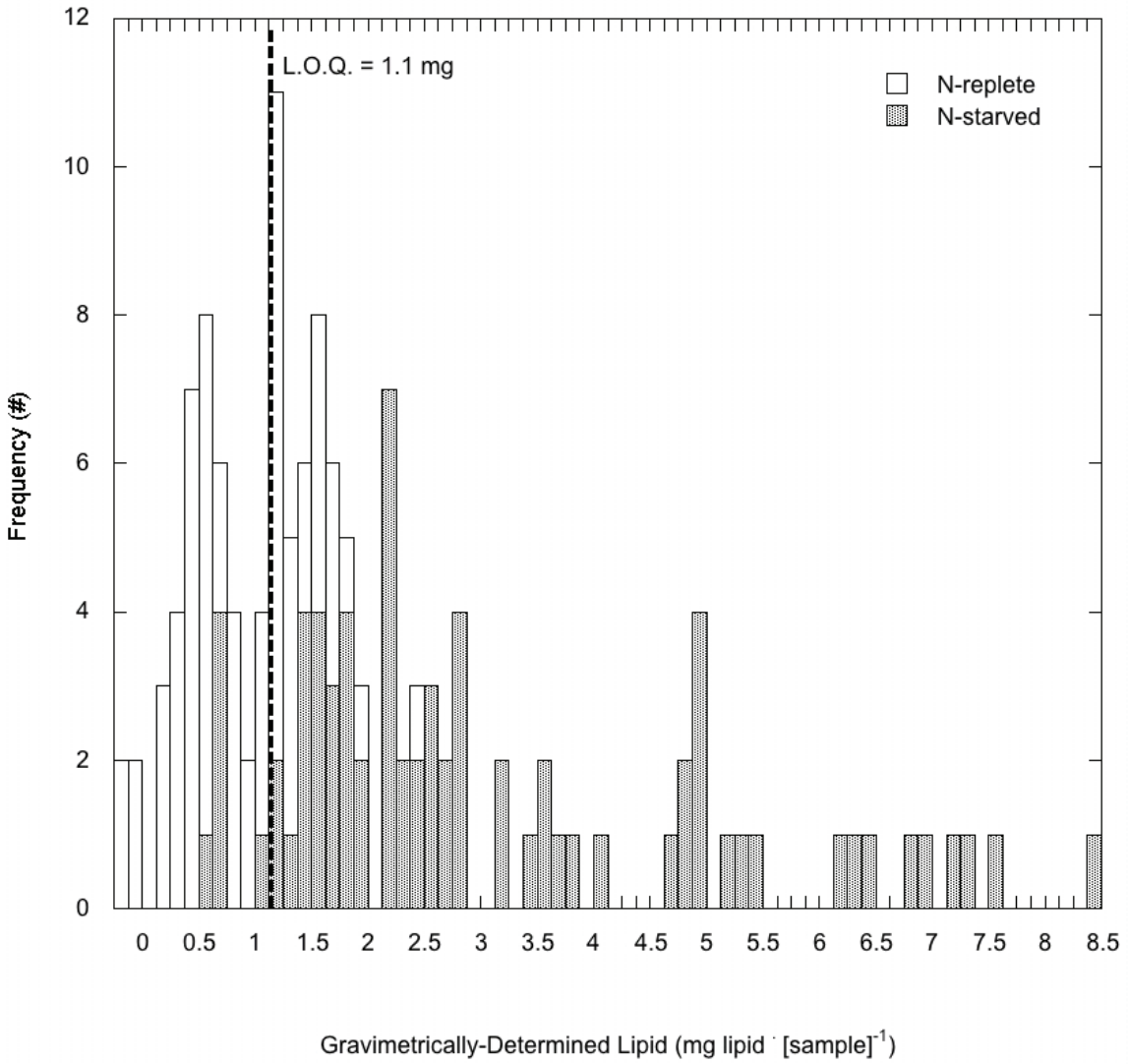

Figure A.12. Frequency of gravimetric total lipids that are above or below the limit of quantification (i.e. 1.1 mg, 10 SE of the blanks, n = 3). Samples taken during the N-replete regime (white bars) were primarily lower than, or close to the L.O.Q, whereas the majority of samples from the N-starvation regime (shaded bars) were above the L.O.Q.

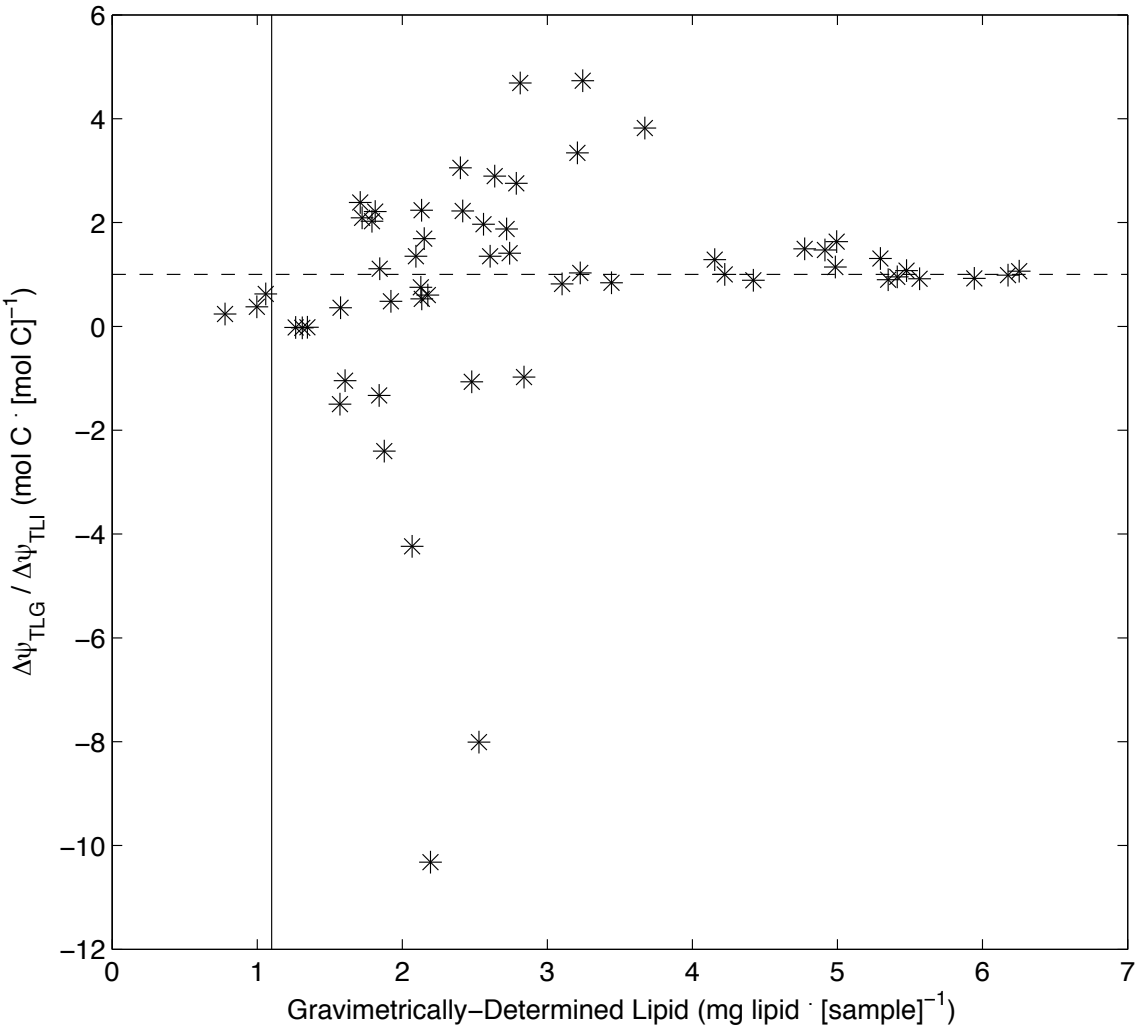

Figure A.13. Comparison of the change in gravimetric total lipid ($\Delta\psi_{TLG}$, mol C_{TLG} · [mol N]$^{-1}$) to the corresponding change in inferred total lipid ($\Delta\psi_{TLI}$, mol C_{TLI} · [mol N]$^{-1}$) as a function of the lipid mass present per sample, as determined by gravimetric means (Gravimetrically-Determined Lipid, mg lipid · [sample]$^{-1}$). Horizontal dashed bar represents the 1:1 line, where the forms of lipid measurements are equivalent. Data falling below the line indicate that gravimetric total lipid detected less lipid than presumably present in the sample, whereas data above the line indicate that gravimetric total lipid detected more lipid than presumably present in the sample. Greater variability, > 10%, was evident for samples of lower gravimetric lipid present per sample.

A.5 Total Nitrogen

As stated in the results, the summation of nitrate (NO_3^-) and particulate organic nitrogen, PON (μmol N L^{-1}) was lower than the expected 100 μmol N · L^{-1} for the majority of the treatments. Possible causes of this included lower than intended nitrate (NO_3^-) concentration in the medium (initial medium nitrate was not verified), and/or biomass that accumulated but was not sampled, e.g. sticking to culture vessel walls. As a new flask was started daily during the N-replete regime, the accumulation of biomass would have only occurred over 24 h. Temporal plots of total N in the flasks provide clues, but not definitive answers (Figure A.14). With the exception of *Tetraselmis* sp., individual species used a single batch of medium. Due to higher than expected dilution ratios, *Tetraselmis* sp. required the use of two batches of medium. Had the NO_3^- concentration of the medium been lower than the 100 μM, PON on the final day of N-starvation (when nitrate concentration is zero) would equal that of the nitrate concentration, if both PON and nitrate had been quantitatively transferred at each dilution. As shown in equation 2.1, dilution ratios were dependent on *in vivo* fluorescence, used as an indicator for algal biomass. If the dilution was correct, but algal biomass stuck to the flask and was not included in the final dilution, the particulate organic nitrogen carryover between flasks would have been lower than what was calculated. The lower concentration of particulate organic nitrogen carryover would result in a lower starting biomass, ultimately resulting with a lower final concentration of PON at the end of N-starvation. Comparatively, if cultures were not homogeneously dispersed in the medium and instead clumped together, a higher than expected biomass could have been transferred; this would have given a total nitrogen greater than 100 μmol N L^{-1}, similar to

what was observed on the first N-replete regime day for *Thalassiosira pseudonana* (Figure A.14). However, without initial measurements of the nitrate in the medium, it cannot be determined if the initial NO_3^- were limiting, or if an incorrect biomass was diluted.

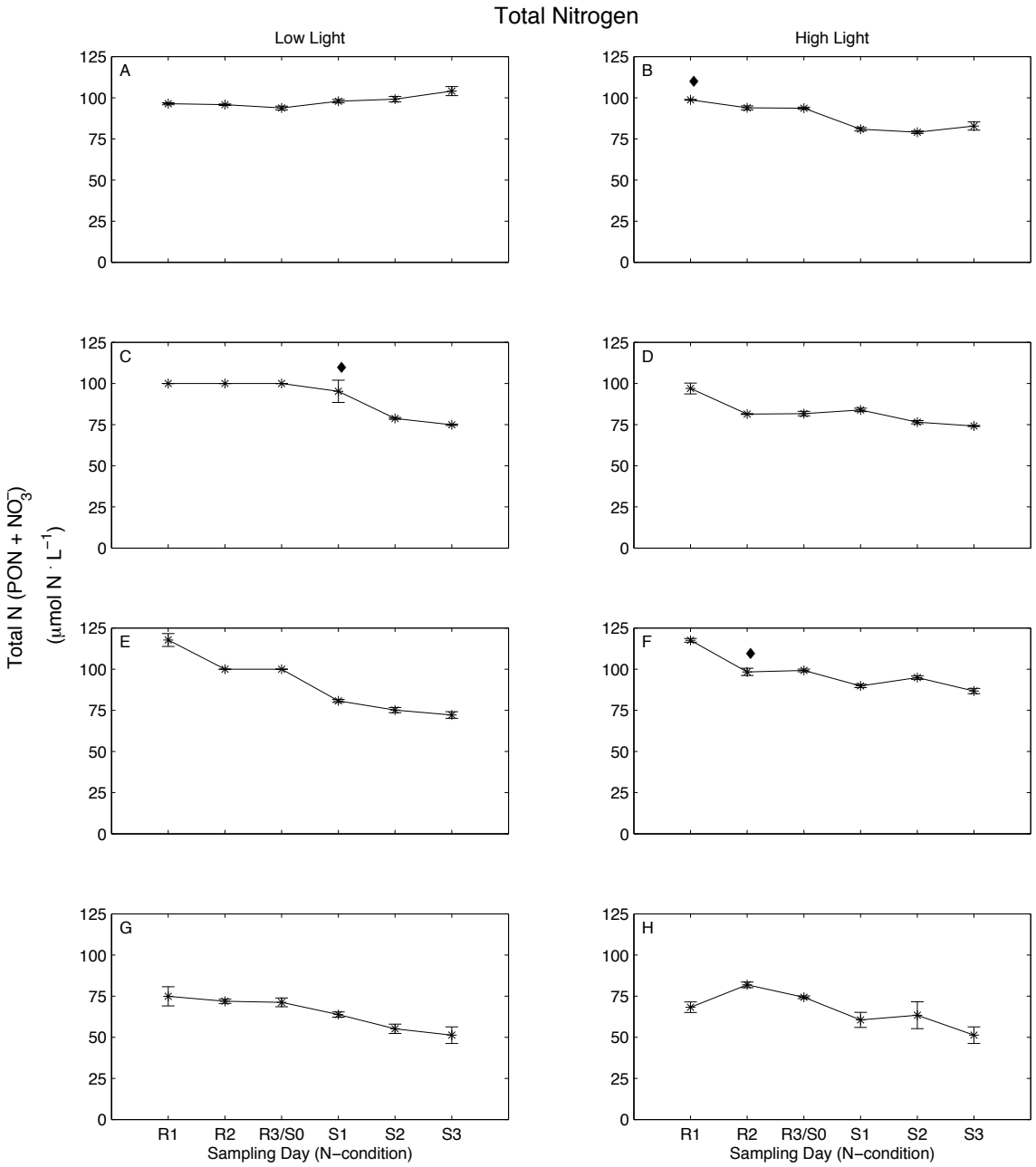

Figure A.14. Calculated total nitrogen for four species of microalgae acclimated to LL (175 µmol quanta m^{-2} s^{-1}) or HL (600 µmol quanta m^{-2} s^{-1}), during periods of nutrient replete growth (R1 – R3) and increasing nutrient starvation (S1 – S3). (A, B) *Chaetoceros muelleri*, (C, D) *Dunaliella salina*, (E, F) *Thalassiosira pseudonana* and (G, H) *Tetraselmis* sp. Values are mean ± SE (n = 3) unless indicated (♦) where values are mean ± range (n = 2).

References

Ben-Amotz, A., Tornabene, T. G. & Thomas, W. H. 1985. Chemical profiles of selected species of microalgae with emphasis on lipids. *Journal of Phycology* **21**:72-81.

Berges, J. A. & Falkowski, P. G. 1998. Physiological stress and cell death in marine phytoplankton: Induction of proteases in response to nitrogen or light limitation. *Limnology and Oceanography* **43**:129-35.

Bligh, E. G. & Dyer, W. J. 1959. A rapid method of total lipid extraction and purification. *Canadian Journal of Biochemistry and Physiology* **37**:911-17.

Boussiba, S., Bing, W., Yuan, J.-P., Zarka, A. & Chen, F. 1999. Changes in pigments profile in the green alga *Haeamtococcus pluvialis* exposed to environmental stresses. *Biotechnology Letters* **21**:601-04.

Brand, L. E., Guillard, R. R. L. & Murphy, L. S. 1981. A method for the rapid and precise determination of acclimated phytoplankton reproduction rates. *Journal of Plankton Research* **3**:193-201.

Brown, M. R., Dunstan, G. A., Jeffrey, S. W., Volkman, J. K., Barrett, S. M. & LeRoi, J.-M. 1993. The Influence of Irradiance on the Biochemical Composition of the Prymesiophyte *Isochrysis* sp. (Clone T-ISO). *Journal of Phycology* **29**:601-12.

Brown, M. R., Dunstan, G. A., Norwood, S. J. & Miller, K. A. 1996. Effects of harvest stage and light on the biochemical composition of the diatom *Thalassiosira pseudonana*. *Journal of Phycology* **32**:64-73.

Bruxton, T., Lyons, H., Lerat, Y., Stanley, M. & Rasmussen, M. B. 2009. A review of the potential of marine algae as a source of biofuel in Ireland. *In*: Ireland, S. E. [Ed.]. Dublin.

Burlew, J. S. 1953. Current status of the large-scale culture of algae. *In*: Burlew, J. S. [Ed.] *Algal culture: From laboratory to pilot plant.* Carnegie Institute of Washing Publication 600, Washington, D.C., pp. 3 - 23.

Canakci, M. & VanGerpen, J. 2001. Biodiesel production from oils and fats with high free fatty acids. **44**:1429-36.

Chan, A. T. 1978. Comparative physiological study of marine diatoms and dinoflagellates in relation to irraidance and cell size. I. Growth under continuous light. *Journal of Phycology* **14**:396-402.

Chen, W., Sommerfeld, M. & Hu, Q. 2011. Microwave-assisted Nile red method for in vivo quantification of neutral lipids in microalgae. *Bioresource Technology* **102**:135-41.

Chen, W., Zhang, C. W., Song, L. R., Sommerfeld, M. & Hu, Q. 2009. A high throughput Nile Red method for quantitative measurement of neutral lipids in microalgae. *Journal of Microbiological Methods* **77**:41-47.

Chisti, Y. 2007. Biodiesel from microalgae. *Biotechnology Advances* **25**:294-306.

Chu, W.-L., Phang, S.-M. & Goh, S.-H. 1996. Environmental effects on growth and biochemical composition of<i>Nitzschia inconspicua</i> Grunow. *Journal of Applied Phycology* **8**:389-96.

Claustre, H. & Gostan, J. 1987. Adaptation of biochemical composition and cell size to irradiance in two microalgae: Possible ecological implications. *Marine Ecology-Progress Series* **40**:167-74.

Conover, R. J. 1966. Assimilation of organic matter by zooplankton. *Limnology and Oceanography* **11**:338-45.

Cullen, J. J. 1982. The deep chlorophyll maximum: Comparing vertical profiles of chlorophyll a. *Canadian Journal of Fisheries and Aquatic Sciences* **39**:791-803.

D'Souza, F. M. L. & Kelly, G. J. 2000. Effects of a diet of nitrogen-limited alga (*Tetraselmis suecica*) on growth, survival and biochemical composition of tiger prawn (*Penaeus semisulcatus*) larvae. *Aquaculture* **181**:311 - 29.

Danger, M., Oumarou, C., Benest, D. & Lacroix, G. 2007. Bacteria can control stoichiometry and nutrient limitation of phytoplankton. *Functional Ecology* **21**:202-10.

Dempster, T. A. & Sommerfeld, M. R. 1998. Effects of environmental conditions on growth and lipid accumulation in Nitzschia communis (Bacillariophyceae). *Journal of Phycology* **34**:712-21.

Deye, J. F., Berger, T. A. & Anderson, A. G. 1990. Nile Red as a solvatochromic dye for measuring solvent strength in normal liquids and mixtures of normal liquids with supercritical and near critical fluids. *Analytical Chemistry* **62**:615-22.

Doney, S. C., Fabry, V. J., Feely, R. A. & Kleypas, J. A. 2009. Ocean acidification: The other CO2 problem. *Annual Review of Marine Science* **1**:169-92.

Dortch, Q., Clayton, J. R., Thoresen, S. S. & Ahmed, S. I. 1984. Species differences in accumulation of nitrogen pools in phytoplankton. *Marine Biology* **81**:237-50.

Dubois, M., Gilles, K. A., Hamilton, J. K., Rebers, P. A. & Smith, F. 1956. Colorimetric method for the determination of sugars and related substances. *Analytical Chemistry* **28**:350-56.

Elsey, D., Jameson, D., Raleigh, B. & Cooney, M. J. 2007. Fluorescent measurement of microalgal neutral lipids. *Journal of Microbiological Methods* **68**:639-42.

Eppley, R. W. 1981. Relations between nutrient assimilation and growth in phytoplankton with a brief review of estimates of grwoth rate in the ocean. *Canadian Bulletin of Fisheries and Aquatic Sciences* **210**:251-63.

Eppley, R. W. & Renger, E. H. 1974. Nitrogen assimilation of an oceanic diatom in nitrogen-limited continuous culture. *Journal of Phycology* **10**:15-23.

Fabregas, J., Maseda, A., Dominguez, A. & Otero, A. 2004. The cell composition of *Nannochloropsis* sp changes under different irradiances in semicontinuous culture. *World Journal of Microbiology & Biotechnology* **20**:31-35.

Falkowski, P. G. & Raven, J. A. 2007. *Aquatic Photosynthesis.* Princeton University Press,

Ferrell, J. & Sarisky-Reed, V. 2010. National Algal Biofuels Technology Roadmap. U. S. Department of Energy Office of Energy Efficiency and Renewable Energy, Washington.

Forster, P., Ramaswamy, V., Artaxo, P., Berntsen, T., Betts, R., Fahey, D. W., Haywood, J., Lean, J., Lowe, D. C., Myhre, G., Nganga, J., Prinn, R., Raga, G., Schulz, M. & Van Dorland, R. 2007. Changes in Atmospheric Constituents and in Radiative Forcing. *In*: Solomon, S., Qin, D., Manning, M., Chen, Z., Marquis, M., Averyt, K. B., Tignor, M. & Miller, H. L. [Eds.] *Climate Change 2007: The Physical Science Basis. Contribution of Working Group I to the Fourth Assessment Report of the Intergovernmental Panel on Climate Change.* Cambridge University Press, Cambridge, United Kingdom.

Galloway, J. N. & Likens, G. E. 1981. Acid precipitation: The importance of nitric acid. *Atmospheric Environment (1967)* **15**:1081-85.

Geider, R. J. & La Roche, J. 2002. Redfield revisited: variability of C:N:P in marine microalgae and its biochemical basis. *European Journal of Phycology* **37**:1-17.

Geider, R. J., La Roche, J., Greene, R. M. & Olaizola, M. 1993. Response of the photosynthetic apparatus of *Phaeodactylum tricornutum* (Bacilliariophyceae) to nitrate, phosophate, or iron starvation. *Journal of Phycology* **29**:755-66.

Geider, R. J., MacIntyre, H. L. & Kana, T. M. 1996. A dynamic model of photoadaptation in phytoplankton. *Limnology and Oceanography* **41**:1-15.

Geider, R. J., MacIntyre, H. L. & Kana, T. M. 1998. A dynamic regulatory model of phytoplanktonic acclimation to light, nutrients, and temperature. *Limnology and Oceanography* **43**:679-94.

Geider, R. J., Osborne, B. A. & Raven, J. A. 1985. Light dependence of growth and photosynthesis in *Phaeodactylum tricornutum* (Bacillariophyceae). *Journal of Phycology* **21**:609-19.

Genty, B., Briantais, J.-M. & Baker, N. R. 1989. The relationship between the quantum yield of photosynthetic electron transport and quenching of chlorophyll fluorescence. *Biochimica et Biophysica Acta (BBA) - General Subjects* **990**:87-92.

Goldman, J. C. 1979. Outdoor algal mass cultures. II. Photosynthetic yield limitations. *Water Research* **13**:119-36.

Gosselin, M., Legendre, L., Therriault, J.-C. & Demers, S. 1990. Light and nutrient limitation of sea-ice microalgae (Hudson Bay, Canadian Arctic). *Journal of Phycology* **26**:220-32.

Granum, E., Kirkvold, S. & Myklestad, S. M. 2002. Cellular and extracellular production of carbohydrates and amino acids by the marine diatom Skeletonema costatum: diel variations and effects of N depletion. *Marine Ecology-Progress Series* **242**:83-94.

Griffiths, M. J. & Harrison, S. T. L. 2009. Lipid productivity as a key characteristic for choosing algal species for biodiesel production. *Journal of Applied Phycology* **21**:493-507.

Guerin, M., Huntley, M. E. & Olaizola, M. 2003. *Haematococcus* astaxanthin: applications for human health and nutrition. *Trends in Biotechnology* **21**:210-16.

Guillard, R. R. L. 1975. Culture of phytoplankton for feeding marine invertebrates. *In*: Smith, W. L. & Chanley, M. H. [Eds.] *Culture of Marine Invertebrate Animals.* Plenum Press, New York, pp. 26 - 60.

Guillard, R. R. L. & Ryther, J. H. 1962. Studies of marine planktonic diatoms. I. *Cyclotella nana* Hustedt and *Detonula confervacea* Cleve. *Canadian Journal of Microbiology* **8**:229 - 39.

Gummert, F., Meffert, M. E. & Stratmann, H. 1953. Nonsterile large-scale culture of *Chorella* in greenhouse and open air. *In*: Burlew, J. S. [Ed.] *Algal culture: From laboratory to pilot plant.* Carnegie Institute of Washing Publication 600, Washington, D.C., pp. 166-77.

Guschina, I. A. & Harwood, J. L. 2006. Lipids and lipid metabolism in eukaryotic algae. *Progress in Lipid Research* **45**:160-86.

Harrison, P. J., Thompson, P. A. & Calderwood, G. S. 1990. Effects of nutrient and light limitation on the biochemical composition of phytoplankton. *Journal of Applied Phycology* **2**:45-56.

Hellebust, J. A. 1965. Excretion of some organic compounds by marine phytoplankton. *Limnology and Oceanography* **10**:192-206.

Hill, J., Nelson, E., Tilman, D., Polasky, S. & Tiffany, D. 2006. Environmental, economic, and energetic costs and benefits of biodiesel and ethanol biofuels. *Proceedings of the National Academy of Sciences* **103**:11206-10.

Hockin, N. L., Mock, T., Mulholland, F., Kopriva, S. & Malin, G. 2012. The response of diatom central carbon metabolism to nitrogen starvation is different from that of green algae and higher plants. *Plant Physiology* **158**:299-312.

Hu, Q. 2006. Environemental effects on cell composition. *In*: Richmond, A. [Ed.] *Handbook of Microalgal Culture: Biotechnology and Applied Phycology.* Blackwell Science, Oxford, pp. 83 - 93.

Hu, Q., Sommerfeld, M., Jarvis, E., Ghirardi, M., Posewitz, M., Seibert, M. & Darzins, A. 2008. Microalgal triacylglycerols as feedstocks for biofuel production: perspectives and advances. *Plant Journal* **54**:621-39.

Huntley, M. & Redalje, D. 2007. CO2 mitigation and renewable oil from photosynthetic microbes: A new appraisal. *Mitigation and Adaptation Strategies for Global Change* **12**:573-608.

Inouye, L. S. & Lotufo, G. R. 2006. Comparison of macro-gravimetric and micro-colorimetric lipid determination methods. *Talanta* **70**:584-87.

Iverson, S. J., C., L. S. L. & Cooper, M. H. 2001. Comparison of the Bligh and Dyer and Folch methods for total lipid determination in a broad range of marine tissue. *Lipids* **36**:1283 - 87.

Kolber, Z., Zehr, J. & Falkowski, P. G. 1988. Effects of growth irradiance and nitrogen limitation on photosynthetic energy conversion in photosystem II. *Plant Physiology* **88**:923 - 29.

Kolber, Z., Zehr, J. & Falkowski, P. G. 1998. Effects of growth irradiance and nitrogen limitation on photosynthetic energy conversion in Photosystem II. *Plant Physiology* **88**:923-29.

Larson, T. R. & Rees, T. A. V. 1996. Changes in cell composition and lipid metabolism mediated by sodium and nitrogen availability in the marine diatom *Phaeodactylum tricornutum* (Bacillariophyceae). *Journal of Phycology* **32**:388-93.

Laws, E. A. & Bannister, T. T. 1980. Nutrient- and light-limited growth of *Thalassiosira fluviatilis* in continuous culture, with implications for phytoplankton growth in the ocean. *Limnology and Oceanography* **25**:457-73.

Laws, E. A. & Chalup, M. S. 1990. A microalgal growth model. *Limnology and Oceanography* **35**:597-608.

Lewis, M. R. & Smith, J. C. 1983. A small volume, short-incubation-time method for measurement of photosynthesis as a function of incident irradiance. *Marine Ecology Progress Series* **13**:99-102.

Lorenz, R. T. & Cysewski, G. R. 2000. Commercial potential for *Haematococcus* microalgae as a natural source of astaxanthin. *Trends in Biotechnology* **18**:160-67.

Lourenço, S. O., Barbarino, E., Lavin, P. L., Marque, U. M. L. & Aidar, E. 2004. Distribution of intracellular nitrogen in marine microalgae: Calculation of new nitrogen-to-protein conversion factors. *European Journal of Phycology* **39**:17-32.

Maberly, S. C., Courcelle, C., Groben, R. & Gontero, B. 2010. Phylogenetically-based variation in the regulation of the Calvin cycle enzymes, phosphoribulokinase and glyceraldehyde-3-phosphate dehydrogenase, in algae. *Journal of Experimental Botany* **61**:735-45.

MacIntyre, H. L. & Cullen, J. J. 2005. Using cultures to investigate the physiological ecology of microalgae. *In*: Anderson, R. A. [Ed.] *Algal Culturing Techniques.* Academic Press, pp. 287 - 326.

Mague, T. H., Friberg, E., Hughes, D. J. & Morris, I. 1980. Extracellular release of carbon by marine phytoplankton; a physiological approach. *Limnology and Oceanography* **25**:262-79.

Mecozzi, M. 2005. Estimation of total carbohydrate amount in environmental samples by the phenol-sulphuric acid method assisted by multivariate calibration. *Chemometrics and Intelligent Laboratory Systems* **79**:84-90.

Meier, R. L. 1955. Biological cycles in the transformation of solar energy into useful fuels. *In*: Daniels, F. & Duffie, J. A. [Eds.] *Solar Energy Research.* University of Wisconsin Press, Madison, WI, pp. 179 - 83.

Moal, J., Martin-Jezequel, V., Harris, R. P., Samain, J. F. & Poulet, S. A. 1987. Interspecific and intraspecific variability of the chemical composition of marine phytoplankton. *Oceanologica Acta* **10**:339-46.

Molina, E., Martinez, M. E., S ánchez, S., Garcia, F. & Contreras, A. 1991. Growth and biochemical composition with emphasis on the fatty acids of *Tetraselmis* sp. *Applied Microbiology and Biotechnology* **36**:21 - 25.

Morris, I. 1981. Photosynthetic products, physiological state and phytoplankton growth. *Canadian Bulletin of Fisheries and Aquatic Sciences* **210**:83 - 102.

Myklestad, S. 2000. Dissolved organic carbon from phytoplankton. *In*: Wangersky, P. J. [Ed.] *The Handbook of Environmental Chemistry.* Springer-Verlag, Berlin, pp. 111-48.

Myklestad, S. M. 1995. Release of extracellular products by phytoplankton with special emphasis on polysaccharides. *Science of the Total Environment* **165**:155-64.

Naik, S. N., Goud, V. V., Rout, P. K. & Dalai, A. K. 2010. Production of first and second generation biofuels: A comprehensive review. *Renewable and Sustainable Energy Reviews* **14**:578-97.

Nigam, P. S. & Singh, A. 2011. Production of liquid biofuels from renewable resources. *Progress in Energy and Combustion Science* **37**:52-68.

Olaizola, M. 2000. Commercial production of astaxanthin from *Haematococcus pluvaialis* using 25,000-liter outdoor photobioreactors. *Journal of Applied Phycology* **12**:499-506.

Oswald, W. J. & Golueke, C. G. 1960. Biological transformation of solar energy. *Advanced Applied Microbiology* **11**:223 - 42.

Panagiotopoulos, C. & Sempere, R. 2005. Analytical methods for the determination of sugars in marine samples: A historical perspective and future directions. *Limnology and Oceanography-Methods* **3**:419-54.

Parkhill, J.-P., Maillet, G. & Cullen, J. J. 2001. Fluorescence-based maximal quantum yield for PSII as a diagnostic of nutrient stress. *Journal of Phycology* **37**:517-29.

Parsons, T. R., Stephens, K. & Strickland, J. D. H. 1961. On the Chemical Composition of Eleven Species of Marine Phytoplankters. *Journal of the Fisheries Research Board of Canada* **18**:1001-16.

Pimentel, D. & Patzek, T. W. 2005. Ethanol production using corn, switchgrass and wood; Biodiesel production using soybean and sunflower. *Natural Resources Research* **14**:65-76.

Platt, T., Gallegos, C. L. & Harrison, W. G. 1980. Photoinhibition of photosynthesis in natural assemblages of marine phytoplankton. *Journal of Marine Research* **38**:687-701.

Powell, R. C., Nevels, E. M. & McDowell, M. E. 1961. Algae Feeding in Humans. *The Journal of Nutrition* **75**:7-12.

Priscu, J. C., Priscu, L. R., Palmisano, A. C. & Sullivan, C. W. 1990. Estimation of neutral lipid levels in Antarctic sea ice microalgae by Nile Red fluorescence. *Antarctic Science* **2**:149 - 55.

Redfield, A. C. 1958. The biological control of chemical factors in the environment. *American Scientist* **46**:230A-21.

Renaud, S. M., Parry, D. L., Thinh, L. V., Kuo, C., Padovan, A. & Sammy, N. 1991. Effect of light intensity on the proximate biochemical and fatty acid compostion of *Isochrysis* sp. and *Nannochloropsis oculata* for use in tropical aquaculture. *Journal of Applied Phycology* **3**:43 - 53.

Renaud, S. M., Thinh, L.-V. & Parry, D. L. 1999. The gross chemical composition and fatty acid composition of 18 species of tropical Australian microalgae for possible use in mariculture. *Aquaculture* **170**:147-59.

Renaud, S. M., Thinh, L. V., Lambrinidis, G. & Parry, D. L. 2002. Effect of temperature on growth, chemical composition and fatty acid composition of tropical Australian microalgae grown in batch cultures. *Aquaculture* **211**:195-214.

Richardson, T. L., Ciotti, Á. M., Cullen, J. J. & Villareal, T. A. 1996. Physiological and optical properties of *Rhizosolenia formosa* (Bacillariophyceae) in the context of open-ocean vertical migration. *Journal of Phycology* **32**:741-57.

Richardson, T. L. & Cullen, J. J. 1995. Changes in buoyancy and chemical composition during growth of a coastal marine diatom: Ecological and biogeochemical consequences. *Marine Ecology-Progress Series* **128**:77-90.

Rodolfi, L., Zittelli, G. C., Bassi, N., Padovani, G., Biondi, N., Bonini, G. & Tredici, M. R. 2009. Microalgae for oil: Strain selection, induction of lipid synthesis and outdoor mass cultivation in a low-cost photobioreactor. *Biotechnology and Bioengineering* **102**:100-12.

Saxena, R. C., Adhikari, D. K. & Goyal, H. B. 2009. Biomass-based energy fuel through biochemical routes: A review. *Renewable and Sustainable Energy Reviews* **13**:167-78.

Schenk, P., Thomas-Hall, S., Stephens, E., Marx, U., Mussgnug, J., Posten, C., Kruse, O. & Hankamer, B. 2008. Second generation biofuels: High-efficiency microalgae for biodiesel production. *Bioenergy Research* **1**:20-43.

Scott, S. A., Davey, M. P., Dennis, J. S., Horst, I., Howe, C. J., Lea-Smith, D. J. & Smith, A. G. 2010. Biodiesel from algae: challenges and prospects. *Current Opinion in Biotechnology* **21**:277-86.

Sheehan, J., Dunahay, T., Benemann, J. & Roessler, P. G. 1998. A look back at the U.S. Department of Energy's Aquatic Species Program - Biodiesel from algae. National Renewable Energy Laboratory, pp. 328.

Shifrin, N. S. & Chisholm, S. W. 1980. Phytoplankton lipids: Environmental influences on production and possible commerical applications. *Algae Biomass.* pp. 627-45.

Shifrin, N. S. & Chisholm, S. W. 1981. Phytoplankton lipids - interspecific differences and effects of nitrate, silicate and light-dark cycles. *Journal of Phycology* **17**:374-84.

Sims, R. E. H., Mabee, W., Saddle, J. N. & Taylor, M. 2010. An overview of second generation biofuel technologies. *Bioresource Technology* **101**:1570-80.

Singh, Y. & Kumar, H. D. 1992. Lipid and hydrocarbon production by *Botryococcus* spp. under nitrogen limitation and anaerobiosis. *World Journal of Microbiology & Biotechnology* **8**:121-24.

Smedes, F. & Askland, T. K. 1999. Revisiting the development of the Bligh and Dyer total lipid determination method. *Marine Pollution Bulletin* **38**:193-201.

Smedes, F. & Thomasen, T. K. 1996. Evaluation of the Bligh & Dyer lipid determination method. *Marine Pollution Bulletin* **32**:681 - 88.

Suggett, D. J., Moore, C. M., Hickman, A. E. & Geider, R. J. 2009. Interpretation of fast repetition rate (FRR) fluorescence: signatures of phytoplankton community structure versus physiological state. *Marine Ecology Progress Series* **376**:1-19.

Sukenik, A., Carmeli, Y. & Berner, T. 1989. Regulation of fatty-acid composition by irradiance level in the Eustigmatophyte *Nannochloropsis* sp. *Journal of Phycology* **25**:686-92.

Sukenik, A. & Wahnon, R. 1991. Biochemical quality of marine unicellular algae with special emphasis on lipid composition. I. *Isochrysis galbana*. *Aquaculture* **97**:61-72.

Sun, M., Zuoguo, Q. & Wei, H. 1984. On the method for determining total dissolved carbohydrates in sea water: Temperature effect of phenol-sulfuric acid method. *Collected Oceanic Works* **7**:84-89.

Terry, K. L., Hirata, J. & Laws, E. A. 1983. Light-limited growth of two strains of the marine diatom *Phaeodactylum tricornutum* Bohlin: Chemical composition, carbon partitioning and the diel periodicity of physiological processes *Journal of Experimental Marine Biology and Ecology* **68**:209-27.

Thomas, W. H., Seibert, D. L. R., Alden, M., Neori, A. & Eldridge, P. 1984a. Yields, photosynthetic efficiencies and proximate composition of dense marine microalgal cultures.1. Introduction and *Phaeodactylum tricornutum* experiments. *Biomass* **5**:181-209.

Thomas, W. H., Seibert, D. L. R., Alden, M., Neori, A. & Eldridge, P. 1984b. Yields, photosynthetic efficiencies and proximate composition of dense marine microalgal cultures. 2. *Dunaliella primolecta* and *Tetraselmis suecica* experiments. *Biomass* **5**:211-25.

Thomas, W. H., Seibert, D. L. R., Alden, M., Neori, A. & Eldridge, P. 1984c. Yields, photosynthetic efficiencies and proximate composition of dense marine microalgal cultures. 3. *Isochrysis* sp. and *Monallantus salina* experiments and comparative conclusions. *Biomass* **5**:299-316.

Thompson, P. A., Guo, M. X. & Harrison, P. J. 1992. Effects of variation in temperature. 1. On the biochemical composition of 8 species of marine phytoplankton. *Journal of Phycology* **28**:481-88.

Thompson, P. A., Guo, M. X. & Harrison, P. J. 1993. The influence of irradiance on the biochemical composition of three phytoplankton species and their nutritional value for larvae of the Pacific Oyster (*Crassostrea gigas*). *Marine Biology* **117**:259 - 68.

Tréguer, P. & Lecorre, P. 1975. *Manuel d'analyse des sels nutritifs dans l'eau de mer (utilisation de l'autoanalyseur Technicon II).* Université de Bretange Occidentale 110.

Utting, S. D. 1985. Influence of nitrogen availability on the biochemical composition of three unicellular marine algae of commercial importance. *Aquaculture Engineering* **4**:175 - 90.

Vrede, K., Heldal, M., Norland, S. & Bratbak, G. 2002. Elemental composition (C, N, P) and cell volume of exponentially growing and nutrient-limited bacterioplankton. *Applied and Environmental Microbiology* **68**:2965-71.

Welschmeyer, N. A. 1994. Fluorometric Analysis of chlorophyll a in the presence of chlorophyll b and pheopigments. *Limnology and Oceanography* **39**:1985-92.

Wilhelm, C., Büchel, C., Fisahn, J., Goss, R., Jakob, T., LaRoche, J., Lavaud, J., Lohr, M., Riebesell, U., Stehfest, K., Valentin, K. & Kroth, P. G. 2006. The Regulation of Carbon and Nutrient Assimilation in Diatoms is Significantly Different from Green Algae. *Protist* **157**:91-124.

Williams, P. J. L. & Laurens, L. M. L. 2010. Microalgae as biodiesel & biomass feedstocks: Review & analysis of the biochemistry, energetics & economics. *Energy & Environmental Science* **3**:554-90.

Wood, A. M. & van Valen, L. M. 1990. Paradox lost? On the release of energy-rich compounds by phytoplankton. *Marine Microbial Food Webs* **4**:103-16.

Wood, L. W. 1985. Chloroform-methanol extraction of chlorophyll a. *Canadian Journal of Fisheries and Aquatic Sciences* **42**:38-43.

Xiao, L., Mjøs, S. A. & Haugsgjerd, B. O. 2012. Efficiencies of three common lipid extraction methods evaluated by calculating mass balances of the fatty acids. *Journal of Food Composition and Analysis* **25**:198-207.

Yu, E., Zendejas, F., Lane, P., Gaucher, S., Simmons, B. & Lane, T. 2009. Triacylglycerol accumulation and profiling in the model diatoms *Thalassiosira pseudonana* and *Phaeodactylum tricornutum* (Baccilariophyceae) during starvation. *Journal of Applied Phycology* **21**:669-81.